AN ELECTRODELESS METHOD FOR MEASURING THE LOW-FREQUENCY CONDUCTIVITY OF ELECTROLYTES

by

MATTHEW JONATHAN RELIS

B.S. in E.E., The City College of New York

(1940)

SUBMITTED IN PARTIAL FULFILLMENT OF THE REQUIREMENTS FOR THE DEGREE OF

MASTER OF SCIENCE

at the

MASSACHUSETTS INSTITUTE OF TECHNOLOGY

(1947)

Signature of Author _____

Electrical Engineering Dept., May 16, 1947

Certified by _____

Thesis Supervisor

_____

Chairman, Department of Electrical Engineering

TO MY WIFE, MIRIAM, WHOSE ENCOURAGEMENT

AND SELF-SACRIFICE MADE POSSIBLE

THE COMPLETION OF THIS RESEARCH.

M. J. RELIS

TABLE OF CONTENTS

I. INTRODUCTION

i. Brief Statement of the Problem. The object of this research is to design and develop instruments for measuring the conductivity of electrolytes without the use of electrodes, using a basic scheme which is described elsewhere in this report. The problem is to develop an instrument in which the deflection of a meter will be directly proportional to the conductivity of the electrolyte being measured, and to develop another instrument functioning on a null principle, in which the conductivity is directly or inversely proportional to an impedance which is adjusted until the circuit is in a null condition. The problem is of importance because when electrodes are eliminated polarization error is absent, as well as error due to mineral deposits, which could become serious in industrial chemical processes where the measuring cell might be immersed in the electrolyte for long periods. A direct-reading conductivity meter would find wide applicability in processes where rapid or continuous measurements of conductivity would be required. Furthermore, an electrodeless method for measuring conductivity is useful in the study of molten metals. Finally, the problem is also of interest because it involves a novel approach to conductivity measurements.

ii. History of the Problem up to the Present. The chief factor which makes electrolytic conductivity measurements different from metallic conductivity measurements is the polarization phenomenon which generally takes place at the surface of electrodes immersed in an electrolyte, when they are connected to a source of emf. Polarization is the building up of a counter emf at this surface when a steady external emf is applied to the electrodes. It occurs in all cases except those in which the nature of the

electrodes is unchanged by deposition. Specifically, when pure copper electrodes are used in a copper sulphate solution, there is no polarization. In general, if the electrodes are originally in an unpolarized condition, and an emf is suddenly applied to them, the current that flows initially is determined only by the conductivity of the liquid and the applied emf, but as time passes the counter emf builds up and the current drops to a value which depends also on the electrolyte and on the electrode material.

In other respects, electrolytic conductivity measurements are very much like metallic conductivity measurements. Electrolytes obey Ohm's law (polarization notwithstanding, since polarization is a surface, rather than a volumetric, phenomenon), except at very high field strengths which are thousands of times greater than those encountered in ordinary types of conductivity-measuring apparatus.[6,11] Furthermore, the conductivity of electrolytes is independent of frequency up to about 10^6 cps.[7] Therefore, if the effects of polarization are taken into account, if electric field strength is kept at a value for which Ohm's law is valid, and if the frequency is kept below 10^6 cps, all methods of measuring conductivity should agree within their limits of accuracy.

To reduce greatly the effects of polarization, Kohlrausch[12], one of the first important investigators in the conductivity of electrolytes, used an equal-arm Wheatstone bridge excited from an a-c source (an induction coil). Alternating current was used because polarization during each half cycle tends to cancel that which occurred during the preceding half cycle, so that the net polarization is very low. The only polarization is that which takes place during a half cycle, the duration of which decreases with increasing frequency, so that polarization effects can be decreased by

increasing the frequency. In fact, it has been shown[11,15] that at audio frequencies the error in conductivity due to polarization varies inversely as the square of the frequency.

In his bridge, Kohlrausch used as the variable arm the helical slidewire which now bears his name. In the unknown arm, he used a conductivity cell consisting of a pair of platinum electrodes immersed in the electrolyte under test. He introduced the technique of depositing platinum black on the electrodes of the conductivity cell because this was found to reduce further the polarization, supposedly because it increases the effective area of the electrodes, and hence decreases the thickness of the ionic layer accumulated by a given current. He also used a variable capacitance across the helical slidewire to balance out the reactance of the conductivity cell. Kohlrausch's apparatus was capable of a maximum accuracy in conductivity determinations of 0.1%.

The apparatus most commonly used today is basically the same as that used by Kohlrausch 50 years ago, and differs only in certain refinements and in the application of modern electronic techniques. Among the earliest improvements made over Kohlrausch's apparatus were:

a. Use of a sinusoidal generator, such as the Vreeland oscillator, to eliminate assymmetrical polarization which occurred with assymetric wave forms supplied by the induction coil used by Kohlrausch, and to facilitate balancing the bridge[24,26].

b. Replacement of the helical slidewire by decade resistors, thereby greatly reducing errors due to the inductance of the slidewire[24,26].

c. Use of a telephone receiver instead of a dynamometer or a galvanometer as a null indicator, increasing the sensitivity[24,26].

Around 1920 and later, the vacuum tube was introduced into conductivity-measuring apparatus, and made possible more efficient, reliable variable-frequency generators and more sensitive detectors[9,11]. The increased sensitivity of the vacuum-tube amplifier permitted reduction of the power supplied to the bridge, without decreasing overall sensitivity, thereby reducing heating of the electrolyte in the cell and the accompanying error.

Later investigators, notably Jones[11], Dike[4], and Shedlovsky[22], increased the precision of measurements by introducing modifications of the Wagner ground to eliminate the effects of detector capacitance to ground. They further reduced the reactive components of the resistance units and developed them to the point where the a-c resistance is equal to the d-c value within 0.01% up to frequencies of 10,000 cps.

Jones and his co-workers[11], in addition to introducing the Wagner ground modification, contributed numerous improvements and eliminated many sources of error, bringing the conductivity bridge to its present state of refinement.

Paralleling the improvement of the bridge circuit, numerous investigators[1,2,5,10,11,14,16,17,22,23,24,26] studied conductivity cells in efforts to minimize or predict polarization errors and apparent variation in the "cell constant*". At high conductivities, it was found that the

---

*Cell constant C = KR where R is the resistance of the cell when filled with a liquid of conductivity K.

"cell constant" varied due to polarization; this effect was minimized by using platinized electrodes of large area, high resistance cells (high cell constant), and higher frequencies (1000 to 3000 cps).

However, another kind of variation in the cell constant appeared at low conductivities and higher frequencies. The cause of this was not discovered until Jones and Bollinger[11] found that it was due to a capacitive-resistive shunt across the electrodes of the cell, which existed because of the type of cell design which had theretofore been used. They established a new cell design which eliminated this error.

Conductivity-measuring equipment of the bridge type has now reached the point where it is consistent to 0.001%, although the absolute accuracy is 0.01%.

Many investigators have studied electrodeless methods of measuring conductivity, which are inherently free of polarization. Electrodeless techniques have been applied in two widely diverse fields; namely, in studies of the resistance of molten metals (where electrodes might dissolve in the molten metal and alter its properties) and in the study of dispersion (variation in the velocity of propagation of electromagnetic fields as a function of frequency) in liquids at high frequencies (where electrodes might introduce unknown boundary conditions).

In the first category, measurements have been made on a coil immersed in or surrounding the medium whose conductivity is to be measured. By observing the change in impedance of the coil when it is removed from the vicinity of the conducting medium, the conductivity of the medium can be determined. Grube and Speidel[8] and Schmid-Burgk, Piwowarsky, and Nipper[21], described such methods. These methods for measuring the conductivity of

molten metals at audio frequencies are not satisfactory for low-conductivity media such as electrolytes, except if extended to higher frequencies, because the change in the coil impedance due to the presence of the medium becomes so small that it cannot be distinguished from instabilities in the coil impedance (caused, for example, by mechanical strain or temperature variations).

Another method in this category used by Grube and Speidel[8] consists in measuring the torque on a molten metal sample whose conductivity is to be determined, in a rotating magnetic field. The torque is directly proportional to the current in the sample, which, in turn, is directly proportional to the conductivity so that the torque is directly proportional to the conductivity.

In the second category, Burton and Pitt[3] described a method in which a test tube of the liquid under test is placed within the plate and grid coils of an oscillator, the coils being wound close together. Inserting the test tube within the coils alters their impedance, as well as the coupling between them, and changes the amplitude and frequency of the oscillations. The rectified output of the oscillator is therefore a function of conductivity. For maximum sensitivity the oscillator is adjusted so that it barely oscillates. By admission of the authors, the circuit adjustments are critical.

Powers and Dull[19] used a method in which a test tube containing the electrolyte is inserted in the coil of a tuned circuit in the grid circuit of an amplifier, driven by an oscillator loosely coupled to the coil. This changes the Q and resonant frequency of the tuned circuit , and hence the gain and output voltage of the amplifier. The output voltage is therefore

a function of conductivity.

Zahn and Rieckhoff[20,27] used a half-wavelength transmission line, one end of which is terminated in a movable bridge (for adjustment to resonance) and the other end in a circular loop. A thin-walled glass cell containing the electrolyte is inserted in the loop. The Q of the transmission line is a function of the conductivity of the electrolyte, due to the energy absorbed therein. The line is loosely coupled to an oscillator and directly to an untuned detector. The current in the line is inversely proportional to the Q of the line, and the indication of the detector is therefore a function of the conductivity of the electrolyte.

Grube and Speidel[8] suggested a method for measuring the properties of electrolytes at high frequencies, in which the electrolyte is placed between the plates of a condenser,in a thin-walled glass cell. The impedance of the condenser is a function of the conductivity and dielectric constant of the electrolyte.

The electrodeless methods just described were either methods for measuring high-conductivity materials (metals) at audio frequencies or low-conductivity materials (electrolytes) at high frequencies. None of these methods is sufficiently sensitive to measure electrolytes at audio frequencies. Some of them have the disadvantage that they are critical as to the exact position, volume, and shape of the sample used. This is true of the Burton-Pitt, Powers-Dull, and Zahn-Rieckhoff methods. Another disadvantage of some of the methods is the fact that the reading of the indicating instrument is not inherently zero for zero conductivity, the conductivity being determined by taking small differences between two large quantities, or what is practically the same thing, by reducing the reading

at zero conductivity to zero by means of a bucking current.

Piccard and Frivold[18] described a method which will measure electrolytic conductivity at low frequencies. This method was conceived of independently by the writer and is the one on which he intends to base his thesis; it was only after many hours of painstaking library research that the writer found that this was proposed some twenty years earlier by the abovementioned scientists. The Piccard-Frivold method was published by virtue of the fact that the Swiss "Archives des Sciences Physiques et Naturelles" presented a report of the April 24, 1920 meeting of the Swiss Physical Society, before which Piccard and Frivold gave an account of some experiments carried out at the Federal Polytechnical School of Switzerland. Because this paper bears directly on the writer's research, an unabridged idiomatic translation from the French is given here:

"Demonstration of Induced Currents Produced without Electrodes in an Electrolyte"

"The following experiment has the double purpose of showing that induced currents are produced in electrolytes exactly as in metallic conductors, and to show that it is possible to measure the resistance of these solutions without electrodes, hence without polarization.

Take a toroid made of iron wire. Put on it a winding, called the primary, of several turns of insulated copper wire through which flows an alternating current. Place against the toroid a second toroid supplied with a winding, called the secondary, of a great number of turns connected in series with a telephone receiver or a string galvanometer. If the primary

toroid is very symmetrical, the telephone receiver or the galvanometer will not indicate any current. Now place a winding common to the two toroids, consisting of a single turn of a column of a liquid conductor. This circuit forms a transformer with the first toroid, of which it acts as the secondary winding; with the second toroid it forms a new transformer, of which it acts as the primary circuit. At the moment when the liquid column is closed, the telephone receiver or the galvanometer indicates the alternating current produced by double induction in the secondary winding of the second toroid.

"Now place a copper wire so as to make one turn around the primary toroid and one turn around the secondary toroid, but in so doing making the second turn in the opposite direction to the first (the wire then forms a figure 8), and put in this circuit an adjustable non-indictive resistance. This wire produces in the second toroid an effect opposite that of the liquid column. The two effects are equal and cancel each other if the two circuits have the same resistance. It is thus easy to determine the resistance of the liquid column by varying the adjustable resistor until the sound disappears in the telephone receiver or the galvanometer string ceases to vibrate.

"It should be noted that the experiment succeeds easily if the liquid column has a large cross-section. This can be accomplished by means of an inverted U tube dipping in a receiver. The top of the tube is equipped with a small suction tube through which it can be filled. The best method, however, is to paraffin the two adjacent toroids so that they can be immersed completely in the liquid.

"These experiments were carried out at the physics laboratory of the Federal Polytechnical School."

The writer searched through "Science Abstracts" covering the interval from 1920 to the present time for further articles by Piccard or Frivold on this subject, but could find none. Likewise, a search of the Swiss patents for a patent of this device by either Piccard or Frivold was fruitless. It therefore appears that they either discontinued or did not publish further work on this device. In a thorough search of "Science Abstracts", no paper written by any other scientist on a similar device could be found.

iii. History of Writer's Interest in Problem. In his work at the Naval Ordnance Laboratory, the writer found that if two coplanar coils are immersed in a conducting medium, their mutual impedance depends on the conductivity of the medium, as well as on their relative orientation, leading him to believe that an electrodeless method for measuring conductivity of liquids could be based on this phenomenon, which is due to currents induced in the medium.

In order to make the mutual impedance of the coils depend only on the conductivity of the medium, it was necessary to eliminate the direct mutual inductance between them. To do this, the writer decided to use a toroid as the driver coil, since ideally it has no external field. To reduce further the mutual inductance (due to leakage flux from the driver coil) and also to eliminate the effects of stray fields from other sources, a toroidal pickup coil was also used. Mechanically, the obvious arrangement was to place the toroids together coaxially, which also results in maximum sensitivity, since all the current in the electrolyte linking one

toroid also links the other.

II. THEORY

i. Simple Theory of the Device. The basis of the method to be used in measuring conductivity is shown in Plate 1. Two toroidal coils are placed one against the other coaxially in an insulating toroidal casing and are immersed in the electrolyte, as shown in Plate 1, which is a sectional view of the toroids, the section being taken through their common horizontal axis, in a vertical plane. A source of alternating voltage, such as an oscillator, is connected to one of the toroidal coils, called the driver coil, or toroid, and a vacuum tube voltmeter is connected to the other, called the pickup coil, or toroid.

An alternating magnetic flux is set up in the core of the driver toroid. We know that around any closed path enclosing this core,

$$\oint \vec{E} \cdot d\vec{s} = - \frac{d}{dt} \int_S \vec{B} \cdot \vec{n}\, dS \qquad (1)$$

where $\vec{E}$ is the electric field intensity, $d\vec{s}$ is an element of the path of integration s, $\vec{B}$ is the alternating magnetic flux density in the core, dS is an element of the surface S over which the integral of $\vec{B}$ is taken, and $\vec{n}$ is a positive unit normal to dS.

The electrolyte is a closed path linking the driver toroid, and since it has a non-vanishing conductivity, current will flow in it and through the hole in the toroidal casing. Thus, the electrolyte acts as the secondary of a transformer, of which the driver coil is the primary.

The current flowing in the electrolyte links the pickup toroid core, setting up an alternating flux therein, which in turn induces a voltage in the pickup coil. The electrolyte therefore acts as the primary of a transformer of which the pickup coil is the secondary.

The integral $\oint \vec{E} \cdot d\vec{s}$ is independent of the path of integration, provided the path completely encloses the core of the driver toroid. Since the integral around any flowline is equal to $\oint \vec{E} \cdot d\vec{s}$ there is a voltage

$$V = - \frac{d}{dt} \int_S \vec{B} \cdot \vec{n} \, dS \qquad (2)$$

tending to send current around any flow line. Then the arrangements of Plate 2(a) and Plate 2(b) are equivalent, since they have the same boundary conditions, namely:

a. The surface of the toroid envelope is a flow surface.

b. Its bisector plane normal to its axis is an equipotential surface.

c. The alternating flux density $\vec{B}$ in the core in Plate 2(a) can be replaced by a generator of voltage

$$V = - \frac{d}{dt} \int_{S'} \vec{B} \cdot \vec{n} \, dS' \qquad (3)$$

which is shown in Plate 2(b).

Then the current I that flows in the electrolyte is the same in both cases, provided the insulating sheet between the surfaces A and B in Plate 2 is of infinitesimal thickness and that surfaces A and B in Plate 2(b) are the same surfaces as A and B in Plate 2(a). The current can be determined by dividing V by the resistance of the electrolyte between the surfaces A and B in Plate 2(b).

ii. Basic Equivalent Circuit. The electrolyte can therefore be replaced by a loop of resistance $R_e = \frac{V}{I}$, the resistance between A and B in Plate 2(b), so that the equivalent circuit, Plate 3(a), may be drawn. All the parameters except R_e are either predetermined or are easily calculated; the calculation of R_e, on the other hand, is in general quite difficult. Means of determining Re will be discussed later. The equivalent circuit is exact, save for the omission of leakage inductance in series

with $n_1^2 R_e$ and capacitance in parallel with $n_1^2 R_e$. The effects of these are usually negligible and will be discussed in a later section.

The detailed development of the circuit theory of the equivalent circuit is carried out fairly completely in Appendix A. In the text, only the more important results, and the ideas on which Appendix A is based, are discussed.

iii. Voltage and Impedance Relationships in the Equivalent Circuits.

In Appendix A the ratio e_p/e_d in this equivalent circuit when the driver and pickup circuits are tuned to the frequency of e_d is shown to be

$$\frac{e_p}{e_d} = \frac{n_2}{n_1}\left[\frac{1}{1+\frac{R_e n_2^2}{Q_p \omega L_p}}\right] \qquad (3)\quad (4A)^*$$

where Q_p is the quality factor of the pickup circuit, i.e. $Q_p = \frac{\omega L_p}{R_p + R_p'}$. When $\frac{R_e n_2^2}{Q_p \omega L_p} > 100$ and $\frac{e_p}{e_d} < \frac{n_2}{100 n_1}$, we can write

$$\frac{e_p}{e_d} \approx \frac{Q_p \omega L_p}{n_1 n_2 R_e} \qquad (4)\quad (5A)$$

with an error of less than one percent.

(4) indicates the basis for a direct-reading conductivity meter; we see that if e_d is held constant, e_p is directly proportional to $G_e = \frac{1}{R_e}$, the conductance of the path linking the toroids. However, a direct-reading arrangement with an untuned pickup circuit is superior because of advantages which will be discussed elsewhere.

---

* The notation for numbering equations is as follows: In the text, the number in the first parentheses indicates the numerical order in the text, while the number and letter in the second parentheses indicate the numerical order in a particular appendix designated by the letter. If only one equation designation is shown, the equation appears only in the text.

It is shown in Appendix A that when the pickup circuit is untuned, we have

$$\left|\frac{e_p}{e_d}\right| = \frac{n_2}{n_1}\left[\frac{1}{1+\left(\frac{R_e n_2^2}{\omega L_p}\right)^2}\right]^{\frac{1}{2}} \qquad (5)\ (19A)$$

Here, when $\frac{R_e n_2^2}{\omega L_p} > 7.07$ and $\frac{e_p}{e_d} < \frac{n_2}{7.07 n_1}$,

$$\frac{e_p}{e_d} \approx \frac{\omega L_p}{n_1 n_2 R_e} \qquad (6)\ (20A)$$

with less than one percent error. We see in (6) the basis for a direct-reading conductivity meter.

In the direct-reading method with tuned pickup circuit, the impedance looking into the input end is shown in Appendix A to be modified by the conducting path according to

$$\frac{Z_d'}{Z_d} = \frac{n_1^2 R_e + \frac{n_1^2}{n_2^2} Q_p \omega L_p}{Q_d \omega L_d + \frac{n_1^2}{n_2^2} Q_p \omega L_p + n_1^2 R_e} \qquad (7)\ (9A),$$

where Z_d is the input impedance when R_e is infinite, and is given by $Z_d = Q_d \omega L_d$. The output impedance is similarly modified to

$$\frac{Z_p'}{Z_p} = \frac{n_2^2 R_e}{n_2^2 R_e + Q_p \omega L_p} \qquad (8)\ (12A),$$

where $Z_p = Q_p \omega L_p$.

For the untuned pickup circuit, the corresponding expressions are

$$\frac{Z_d'}{Z_d} = \frac{n_1^2 R_e + j\omega L_p \frac{n_1^2}{n_2^2}}{Q_d \omega L_d + n_1^2 R_e + j\omega L_p \frac{n_1^2}{n_2^2}} \qquad (9)\ (21A)$$

and

$$\frac{Z_p'}{Z_p} = \frac{n_2^2 R_e}{n_2^2 R_e + j\omega L_p} \qquad (10)\ (22A).$$

In certain special cases, especially when the driver and pickup coils are of low Q, it may be necessary to use equation (17A) for the untuned pickup arrangement, rather than (19A) or (20A).

L_p in (19A) and (20A) is the low-frequency inductance of the pickup coil, i.e. it is the inductance at a frequency lower than and sufficiently remote from self-resonance that the effect of self-capacitance and incidental circuit capacitance is negligible. In practice, however,

these capacitances are not negligible and cause an apparent increase in the inductance of the pickup toroid. Usually when the pickup toroid is untuned, it is terminated in a resistive load which is used as a voltage divider.

The ratio e_p/e_d given by (6), as modified by the abovementioned capacitances and resistive load is shown in Appendix A to become

$$\left|\frac{e_p}{e_d}\right| = \frac{\omega L_p' R_L}{Re\, n_1 n_2}\left[\frac{1}{(R_L)^2 + (\omega L_p')^2}\right]^{\frac{1}{2}} \qquad (11)\ (30A)$$

where L_p' is the apparent inductance of the pickup toroid measured in the presence of the self-capacitance and incidental capacitance at frequency $f = \frac{\omega}{2\pi}$ and R_L is the value of the resistive load. In general, the effect is to increase the pickup voltage in the ratio

$$\left|\frac{e_p'}{e_p}\right| = \frac{R_L L_p'}{L_p}\left[\frac{1}{(R_L)^2 + (\omega L_p')^2}\right]^{\frac{1}{2}} \qquad (12)\ (29A).$$

In the Piccard-Frivold null method for measuring conductivity, a single loop is wound around the toroids in such a way that in relation to the electrolytic loop, it is wound in the same sense on one toroid and in opposite sense on the other, i.e. in the form of a figure '8', as shown in Plate 4(a). Then a resistance in the figure-8 loop will cause a voltage to be induced 180 degrees out of phase with the voltage resulting from a resistance inserted in the electrolytic loop. If the mutual inductance between one loop and the driver toroid is equal to that between the other loop and the driver toroid, and if the same is true of the mutual inductances with the pickup toroid, then the voltage at the output of the pickup circuit will go through a null when the resistances in the two loops are equal (neglecting the effects of leakage inductance and displacement currents, which will be discussed in a later section). Since greater sensitivity is required in a null circuit, the tuned pickup arrangement was used in the Piccard-Frivold null method. The most important relationships

are those which occur at balance. It is shown in Appendix A that the input impedance of the toroid system at balance in the Piccard-Frivold null method is

$$\frac{Z_d'}{Z_d} = \frac{\frac{n_1^2 R_e}{2}}{\frac{n_1^2 R_e}{2} + Q_d \omega L_d} \qquad (13)\ (32A)$$

and that the output impedance (assuming a generator of zero internal impedance) is

$$\frac{Z_p'}{Z_p} = \frac{\frac{n_2^2 R_e}{2}}{\frac{n_2^2 R_e}{2} + Q_p \omega L_p} \qquad (14)\ (33A).$$

If $n_1^2 R_e \gg Q_p \omega L_p$ the sensitivity at balance is

$$\frac{\Delta e_p}{\frac{\Delta R_e}{R_e}} = - \frac{Q_p \omega L_p e_d}{n_1 n_2 R_e} \qquad (15)\ (36A).$$

These expressions are based on the assumption that the mutual inductances between a toroid and either loop are equal, a valid assumption for perfect toroids, since all the magnetic flux set up by either toroid is mutual flux with any closed circuit linking the toroid. Because of the identity of mutual inductances, the figure-8 loop is represented in the equivalent circuit of the Piccard-Frivold null method by an ideal phase-inverting transformer of unity ratio, in cascade with the balancing resistor, as shown in **Fig.** 5A*.

iv. Displacement Currents in the Loop. The equivalent circuit of Plate 3(a), as well as the equivalent circuits drawn elsewhere in this report, neglects two factors. The first of these is the effect of displacement currents. If the boundary conditions on the displacement current were the same as those on the conduction currents, they would be divided into two parts, those in the toroid casing and those in the electrolyte. Those in the casing would be constant and their effect would be balanced out by a suitable bucking voltage applied to the pickup circuit; those in

---

* The convention for numbering figures in the appendices is identical with that for numbering equations.

the electrolyte would depend on the dielectric constant of the electrolyte and could be evaluated. Since most electrolytes are aqueous solutions, and since the dielectric constant of water at low frequencies is of the order of 80, in most cases the displacement currents in the electrolytes would be much greater than those in the casing. In Appendix A it is shown that displacement currents in the electrolyte introduce a reactive component in the impedance of the loop, such that it becomes

$$Z_e = \frac{R_e \left[\tan^{-1}(8.842\times10^{-14}K\rho)\right]}{\left[(8.842\times10^{-14}K\rho)^2 + 1\right]^{\frac{1}{2}}} \qquad (16)\ (41A).$$

We see that the magnitudes of Z_e and R_e would begin to differ appreciably only for large values of K and ρ.

We can expect that the presence of conductors within the toroid casing will alter the configuration of displacement currents from the above-mentioned ideal situation. Unquestionably such conductors will cause large displacement currents to cross the insulation in the casing and pass into the electrolyte, but it is difficult to evaluate their effect quantitatively.

In the Piccard-Frivold null method, the effect of displacement currents is to require a shunt capacitance balance in addition to the resistive balance.

v. Leakage Inductance in the Loop. The second factor not included in the equivalent circuit is the leakage inductance of the loop containing R_e. The total inductance of this loop may be divided into three components. The first component is due to the mutual flux between the loop and the driver toroid plus the mutual flux between the loop and the pickup toroid, and is represented in the equivalent circuit by the two mutual inductances. The second component is due to flux in the toroid casing (exclusive of the mutual flux) and is part of the leakage inductance. The remainder of the

leakage inductance is the internal inductance of the electrolytic path.

The effect of leakage inductance is to change (3) to

$$\frac{e_p}{e_d} = \frac{n_2}{n_1}\left[\frac{1}{1+\frac{n_2^2}{Z_p}(R_e+j\omega L_e)}\right] \qquad (17)\ (44A)$$

and to change (5) to

$$\left|\frac{e_p}{e_d}\right| = \frac{n_2}{n_1}\left[\frac{1}{\left(\frac{R_e n_2^2}{\omega L_p}\right)^2+\left(\frac{L_p+n_2^2 L_e}{L_p}\right)^2}\right]^{\frac{1}{2}} \qquad (18)\ (45A),$$

where L_e is the total leakage inductance of the loop.

Ordinarily, the permeability of the toroid cores will be high (greater than 100) and the leakage inductance will be only a small fraction of the total inductance. Only when low-permeability cores are used, and the conductivity of the electrolyte is such that ωL_e is of the same order of magnitude as R_e, will leakage inductance have an appreciable effect.

In the Piccard-Frivold null method, the effect of leakage inductance is to impose the balance condition $L_e = L_e'$. If the effect of displacement currents is present, the displacement current and leakage inductance balance may be effected by one control, since they are both reactive. However, this balance would be a function of R_e. By using a separate series inductance balance and a separate shunt capacitance balance, independence of the reactive balances from R_e may be obtained.

vi. Considerations on R_e and Inductance Analogue. It is desirable to predict from theoretical considerations the value of R_e. The boundary conditions on the conduction current induced in an infinite homogeneous isotropic conducting medium, when an insulated toroidal core carrying alternating magnetic flux circumferentially is inserted therein, are exactly analogous to those on the magnetic flux induced in an infinite homogeneous insulating medium, when the boundary surface of the abovementioned toroid, carrying current circumferentially, is inserted therein. Hence the resistance of

the conducting path in the former case may be determined from the reluctance of the conducting path in the latter, and since the reluctance of a path linking a conductor, and the inductance of the conductor, are related, the resistance of the path in the former case may be determined from the inductance of the conductor in the latter.

It is shown in Appendix B that this relationship is

$$R_e = \frac{4\pi\mu\rho}{10^9 L} \qquad (19)\ (10B),$$

where R_e is the resistance of the conducting path in ohms, μ is the permeability of the medium in which the conductor of external (high-frequency) inductance L henries is located, and ρ is the resistivity in ohm-cm of the conducting path. Therefore, if we wish to determine the resistance of a conducting path linking an insulated toroidal casing, we can calculate it from the high-frequency inductance of a conductor having the same dimensions as the casing.

Of course, the calculation of L from fundamental considerations is the same problem as calculating R_e, and it appears to be extremely difficult in most cases. An approximate solution exists for the case of a toroidal conductor of circular cross-section, whose circumferential inductance is [28]

$$L = 0.01257a\left\{2.303\log_{10}\frac{16a}{d} - 2\right\} \qquad (20)$$

in air, with good accuracy when $\frac{d}{2a} < 0.2$, at frequencies at which the current flows only on the surface of the toroid. L is the inductance in microhenries, a is the mean radius of the toroid, and d is the diameter of the cross section, both in cm. Then

$$R_e = \frac{4\pi\rho}{0.01257a\left\{2.303\log_{10}\frac{16a}{d} - 2\right\}} \qquad (21)$$

where ρ is in ohm cm.

If a toroidal casing of circular cross-section were used, therefore, the electrodeless method for measuring electrolytic conductivity would be an absolute method. For practical reasons, in this research a rectangular cross-section was used instead, and since no accurate formulae are available for the high-frequency inductance of a toroidal conductor of rectangular cross-section, absolute measurement of resistivity was not possible.

R_e/ρ can be calculated from experimentally determined values of L where L cannot be calculated. It can also be measured directly by placing electrodes in the casing, as shown in Plate 2(b), measuring the resistance between these electrodes in a solution of known conductivity, and correcting for the thickness of the insulation between the plates. Finally, R_e/ρ may be determined by means of the electrodeless method, by determining R_e in a solution of known conductivity.

III. MODES OF USE AND DESIGN CONSIDERATIONS

i. Introduction. There are two basic ways in which the toroid assembly may be used to measure resistance in a loop linking it. They are:

a. Direct-reading methods.

b. Null methods.

In general, an optimum design for one of these modes of operation is not necessarily an optimum design for the other. A discussion of the design requirements for the two modes is given below. Requirements common to the two methods are:

a. The indication of the instrument should always be the same for a given resistance in the loop linking the toroid assembly.

b. The indication should be a linear function of the loop resistance. *or conductance.*

c. A wide range of resistance values should be measurable.

There is one important source of error in both the direct-reading and null methods, namely, direct coupling between the driver and pickup toroids, which must be corrected if requirements a, b, and c are to be met. In Appendix A and in the text up to this point, it was assumed that if R_e were infinite, there would be no voltage induced in the pickup coil. Actually, this is not the case. Even if the toroids were perfectly astatic, there is electrostatic coupling between them. To eliminate this coupling, the driver toroid and its circuit must be thoroughly shielded electrostatically from the pickup toroid and its circuit. Furthermore, the toroids are in fact never perfectly astatic. After the conventional precaution is taken of winding the toroids so that there is no current circulation about their axes, some of the driver toroid flux still links the pickup toroid because of non-uniformity of the windings or inhomogeneity of the cores. The effect of these irregularities is to cause the driver toroid to set up a small external field as though it were a dipole oriented in a random direction normal to the toroid axis, and to cause the pickup toroid to behave as a small coil with axis in a random direction normal to the toroid axis. By rotating the axis of the dipole with respect to the axis of the coil until the two are at right angles, the coupling between them is minimized. This condition may be reached by rotating one toroid with respect to the other until the voltage induced in the pickup coil goes through a minimum. It is possible that this residual voltage may be further reduced by a large factor, by placing a high-permeability ring between the

two toroids.

This minimum residual voltage may still be of sufficient magnitude to cause errors in both the direct-reading and null methods when high resistances are being measured. To remove this voltage, a balancing circuit may be used, in which two small variable voltages spaced 90° apart in phase, derived from the generator of frequency $f = \frac{\omega}{2\pi}$, are injected into the pickup circuit and adjusted until they completely balance out the residual voltage.

Although large residual voltages may be balanced out in this way, it is desirable that the residual unbalance voltage be made as low as possible. Otherwise, the condition will exist where the residual voltage after balancing is the difference between two large quantities, with the poor stability which is inherent in such cases.

After all precautions are taken to reduce the pickup voltage to zero when R_e is infinite, there will still be a residual voltage consisting of harmonics of f . This voltage causes an error in readings in the direct-reading method, and obscures the null in the null method. Its effect is greatly reduced by adequate filtering in the amplifier of the pickup voltage, and by the pickup circuit if tuned.

ii. Direct-Reading Method. Requirements a, b, and c above determine whether a tuned or untuned pickup circuit is to be used in the direct-reading method. Referring to (4), one sees that where the pickup circuit is tuned, the pickup voltage is directly proportional to the parallel-resonant impedance of the pickup circuit, at resonance. This impedance is given by

$$Q_p \omega L_p = \frac{\omega^2 L_p^2}{R_p + R_p'} \quad .$$

R_p, representing the "copper" loss in the pickup coil, is a function of temperature, varying at the rate of approximately 0.4 percent per degree C

for copper. R_p', representing the core loss, is made up chiefly of two components, namely, R_h representing hysteresis and R_e representing eddy-current loss. The latter has a temperature coefficient of the same order of magnitude as that of R_p. No figures for the temperature coefficient of R_h are on hand, but even if it should be zero, we already have appreciable deviations from requirement a as a function of temperature. R_h is a function of the voltage across the pickup coil. Therefore, under certain conditions variation of the pickup voltage may cause deviation from requirement a.

In (6), one sees that where the pickup circuit is untuned, the calibration has no dependence whatever on R_p or R_p'.

(4) assumes that the condition of resonance obtains in the pickup circuit. If resonance does not obtain, $Q_p \omega L_p$ is replaced by the actual impedance of the pickup circuit. If Q_p is high, the impedance of the pickup circuit (and hence the calibration) will vary to a considerable extent for relatively small deviations of ω from the resonant frequency of the pickup circuit. For example, if Q_p is 100, a one-half percent change in frequency from resonance will cause a 30 percent decrease in sensitivity; whereas (6) shows that in the untuned pickup circuit, the corresponding change in sensitivity is one-half percent.

It was shown that the condition for (3) to reduce to (4) was $\frac{Re\, n_2^2}{Q_p \omega L_p} \rangle 100$, while that for (5) to reduce to (6) was $\frac{Re\, n_2^2}{\omega L_p} \rangle 7.07$. If $Q_p = 100$, $\frac{Re\, n_2^2}{\omega L_p} \rangle 10000$ is required in the former case and $\frac{Re\, n_2^2}{\omega L_p} \rangle 7.07$ in the latter. Thus, the untuned arrangement in this case will measure resistance on a linear scale to 1/1410 the value that the tuned arrangement will measure.

Although for a given pickup coil the tuned arrangement will develop

Q_p times the voltage of the untuned arrangement, the higher stability and wider linear range are more important considerations. Consequently, the untuned pickup arrangement was selected for the direct-reading method in this research.

Referring now to the untuned pickup arrangement, the other conditions necessary to meet requirement a must be determined.

In the first place, it should be possible to adjust e_d to some predetermined value, at which it should remain thereafter within close limits (an important consideration in the design of the associated electronic circuits). Furthermore, the instrument which measures e_d should have a stable calibration.

L_p and R_e/ρ are functions of temperature, but in general the variations are negligible over the usual temperature range. For example, if the coils are wound on molybdenum-permalloy dust cores, the temperature coefficient of inductance will be about 0.02 percent per degree C. R_e/ρ will vary with temperature directly as the linear dimension because of variation in the outer dimensions of the toroid assembly. For a thermal expansion coefficient of 100×10^6 per degree C, we have a 0.001 percent per degree C change.

To recapitulate, for the direct-reading conductivity meter, the untuned pickup circuit should be used, and e_d, ω, and the calibration of the instrument measuring e_p, should all be held constant within limits of an order of magnitude better than the required overall accuracy. Changes in L_p and R_e/ρ will usually be negligible, and n_1 and n_2 are of course constant.

For a solution of given resistivity, the voltage e_p should be as large as possible, in order that a reasonable gain be required of the

amplifier driving the indicating instrument. e_p may be increased by several expedients, which are enumerated below and critically discussed.

a. Increasing e_d. This increases the power requirements on the generator of frequency $\frac{\omega}{2\pi}$ and increases the power dissipated in the toroid assembly.

b. Decreasing n_1. This results in lower input impedance and consequent increase in the power demand on the source of frequency $\frac{\omega}{2\pi}$ and in the power dissipated in the toroid assembly. Hence, the effect is the same as that of increasing e_d.

c. Increasing ω. This decreases the highest resistivity that can be measured before the effect of displacement currents becomes appreciable. Furthermore, ω should not be increased above a value at which resonance effects begin to appear. As a general rule, conditions should be such that the increase in inductance of the pickup coil due to incipient resonance should not exceed 10 percent of the low frequency inductance.

d. Increasing L_p. If this is done by increasing the permeability of the core, stability becomes poorer as the permeability is increased. For example, excellent stability is obtained with molybdenum-permalloy dust cores having a permeability of ~125, because of the large demagnetizing factor resulting from the interstitial air gaps. If permalloy strip having a permeability of 20,000 is used, the permeability is sensitive to mechanical shock and temperature, and does not reproduce closely from core to core. Of course, there are core materials of intermediate permeability which might be used. If L_p is

increased by increasing n_2, an improvement is obtained which is directly proportional to n_2. If the dimensions of the core are all increased in the same proportion, the sensitivity will increase because of the resultant increase in the ratio L_p/n_2 (see (1e)). Note that if L_p is made sufficiently large, resonance effects will appear and L_p should not be so large that $\frac{L_p' - L_p}{L_p} > 0.1$.

e. Increasing n_2. This was discussed under L_p.

f. Decreasing R_e for a given value of ρ. This may be done by increasing all the dimensions of the toroid assembly in the same proportion (see (21)). This will require increase in the dimensions of the cores, and will in general result in increased inductance and Q, and an additional increase in sensitivity. However, since the ratio R_e/ρ is only inversely proportional to linear dimension, startling improvements in sensitivity will be obtained only if radical changes in dimensions are made from those that are fixed largely by mechanical considerations.

It hardly seems worthwhile to go into the sensitivity problem analytically. By keeping all the requirements in mind and following the abovementioned principles to obtain high sensitivity, a satisfactory design may be arrived at. After a preliminary design is completed, the sensitivity may be calculated (using an approximate value of R_e/ρ obtained from the low-frequency inductance of the inductance analogue), and the amplification necessary to drive an indicating instrument may be determined. If this requirement is reasonable, the design is satisfactory. If not, it will be

fairly simple to make a new design (using the original design as a guide) that will have the required sensitivity.

Note that varying R_e/ρ , L_p/n_2^2, or ω varies the value of φ at which (5) reduces to (6), in such a way as to reduce the range of sensitivities for which (6) is valid, as the sensitivity is increased. However, since high sensitivities are required where high resistivities are to be measured, for the measurement of low resistivities L_p/n_2^2, or ω may be reduced sufficiently and R_e/ρ increased sufficiently to make (6) valid in that range.

iii. Null Methods. The object of null methods is to obtain greater reproducability of measurements than direct-reading methods. Whereas in direct-reading methods, reproducability might be within 2 percent; in a null method it might be 0.1 percent or better. If the same minimum conductivity is to be measured by both methods, the null method must be able to detect a voltage $\frac{\epsilon}{100}$ as great as that which the direct-reading method must detect, where ϵ is the error in reproducing the same reading for a given conductivity, in percent. Hence, null methods must have higher overall sensitivity than direct-reading methods, to cover the same conductivity range at full accuracy. Some of this increased sensitivity may be obtained by using a tuned pickup circuit and by applying some of the principles discussed under the direct-reading method. The remainder must be obtained by increasing the gain of the amplifier.

Referring to (15), one sees that the sensitivity of the Piccard-Frivold method in the vicinity of balance, expressed as the change in voltage for a given percent change in R_e, is inversely proportional to R_e. Thus, the lower the maximum value of R_e that is to be measured, the lower the sensitivity may be.

In the Piccard-Frivold null method, the conditions of balance are $R_e = R_e'$, $L_e = L_e'$, and $C_e = C_e'$, where L_e and L_e' are the leakage inductances in the R_e and R_e' loops, respectively, and C_e and C_e' are the shunt capacitances across R_e and R_e', respectively. It was shown in Appendix A that the balance was independent of any other factors. All those factors discussed in the direct-reading method which affected the calibration have no effect on the calibration of the Piccard-Frivold null method, except for the ratio R_e/ρ where ρ rather than R_e is being measured. Hence, in the Piccard-Frivold null method, the tuned pickup arrangement may be used, high-permeability cores are permissible, e_d may vary, ω may vary, and no special pains need be taken to stabilize the gain of the amplifier driving the null indicator. Note also that whereas in the direct-reading method there is an upper limit to the value of $G_e = \frac{1}{R_e}$ that can be read on a linear scale, in the Piccard-Frivold null method, theoretically there is no lower limit of G_e at which the abovementioned balance conditions cease to be true.

Other null methods are possible, in which a fraction of the voltage applied to the driver toroid is injected into the pickup circuit in such a way as to buck out the voltage developed therein. Such methods have the advantage over the Piccard-Frivold null method that they do not require the figure-8 loop, simplifying the construction of and connections to the toroid assembly, but they also have certain disadvantages.

One such method was incorporated into the experimental circuit for this research, but time did not permit its analysis or experimental investigation. This circuit is shown in simplified form in Plate 3(b). The voltage across the driver toroid is applied to a 90 degree phase-

shifting network, a fraction of whose output is injected into the pickup circuit 180 degrees out of phase with e_p and is adjusted until the voltmeter V indicates a null. The value of R_e may be determined from the ratio $\frac{R_1}{R_1 + R_2}$ of the voltage divider, and $G_e = \frac{1}{R_e}$ is directly proportional to this ratio. A more detailed description of the circuit used in this method is given under IV, "Description of Apparatus".

This, as well as other null methods, are discussed under suggestions for further work.

The thickness, t, of the toroid winding is also a design parameter of importance in both direct-reading and null methods. For a given set of cores, increasing t will allow the use of more copper and will result in higher Q. On the other hand, increasing t decreases the cross-section area and increases the length of the electrolytic path, increasing the ratio R_e/ρ and decreasing the sensitivity. The Q of the coils should therefore be no higher than is necessary to meet the requirements of frequency stability, oscillator power, and in the case of methods using the tuned pickup circuit, sensitivity. There is little value in increasing the amount of copper on the toroids much beyond the point where the copper losses become less than the core losses, since beyond that point an improvement of only a factor of two in Q is obtained, even if copper losses are reduced to zero.

IV DESCRIPTION OF APPARATUS

1. Toroid assembly. The toroids are wound on Western Electric molybdenum-permalloy dust cores no. 475866. Design data on these cores is given in Appendix C. Molybdenum-permally dust cores are used because of their high magnetic stability, and the no. 475866 core in

particular was used because among the cores available, it had the largest dimensions (making possible a large toroid casing and hence a large value of ρ/R_e) together with one of the lowest values of K (large L/n^2), making for high sensitivity.

Somewhat arbitrarily, it was decided that the resonant impedance of the driver and pickup tuned circuits should be 1 megohm. A high value was selected so that the power dissipated in the toroid would be kept in the order of several milliwatts, minimizing the heat generated in the toroid assembly and the power demand on the oscillator. An operating frequency of 10000 cps was selected. It was made as high as possible , since fewer turns of wire are required on the toroid to obtain a given impedance level as the frequency is increased, and since it was considered desirable to operate at as remote a frequency from 60 cps as possible. The upper frequency limit is determined by the losses in the toroid cores; in the no. 475866 cores the losses increase rapidly above 10000 cps. Another factor determining the upper frequency limit is the permissable error due to displacement current. The maximum resistivity that can be measured, such that the displacement current error not exceed 1 percent, was calculated at 10000 cps for water, by (16), to be 3.2×10^5 ohm-cm, which is sufficiently high to permit satisfactory operation at this frequency.

A voltage e_d of 30 volts rms was selected; it was not made larger because of oscillator design considerations which will be discussed later.

A winding thickness t of 0.1 inch was selected, being large enough to yield high-Q toroids, yet small enough to not increase the length and decrease the cross-section area of the conducting path.

The abovementioned design values were chosen before a complete

picture of the design considerations had been developed, and do not neccesarily represent an optimum design.

In Appendix C it is calculated that in order to have a parallel resonant impedance of 1 megohm at 10000 cps when the voltage applied to the coil is zero, the no. 475866 cores should be wound with 722 turns of no. 25 B & S ga. copper wire with heavy Formex insulation. With 45 volts across the coil, it was calculated that the number of turns chould be 737. These figures are based on a winding thickness t of 0.1 inch.

The coils are wound in two equal sections, and the leads are connected so that there is no net circulation about the axis of the core. The coils are wound as uniformly as possible.

Four toroids were wound, two for the no. 1 toroid assembly, which was not satisfactory and later became defective, and two for the no. 2 toroid assembly, which was almost identical in design with the former but was assembled with greater care and was satisfactory. All four toroids were wound with no. 25 B & S ga. heavy Formex insulated copper wire.

The data on the toroids is as follows:

No. 1 toroid assembly:

n_1= 737 turns, $L_d' \doteq$ 83.7 mh. at 30 v. rms and 10000 cps.

n_2= 722 turns, $L_p' \doteq$ 83.0 mh. at 30 v. rms and 10000 cps.

No. 2 toroid assembly:

n_1= 737 turns, L_d' = 86.3 mh. at 30 v. rms and 10000 cps.

n_2= 737 turns, L_p' = 89.6 mh. at 30 v. rms and 10000 cps.

The inductance measurements were made by a resonant method, with the toroids in the toroid casing and connected to the measuring circuit through the toroid-assembly cables.

With one of the toroids uncased and connected through short leads to the inductance-measuring circuit, its inductance measured at 30 volts rms and 10000 cps was 80.7 mh. with a Q of 143, giving a parallel resonant impedance of 725000 ohms, compared with the assumed value of 1 megohm. The discrepancy is probably partially due to proximity losses in the winding, which were not considered in the calculations, and partially because the measured Q included the losses in the mica-dielectric tuning condenser. The value of parallel resonant impedance is not critical, and is effective only in determining the power dissipated in the driver toroid and the sensitivity of the Piccard-Frivold null method and other null methods where a tuned circuit is used.

External dimensions of the toroid casing were the same for the no. 1 and no. 2 toroid assemblies, but the internal dimensions were somewhat larger in the latter. Plate 7 and Plate 8 show the dimensions of the parts of the toroid casing, for the no. 2 toroid assembly. Leads enter the casing through hollow plastic tubing which is fitted into the holes seen at the top of the casing in Plate 7.

The end caps in Plate 8 fit into the ends of the casing in Plate 7. Polystyrene is used because of its negligible water absorption and the ease with which two pieces may be cemented together. Plate 9 and Plate 10 show views of the toroid assembly. Plate 4(b) is a section through the axis of the assembly, and is complete with the exception that the figure-8 loop is not shown.

Each toroid is individually and completely shielded electrostatically by 3 mil brass shim stock cut to fit snugly against and cemented to the inside walls of the toroid casing. The shields are shown in the sectional view, Plate 4(b). Each shield is split so that it does

not act as a short-circuited turn.

Leads are brought into the toroid casing through 0.125 inch o.d. polyethylene-insulated coaxial tubing, running the length of the polystyrene tubing. The coaxial tubing is in turn connected through RG-58/U cable to the electronic circuits. At the lower left corner of Plate 5, which shows the complete circuit of the conductivity-measuring apparatus developed in this research, the toroid assembly is shown schematically with all electrical connections.

In the no. 1 toroid assembly, the toroids were placed in their receptacles without any attempt to minimize the coupling between them and without securing them to prevent relative motion, and the end caps were cemented in place, on the assumption that the coupling between the toroids would be negligible. This was hardly the case and with e_d= 30 volts, the voltage in the pickup circuit was 4 millivolts, an excessive value since the intention was to measure voltages as low as 2 microvolts. A balancing circuit was therefore introduced, which made possible the balancing of e_p down to much less than 2 microvolts. An extremely unstable balance was obtained, because in balancing, the difference is taken between two large quantities, of which one, the initial unbalance voltage in the pickup circuit, varied since the toroids were not fixed in place in the casing. If toroid assembly no. 1 were moved about vigorously, the unbalance voltage would change by as much as 100 microvolts.

Toroid assembly no. 2 was built to replace no. 1 which became defective because of water leakage and rough handling. In the new assembly, one of the toroids was wedged firmly in the casing by means of small wooden

wedges; the other toroid was then placed in the casing and rotated until the initial unbalance voltage reached a minimum, whereupon the toroid was wedged in place and the end caps were cemented on. The initial unbalance so minimized was 50 microvolts, a factor of 80 less than in the toroid assembly no. 1. When this voltage was balanced out by means of the balancing circuit, only very rough handling of the probe would cause the unbalance voltage to change as much as 2 microvolts. Such high stability was a result of the low initial unbalance voltage and the improved mechanical stability of the system.

The parts of the toroid assembly were joined by means of polystyrene cement, and the cemented parts were clamped together until the cement hardened. Strains set up by the clamps caused crazing of the polystyrene; repeated dipping of the toroid assembly in a polystyrene solvent dissolved a surface layer of polystyrene sufficiently to cause it to flow into the cracks, making the unit watertight.

ii. Electronic circuits. The complete electronic circuit is shown in Plate 5, and a complete list of components appears in Plate 6.

In the upper left corner of Plate 5 is the power unit, a conventional one which supplies the a-c heater voltage and the 300 volt d-c stabilized voltage for the plate supply of the amplifier and oscillator.

Slightly higher and to the right of the power supply is the balancing circuit, which derives from the driver circuit two voltages 90° apart in phase and injects them in series with the pickup coil to balance out any voltage due to direct coupling between the driver and pickup circuits. Each voltage may be adjusted by either a coarse or a fine control.

Below the balancing circuit is the amplifier which amplifies the resultant voltage in the pickup circuit. It is a three-stage amplifier, with first and second pentode stages V_6 and V_7 and an output cathode-follower V_8. The amplifier has about 27 db. of negative feedback from the cathode circuit of the cathode-follower to the cathode of the first pentode, for stabilizing the gain.

A 10000 cps tuned circuit from plate of the second pentode to ground causes the high and low cutoff frequencies of the amplifier to be closer to 10000 cps than they would be with R-C coupling alone, while maintaining a flat-topped frequency response in the vicinity of 10000 cps, an important feature in the direct-reading method where changes in the oscillator frequency should not cause changes in the amplifier calibration.

It was found that the gain of the amplifier is not attenuated sufficiently at 60 cps and its low multiples and at low multiples of 10000 cps to give adequate filtering . Therefore a half-octave band-pass filter with a mid-band frequency of 10000 cps and a characteristic impedance of 1000 ohms is connected at the output of the amplifier. A Ballantine Model 300 vacuum-tube voltmeter is connected to the output of the filter. The frequency response of the filter is shown in Plate 14; the frequency response of the filter plus amplifier, with and without feedback, is shown in Plate 15.

The overall gain from amplifier input to filter output with feedback is adjusted to 500 at 10000 cps; without feedback it is about 20000. Since the Ballantine voltmeter will read a minimum voltage of 1 millivolt, the minimum amplifier input voltage that can be measured is 2 microvolts. With feedback, the amplifier noise is below this level.

A decade attenuator is connected in the input of the amplifier, supplying attenuations of 1, 0.1, 0.01, and 0.001. A fifth position on this switch places a tuning condenser across the pickup coil, for use in the Piccard-Frivold null method and other null methods. The input resistance of the attenuator is 25000 ohms.

Curves of filter output as a function of the input to the first grid of the amplifier at 10000 cps, with and without feedback, are shown in Plate 16.

Below the amplifier circuit in Plate 5 is the oscillator circuit, which applies a constant 30 volt rms 10000 cps voltage to the driver toroid. The circuit is essentially an L-C oscillator with the driver toroid acting as the tank coil, and with a novel arrangement for stabilizing the amplitude. The diode, V_9, is the stabilizing or limiting element, the first pentode V_{10} is a phase splitter (for supplying positive feedback without requiring a tapped driver toroid) and the second pentode V_{11} is the oscillator. The stabilizing circuit maintains e_d substantially constant, independent of wide variations in the gain of the oscillator tube or in the tank circuit impedance.

In operation, the cathode of the diode V_9 is adjusted to some positive d-c voltage smaller than the normal peak amplitude of e_d in the absence of the stabilizing circuit. During oscillation, the diode conducts whenever the driver voltage swings sufficiently positive to exceed the voltage on the cathode of the diode, and in so doing applies a negative feedgack pip to the grid of the oscillator tube, V_{11}, through R 42. If the amplitude of oscillation should increase by a given percentage, the amount of nega tive feedback increases by a much larger percentage, opposing the increase in amplitude. Decreases in amplitude are prevented

in a similar way. The oscillator stabilizes at a voltage e_d whose peak value is slightly larger that the d-c bias on the diode cathode.

Plate 18 shows the effectiveness of this arrangement. To obtain this data, the circuit was broken between C_{18} and R_{41} and an alternating voltage at 10000 cps was applied to the loose end of R_{41}. The voltage at the cathode of V_{10} was measured as a function of this input voltage, in one case with V_9 removed and R_{42} disconnected from the grid of V_{11} (upper curve in Plate 18) and in the other curve with V_9 in the circuit and R_{42} connected (lower curve). With the limiter circuit connected, the output increases roughly in proportion to the input, until it reaches a value where the diode conducts, above which the output increases only slightly for increasing input. The two curves differ below the point where the diode begins to conduct, because of the loading effect of R_{42} which was not connected when the upper curve was taken.

In this type of amplitude control, negligible distortion is introduced, since the diode draws negligible energy from the tuned circuit. Although the negative feedback pulse applied to the oscillator tube V_{11} is rich in harmonics, V_{11} acts as a tuned amplifier and amplifies the fundamental-frequency component of this pulse much more than the harmonics.

With a 45 volt positive bias on the diode cathode, and a 6.3 volt rms heater voltage throughout, the voltage at the cathode of V_{10} varied from 32 volts rms to 33 volts rms, when the plate supply voltage of the oscillator was varied from 200 to 350 volts, and the frequency changed by 0.02 percent over this same range. With the plate supply voltage held constant at 300 volts, the voltage at the cathode of V_{10} varied from 31 volts rms to 33 volts rms when the heater voltage was varied from 7 volts

rms to 5 volts rms, and the frequency changed by 0.01 percent over this same range.

The oscillator voltage is stabilized against changes in the impedance of the oscillator tank circuit, provided the impedance does not drop so low that the peak value of the voltage e_d in the absence of the limiting diode drops below the value of the diode bias, since if this condition obtains the diode never conducts.

High-conductivity solutions cause a decrease in the impedance of the driver (tank) circuit, according to (7). In order to permit direct-reading measurement of as high conductivity as possible, the voltage at which e_d stabilizes should be low. On the other hand, for high sensitivity e_d should be high. A value of 30 volts rms was selected for e_d, as a compromise between these two requirements.

To the left of the oscillator circuit in Plate 5 is null circuit B. This is the null arrangement that was shown in simplified form in Plate 3 (b). The phase splitter V_{10} is used to supply the voltage to the phase-shifting network of this null circuit. A decade attenuator receives the output of the phase-shifting network, and in turn applies its output to a General Radio type 654-A decade voltage-divider. A nulling voltage from the output of the decade voltage-divider is injected into the pickup circuit, in series with the pickup coil. In obtaining a balance by this method, it will be necessary to adjust the phase control C_{24} to take care of incidental phase shifts.

This null circuit is intended to measure resistances as high as 14000 ohms with an accuracy of 0.1 percent, and resistances as high as 140000 ohms with an accuracy of 1 percent.

Although the phase-shifting network in Plate 5, consisting of

R_{48}, C_{23}, C_{24}, R_{39} and R_{37}, looks like the conventional bridge-type R-C phase-shifter, it is a generalization of the latter. In the ordinary R-C bridge phase-shifter, of the type shown in Fig. 1,

$$\frac{e_o}{e_i} = \frac{1}{2} \angle 2\tan^{-1}\frac{n'}{n} \qquad (22)\ (15D),$$

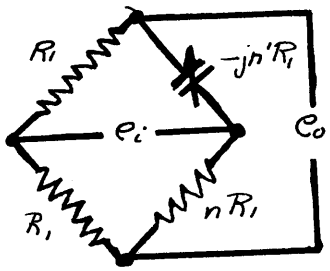

Fig. 1

provided the source of e_1 has zero internal impedance and the impedance across the output is infinite. If these requirements are not met, $|e_o/e_i|$ is not independent of the phase shift, and the phase shift is not given by the simple expression $\phi = 2\tan^{-1}n'/n$. In the use of the circuit shown in Fig. 1, the source impedance should be negligible compared with the input impedance of the bridge and the load impedance should be large compared with the output impedance of the bridge.

There are many cases where these requirements cannot be easily filled, yet where it is desirable to have a phase-shifter which behaves according to an expression similar to (22).

In Appendix D, the author determined the conditions for which the bridge-type R-C phase shifter, fed from a source with non-vanishing internal resistance and supplying a load of finite resistance, would shift the phase of the output voltage up to 180° without change in the magnitude of the output voltage, if the input voltage is maintained constant. Fig. 1D shows the circuit diagram for this phase shifter. The condition for constant output voltage is shown in Appendix D to be

$$p = \frac{2n^2}{1 + 2m - n^2} \qquad (23)\ (7D).$$

In order for p to be positive,

$$1+2m)n^2 \qquad (24) \quad (20D).$$

When (23) obtains,

$$e_o = \frac{e_i\, m(1+2m-n^2) \angle 2\tan^{-1}\frac{n}{n}}{4m[1+m+n]+(1+n)^2} \qquad (25) \quad (13D).$$

(23) and (25) were used in the design of the phase-shifting network used in null circuit B, since it is driven by a generator with non-vanishing internal impedance and drives a load of finite impedance.

The circuit in Fig. 1 is only a special case of that in Fig. 1D.

Between null circuit B and the toroid assembly in Plate 5 is null circuit A, which consists merely of the standard variable resistor and standard variable capacitor used for obtaining balance in the Piccard-Frivold null method.

The circuits of the power supply, amplifier, oscillator, and null circuit B (exclusive of the decade voltage-divider) are all on one chassis and panel assembly. A front view of this assembly appears in Plate 12 and a rear view in Plate 13. In Plate 12, the label AMPLIFIER MULTIPLIER is incorrect; it should read AMPLIFIER ATTENUATOR. The DIRECT READING- NULL switch is SW 1 in Plate 5; it is thrown in the NULL position when null circuit B is used. The control labeled QUADRATURE is the phase control in Plate 5. The two connectors lying in front of the panel connect to the external voltage divider for null circuit B.

The balancing circuit and the output filter are on separate small chassis. Cables connect the toroid assembly to the balancing circuit, which is connected to the main chassis, also by means of cables. Plate 10 is a view of the toroid assembly and the balancing circuit. The filter chassis is not shown.

iii. Measurement of electrolytic conductivity. These were made in a five-gallon

Pyrex battery jar. Instead of using standard solutions, the conductivity of the electrolyte was measured by means of a conventional conductance bridge and a dip cell. The bridge is a Leeds and Northrup type 4960 portable electrolytic resistance indicator, having a resistance range from 0.3 to 30000 ohms, with a ± 1 per cent limit of error when measuring resistance near the center of the slidewire scale. The cell is a Leeds and Northrup type 4920 dip cell. This cell is intended for use with low-conductivity solutions, and uses platinized electrodes of 3.1 sq. cm. area per electrode, spaced about 0.3 cm. apart, and has a cell constant of 0.975 $cm.^{-1}$ The electrolyte enters the glass case containing the electrodes, through flow holes.

A model of the toroid casing was made, to be used in determining the ratio R_e/ρ . This model has the same external dimensions as the toroid casing, with the exception that in the center hole are two copper disc electrodes at right angles to the axis and of the same diamter as the hole, and separated by a polystyrene wall. The outer surfaces of the discs are spaced 0.17 inch apart..Leads to the electrodes are brought in through polystyrene tubes corresponding to those in the toroid assembly.

An inductance analogue was also made. This is a toroidal aluminum conductor of the same external dimensions as the toroid casing, cut into two equal C's along a plane containing its axis, so that a sheet of dielectric material can be placed between them. The C's are held together by a wood framework having a long dielectric path.

In Plate 11, the upper object is the inductance analogue and the lower one is the model with electrodes.

V. DESCRIPTION OF EXPERIMENTS AND DISCUSSION OF RESULTS

i. Model with Electrodes. A value of R_e/ρ was determined, using the model of the toroid assembly with copper electrodes, which was described under IV, "Description of Apparatus", and shown at the bottom of Plate 11. The procedure was to immerse the model in a battery jar (whose dimensions are large compared with the toroid assembly) containing a copper sulphate solution, and to measure the resistance of the model, using the L and N bridge. Resistivity of the solution was determined with the same bridge and the L and N dip cell. After a measurement was made at a given conductivity, copper sulphate was added to the solution and measurements were made again; this procedure was repeated several times.

To get the true value of R_e/ρ, it was necessary to make an additive correction to the resistance of the model as measured, to account for the decrease in path length in the model due to the spacing between the electrodes.

The test was begun with freshly-brightened electrodes. The first point taken is indicated by the number 1 in Plate 19; the numbers indicate the order in which the measurements were made. Note that for successive measurements, the points deviate more and more from a straight line through the origin and point 1, and indicate a higher ratio of R_e/ρ. After point 5 was taken, it was noticed that the model electrodes had darkened. On the suspicion that this darkening of the electrodes was related to the deviation from linearity, the electrodes were cleaned with an abrasive and point 6 was taken, which falls on the straight line joining point 1 and the origin.

On the assumption that the ratio R_e/ρ was increased over the true value by darkening of the electrodes at points 2, 3, 4, and 5, the

straight line through points 1, 6, and the origin was taken as the true relationship of R_e vs. ρ . From the slope of this line, a value of R_e/ρ = 0.758 is obtained.

The darkening effect was studied further, and the results are shown in Plate 20. Here, the apparent increase in resistance of the model is plotted as a function of time, measurements being made in a solution of fixed resistivity and temperature. There is a rapid increase in resistance at first, and later an asymptotic approach to a limiting value. This effect cannot be attributed to some sort of polarization due to the bridge current, since the bridge current was applied for a negligible fraction of the duration of the entire test. At the beginning of the test, the model electrodes were bright and shiny; at the end they had a dark rouge hue. It appeared certain that the darkening was due to the formation of cuprous oxide. This conviction was strengthened by the observation of a photo-voltaic effect when a strong light was played on the electrodes while the model was immersed in the copper sulphate solution.

Plate 21 shows the effect of proximity to the walls of the jar on the resistance of the model with electrodes. The increase in the resistance of the model is plotted as a function of its position. As the model approaches the walls, one would expect the resistance to increase because of constriction of the conducting path. A greater increase would be expected for a broadside approach than for an edgewise approach, since in the former case the central hole becomes obstructed. The variation should obey some higher-power law, similar to the variation in inductance of a coil in proximity to a conducting sheet when the frequency is so high that there is negligible penetration. All these expectations are verified in Plate 21, where the

curve showing the larger effect is for broadside approach. Since the current flow in the electrolyte is the same for the toroid assembly as for the model, these curves apply equally well to the toroid assembly. In order to avoid this effect as much as possible, the toroid assembly or model was placed at the center of the tank where the variation of the resistance with position is negligible.

In (149), p. 129, ref. 29, the effect of a cylindrical conducting shield on the inductance of a coil symmetrically placed within it coaxially is given as

$$\frac{\text{Actual inductance}}{\text{Inductance in absence of shield}} = \left[1 - \left(\frac{r_c}{r_s}\right)\frac{2l_c}{l_s}\frac{1}{K}\right] \qquad (26)$$

where r_c and r_s are the respective radii of the coil and the shield, l_c and l_s are the respective lengths, and K is a function of the diameter-to-length ratio of the coil.

On the basis of the inductance analogue, this expression applies to the model in the battery jar. Since the axis of the tank was at right angles to the axis of the model in all the measurements, the conditions on which (26) is based are not fulfilled. Since a section through the axis of the tank is square, however, interchanging the length and diameter of the tank should have little effect (this is further justified by the fact that (26) was derived by replacing the actual shield with a sphere of diameter equal to the geometric mean of the three dimensions of the actual shield). We can therefore write

$$\frac{\text{Resistance in absence of tank}}{\text{Actual resistance of model}} = \left[1 - \left(\frac{d_m}{l_t}\right)^2 \frac{\tau_m}{d_t}\frac{1}{K}\right] \qquad (27)$$

where d_m and d_t are the respective diameters of the model and tank, and l_m and l_t are the respective lengths.

Using the dimensions shown in Plate 21, we find that the diameter-to-length ratio of the model is 1.8. According to Fig. 88, p. 130, ref. 28, K is 0.57, and we get

$$\frac{\text{Resistance in absence of tank}}{\text{Actual resistance of model}} = 0.9765 \qquad (28)$$

i.e. there is a 2.35 percent increase in the resistance due to the presence of the tank. The value of R_e/ρ of the model, after applying this correction, is

$$R_e/\rho = 0.741 \qquad (29).$$

ii. Inductance Analogue. R_e/ρ was also determined by the inductance analogue method, using a split toroidal conductor like that described in IV, "Description of Apparatus", with the exception that the axial length was inadvertently made 1.83 inches instead of 1.87 inches.

A sheet of dielectric material was placed between the two halves of the conductor, which were then matched up and clamped in the wood framework, and the capacitance between them was measured at 1000 cps on a General Radio type 716-B capacitance bridge. Care was taken to account for all lead capacitances.

The conductor was then coupled loosely to a loop connected to the output of a General Radio type 857-A u.h.f. oscillator. A general Radio type 726-A vacuum-tube voltmeter indicated the voltage developed across the loop (see Plate 22). The frequency of the oscillator was varied until the loop voltage dipped, due to resonance of the conductor. The separation between the conductor and the loop was then increased until the dip could just barely be observed (minimizing reaction of the loop circuit on the conductor), the oscillator was retuned for maximum dip, and the resonant

frequency was recorded. This procedure was repeated with two, three, and four thicknesses of dielectric material between the halves of the toroid conductor.

In Plate 22, the resonant frequency is plotted as a function of one-fourth the capacitance measured by the bridge, since the capacitance measured with the bridge is four times the effective capacitance in series with the conductor.

The capacitances C_A and C_B (see the drawings in Plate 22) are not necessarily equal, due to varying thickness of the air gap between the conductors and the dielectric sheet, and varying thickness of the dielectric sheet. In Appendix B, the error is evaluated, from assuming $C_A = C_B$ when in reality $C_A = C_B$, and it is shown to be negligible for reasonable differences between C_A and C_B.

In order for this method to be successful, the dielectric constant of the dielectric sheet should be independent of frequency from 1000 cps up to the top frequency used; for this reason polystyrene was employed.

If the measurements are accurate, all the measured points should lie on a straight line having a negative slope of one-half, when plotted on log-log paper. In Plate 22, a straight line was drawn through the experimental points (the clusters of points were obtained by varying the capacitance slightly, this being done by changing the clamping pressure applied by the framework to the two halves of the conductor). Twice the Y intercept of this line was laid off on the X axis. The difference between the resultant point (located in Plate 22 by a small arc intersecting the X axis) and the actual X intercept is one indication of the reliability of measurement, and we see that the agreement is excellent.

The inductance was calculated as the average of the extreme inductances represented by the X and Y intercepts in Plate 22, i.e. by the points F_1, C_1 and F_2, C_2 in Plate 22, and has a value of

$$L = 0.0171 \text{ microhenry} \qquad (30).$$

Using this value in (19), we get for R_e/ρ ,

$$R_e/\rho = 0.735 \qquad (31).$$

This value is obtained from the inductance of a conductor which is axially shorter than the toroid assembly by 0.04 inch. To obtain the value for a conductor of the same size as the toroid assembly, we first note that the resistance of the central hole in the toroid assembly is given by

$$R_e/\rho = 0.487 \qquad (32),$$

which is about 65 percent of (31). The remainder of the resistance is made up of two radial paths and an axial path, and hence this last path contributes only a small fraction of the total resistance. Since a small change in the axial length of the toroid assembly has little effect on the resistance of the axial paths, most of the increase in R_e/ρ for a small change in axial length is due to increase in the length of the central hole.

For a 0.04 inch increase in length, this increase in R_e/ρ is

$$\Delta R_e/\rho = 0.012 \qquad (33).$$

For an axial length of 1.87 inch, the value of R_e/ρ is given by (31) plus (33), or

$$R_e/\rho = 0.747 \qquad (34).$$

iii. Measurement of Resistance by Direct-Reading Method. One experiment was successfully concluded with toroid assembly no. 1; this was measurement of the pickup voltage e_p as a function of the resistance of a decade resistor in an external loop linking the toroid assembly, using an untuned pickup

circuit. Prior to the test, e_p was balanced down to well below 2 microvolts, with the external loop open-circuited. Plotted in Plate 23 are the results of this experiment, showing $e_p/2$ as a function of the loop resistance in ohms. As predicted in (6), the pickup voltage is inversely proportional to the loop resistance R_e. From the slope of the line in Plate 23, it is calculated that

$$e_p = 0.296/R_e \text{ volts} \qquad (35) .$$

Using (11) and the following data on toroid assembly no. 1:

e_d= 30 volts rms
$\omega = 2\pi f$= 62800 rps
n_1= 737 turns
n_2= 722 turns
R_L= 25000 ohms
L_p= 83.0 mh., we get

$$e_p = 0.288/R_e \text{ volts} \qquad (36) .$$

The discrepancy between the theoretical and experimental values is 2.7 per cent, and may be due to the normal tolerance in the permeability of the cores, errors in counting the number of turns on the the toroids, and experimental errors.

Note the deviation in the high-voltage end of the curve, from a straight line. This could not be explained by the derived equations for e_p, and was later found to be caused by failure to include in the value of R_e the resistance of the wire used in the external loop, as well as the "zero" resistance of the decade resistor.

A similar experiment was carried out with toroid assembly no. 2. Plotted in Plate 24 are the results of this experiment. From the slope of the straight line in Plate 24, we get

$$e_p = 0.296/R_e \text{ volts} \qquad (37) .$$

Using (11) and the following data on toroid assembly no. 2:

e_d= 30 volts
$\omega = 2\pi f$= 62800 rps
n_1= 737 turns
n_2= 737 turns
R_L= 25000 ohms
L_p= 89.6 mh., we get

$$e_p = 0.303/R_e \text{ volts} \qquad (38),$$

yielding a discrepancy of 2.4 percent between the experimental and theoretical values.

In Plate 24, as in Plate 23, there is a deviation from the straight line at the extreme right, for the same reason.

Another experiment of this type was carried out with toroid assembly no. 2, for lower values of resistance, with the resistance of the wire in the external loop and the zero resistance of the resistance box included in R_e. The results are plotted in Plate 25. Note that the deviation from a straight line now commences at a lower value of resistance. A portion of this deviation is a result of the decrease in e_d as R_e decreases. Although the oscillator is amplitude-stabilized, the impedance reflected into the tank circuit when R_e= 0.1 ohm is $(737)^2 \times 0.1$= 54000 ohms which reduces the tank impedance from its normal value of 600000 ohms to only 50000 ohms. A drop in e_d under these conditions is understandable. e_d was measured as a function of R_e, and the curve in Plate 25 was then corrected for the drop in R_e, yielding a new curve which is so labeled. The deviation of the new curve from the straight line is smaller, and could be caused by a 0.01 ohm error in the determination of the total resistance of the loop. In Plate 25, the value of e_p is once more

$$e_p = 0.296/R_e \text{volts} \qquad (39).$$

Note that in Plates 23, 24, and 25, the deviation of the points from the line over the straight portion does not exceed $\pm$ 2 percent.

These tests verify (11) and demonstrate the feasability of a direct-reading conductivity and conductance meter.

iv. Measurement of Electrolytic Conductivity by Direct-Reading Method. An attempt was made to measure e_p as a function of the conductivity of an electrolyte, using toroid assembly no. 1. The pickup voltage was first reduced to about 0.1 microvolt by means of the balancing circuit. Upon immersion of the toroid assembly in the electrolyte, e_d increased immediately but did not reach a stable value; it continued to drift upwards and upon removal of the assembly from the electrolyte, a large unbalance voltage remained. The behavior was erratic and entirely unsatisfactory, and was attributed to leakage of electrolyte into the toroid casing. Upon opening the casing, several droplets of water were found therein, and it was observed that one of the polystyrene tubes had not been thoroughly cemented into the toroid casing.

Two experiments were carried out in which e_p was measured as a function of the resistivity of the electrolyte, using toroid assembly no. 2, placed at the center of the glass battery jar filled with electrolyte. In these tests, e_d was balanced to less than 0.1 microvolt before immersion, and upon removal after completion of the tests, there was no noticable change in the balance.

In the first test, the experiment began with a sodium chloride solution with a resistivity of about 70000 ohm-cm., and e_d was measured as a function of the resistivity of the electrolyte, which was decreased repeatedly in steps of approximately a factor of two by addition of sodium chloride. The resistivity was measured independently using the Leeds and Northrup conductivity cell and portable resistance indicator.

The resistance R_e of the electrolytic path was calculated from e_d, using (37), and the ratio of this resistance to the resistivity of the electrolyte is plotted as a function of resistivity in Plate 26, showing a substantially constant value of R_e/ρ of

$$R_e/\rho = 0.760 \qquad (40)$$

over a resistivity range from 15 ohm-cm. to 20000 ohm-cm. Applying the correction given by (28), we get

$$R_e/\rho = 0.743 \qquad (41).$$

In this experiment, at the low-resistivity end the resistance of the L & N conductivity cell was so low that it was necessary to take into account the calculated resistance of the leads connected thereto. Measurement of the lead resistance was impossible because the cell end of the cable is inaccessible.

The points on the dotted curve on the left in Plate 26 were taken when the voltage e_d had dropped about 2 percent below its normal value, possibly due to a sudden change in the operating voltage of one of the type 991 regulator tubes in the stabilized power supply, which in turn would cause a drop in the bias voltage on the cathode of the diode V_9. The solid curve, which is for a normal value of e_d of 30 volts rms, was therefore extended parallel to the dotted curve to correct for the drop in e_d.

On the basis of the theory developed in Appendix A, the drop in the curve at low resistivities cannot be attributed to the toroid assembly. The error in the measurement of resistance required to cause the observed drop at a resistivity of 10 ohm-cm. is about 0.04 ohm, since the resistance of the cell for this resistivity is about 1 ohm.

Plate 25 shows not only that e_p is a linear function of the loop conductance to a conductance 20 times higher than that at which the decrease at the left side in Plate 26 begins to appea r, but also that the deviation in e_p from linearity when it does occur is such as would cause an apparent increase in R_e/ρ.

Conductivity cells are designed so that polarization errors are negligible over the range of conductivities for which they are intended. Since the cell used is described by the manufacturer as being "for low conductivity solutions", it is unlikely that precautions were taken to minimize polarization errors at high conductivities. It is therefore reasonable to attribute the observed drop at low resistivities to polarization error in the cell. Polarization causes an apparent increase in resistivity, which is in agreement with the observed decrease in the ratio R_e/ρ.

At the high-resistivity end of the curve in Plate 26, decrease in R_e/ρ is observed to commence at about 20000 ohm-cm. In order to observe the effect at higher resistivities, an experiment similar to the previous one was carried out, starting with resistivities of the order of 10^6 ohm-cm.; the results are plotted in Plate 27. A curve of the theoretical effect of displacement currents linking the toroid assembly, calculated from (16), is plotted on the same sheet for comparison. Note that the resistivity scale is not the same for the two curves, which show that the theoretical effect occurs at approximately 20 times the resistivity at which the experimental effect appears.

At first, one might attribute this discrepancy to circulating currents entering the shield through the shield-to-electrolyte capacitance. This explanation may be studied with the aid of Fig. 2, which shows one half

of a sectional view through the axis of the toroid assembly.

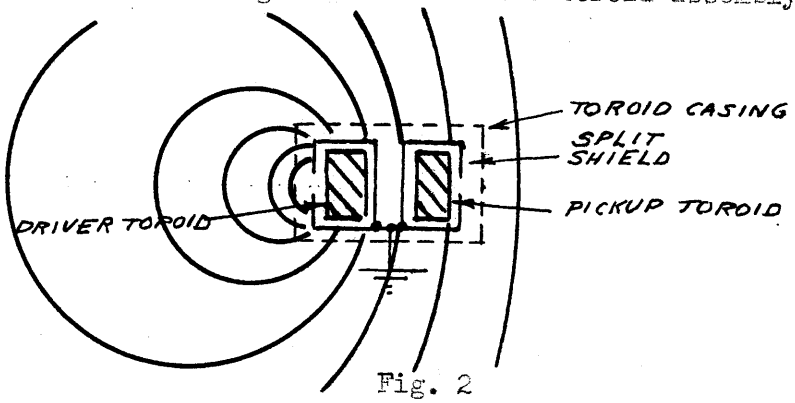

Fig. 2

A rough picture of the current flow lines is shown, appreciable displacement currents flowing from the shield into the electrolyte. One sees that none of the current entering the shield links the pickup toroid; hence the effect of this current appears to reduce the amount of current linking the pickup toroid, which is contrary to the observed effect, and would cause an increase, rather than a decrease in R_e/ρ with increasing resistivity. There seems to be no way of explaining the effect by reasoning along these lines.

A plausible explanation attributes the effect to electrostatic coupling between the driver and pickup toroids through the electrolyte. A phenomenon was observed which strengthens the conviction that this explanation is correct. In the range of high resistivities where the decrease in the experimental value of R_e/ρ occurs, it was found that touching the battery jar with the hand decreases the value of e_p markedly at the highest resistivites, and by decreasing amounts as the resistivity decreases, becoming negligible when the decrease in R_e/ρ becomes negligible.

If the decrease in R_e/ρ were due to change in the path of the circulating currents linking the toroid assembly, this phenomenon would not have occurred, since the circulating currents near the walls of the

battery jar are small compared with the total circulating current linking the toroids, as is evident from Plate 21.

However, if we consider the electrostatic coupling between the two toroids to consist of an equivalent T network with the center leg grounded, the body capacity would change the impedance of the center leg appreciably (since body capacity is of the order of several hundred micromicrofarads to ground), changing the coupling and causing the observed decrease in pickup voltage. At high conductivities, the coupling is shorted to ground, and the voltage due to it becomes negligible compared with that due to circulating conduction currents.

In Plate 26, the deviation of the points from the curve is about ± 1 percent, indicating that a highly accurate electrodeless conductivity meter has been developed. Where the instrument is not direct-reading, e. g. where R_e/ρ decreases for high resistivities, curves similar to Plate 26 and Plate 27 may be used as correction curves.

In the preceding experiments, three values of R_e/ρ were obtained by three different methods. They are shown in the following table.

Method		Value of R_e/ρ
Model with electrodes	(29)	0.741
Inductance analogue	(34)	0.747
Toroid assembly	(41)	0.743

The agreement is within experimental error and proves the validity of the reasoning used herein.

v. Piccard-Frivold Null Method. Plate 28 shows the results of an experiment to determine the performance of the Piccard-Frivold null method, using toroid assembly no. 2 with tuned pickup circuit, and the electronic circuits developed for this research. In this experiment the decade resistance

boxes R_1 and R_2 are connected to the figure-8 loop and to an external loop snugly linking the toroid assembly, as shown in the circuit diagram in Plate 28. Both switches are in an up or down position, so that when R_1 is in the external loop, R_2 is in the internal loop, and so that R_1 and R_2 may be interchanged by throwing the switches. The resistance in the external loop is called R_e; that in the internal loop R_e'.

The procedure is to first reduce e_p to zero by means of the balancing circuit, with both loops open-circuited, and then to set the switches such that, say, $R_e = R_1$ and $R_e' = R_2$. R_1 is set at some value R_A, and R_2 is adjusted to the value required for balance, R_B. Because of the unequal lead capacitances across the resistance boxes, a capacitive balance is required. A fixed 500 mmf. condenser C_2 is placed across R_2 and a standard variable air condenser with an 100 mmf.- 1100 mmf. range is placed across R_1.

After balance is obtained, the error is taken as the deviation of R_e' from R_e in percent, i. e.,

$$\epsilon' = \frac{R_B - R_A}{R_A} \times 100 \qquad (42).$$

After throwing both switches, R_2 is set at R_A and R_1 is adjusted to a new value required for balance, R_B'. The error in this case is

$$\epsilon'' = \frac{R_B' - R_A}{R_A} \times 100 \qquad (43).$$

The difference between ϵ' and ϵ'' is a check on the measurements and a check on the accuracy of the resistance boxes. The average of ϵ' and ϵ'' is used, giving

$$\epsilon = \frac{\epsilon' + \epsilon''}{2} = \frac{R_e' - R_e}{R_e} \times 100 \qquad (44).$$

As the resistance R_e is decreased, the capacitance C_1 assumes values which differ more and more from C_2. If only shunt capacitance were present, the capacitance balance would be independent of R_e.

Since the capacitance balance changes, it appears that series inductance is present. In one experiment, C_1 was left at the value required for balance when R_e= 100000 ohms; in order to obtain balance at 100 ohms without changing C_1, it was necessary to add an inductance L_e' of 12 microhenries in series with R_e'. No explanation is forthcoming for this large value of inductance required for balance, since the largest part of the inductance of each loop, that contributed by the toroids, is only 0.30 microhenry.

In Plate 28, ϵ is plotted as a function of R_e. For values of R_e less than 3000 ohms, ϵ is within 0.1 percent of 2 percent; above 3000 ohms, ϵ increases rapidly to about 6 per cent at 110000 ohms.

Such errors are surprising and difficult to explain. It was pointed out in the theory that if the toroids are perfectly symmetrical, R_e=R_e', since the mutual flux between a toroid and either loop must be the same. A constant error, independent of R_e, could be attributed to assymmetry of the toroids, since in this case, in general one loop would link more of the toroid flux than the other. The loop of larger diameter would usually link more flux, and hence for balance the resistance in that loop would have to be higher than that in the other loop. In the experiment under discussion, this is the case, since the higher resistance is in the external loop, which is of greater diameter than the internal loop.

No plausible explanation has been found for the large increase in error shown in Plate 28, when R_e exceeds 3000 ohms.

The failure to find explanations of some of the results obtained with the Piccard-Frivold method indicates that the equivalent circuit in Appendix A for this method is not complete. For one thing, it neglects the mutual inductance between the two loops. If perfect symmetry were

maintained, we would expect this mutual inductance to be zero, since the mutual inductance between one-half of the figure-8 loop and the external loop is of opposite sign to that between the other half and the external loop. In general, however, these mutual inductances do not balance out, and a complete equivalent circuit for the Piccard-Frivold method should include this mutual inductance.

It may be that some of the unexplainable effects are due to some unintended mutual impedance involving the driver, pickup, and loop circuits. Every precaution was taken to avoid such impedances; the shields of the driver and pickup circuits were separately grounded, the driver shield being grounded directly to C_A, to prevent flow of driver current in the chassis.

Unfortunately, time does not permit further work on the Piccard-Frivold method, although a considerable amount remains to be done. The direction that this work might follow is given in VII, "Suggestions for Further Work".

If the error in R_e is independent of R_e, it is tolerable, since it can be corrected by means of a constant factor. We see in Plate 38 that the Piccard-Frivold method using the circuits of this research is satisfactory for measuring resistances below 10,000 ohms. Undoubtedly, it can be improved.

VI CONCLUSIONS

1. An electrodeless direct-reading conductance meter has been developed, in which the output voltage is directly proportional to conductance over the conductance range from 10 micromhos to 10 mhos. The meter can be calibrated to read conductance directly, and is accurate to ± 2 percent. The theory of this instrument has been developed, and the experimental results agree with the theory, within experimental error.

ii. An electrodeless direct-reading conductance meter has been developed, in which the output voltage is directly proportional to electrolytic conductivity over the range of conductivities from 50 micromho-cm.$^{-1}$ to greater than 0.1 mho-cm.$^{-1}$. The meter can be calibrated to be direct-reading in conductivity over this range, with an accuracy of ± 1 percent. Lower conductivities may be measured if a calibration curve is used.

The heart of the device is an insulated assembly containing two toroids, in the form of a toroidal casing with an outside diameter of 3.4 inches and an axial length of 1.87 inches. Provided the dimensions of the non-conducting tank in which the measurements are made are greater than three times the diameter of the toroid assembly, the calibration of the device is decreased by less than 3 percent by the finite extent of the conducting medium, and the calibration is independent of the posiiton in the tank within 2 percent provided the spacing between the toroid assembly and the tank is not less than the axial thickness of the assembly.

The theory of this instrument has been developed, and the experimental results agree with the theory within experimental error, over the conductivity range in which the output is a linear function of conductivity. At lower conductivities the deviation from linearity is attributed to electrostatic coupling between the toroids, through the electrolyte, but no quantitative theoretical explanation of the experimental results at low conductivities has been obtained.

iii. Using the null method proposed by Piccard and Frivold, resistance was measured over a resistance range from 100 ohms to 100000 ohms, with an error which was constant within 0.1 percent of 2 percent

up to 3000 ohms, and which increased rapidly to 6 percent at 100000 ohms. Although the constant error may be explained by asymmetry of the toroids, no explanation has been found for the error at low conductances.

iv. An equivalent circuit of the toroid assembly has been developed, which explains its behavior adequately over a wide conductance range. A coupling element in the equivalent circuit represents the resistance of the path linking the toroids. This coupling element has been measured by three different methods:

a. The output voltage of the toroid assembly was determined under known conditions, and this in conjunction with the equivalent circuit was used to determine the value of the coupling element.

b. The resistance of the path was determined by inserting electrodes therein.

c. The resistance of the path was calculated from a knowledge of the high-frequency inductance of a conductor having the same external dimensions as the toroid assembly, using a formula developed in the theory, which gives the relationship between high-frequency inductance and resistance. The effect of an insulated container of finite dimensions on the path resistance may be determined by measuring the high-frequency inductance in a conducting container of the same dimensions.

The values obtained for the coupling element by these three methods are in close agreement.

v. the converse of iv(c) is useful; the high-frequency inductance of a conductor may be determined from measurements of the resistance of the conducting path linking an insulated model of the same dimensions.

vi. A new type of amplitude-stabilized vacuum-tube oscillator has been developed, in which the amplitude of oscillation is independent of wide changes in the plate supply voltage, heater voltage, parameters of the oscillator tube, and tank circuit impedance.

vii. The conditions have been determined for which the magnitude of the output voltage of a bridge-type R-C phase-shifting network is independent of the phase shift, when the source resistance is non-vanishing and the terminal resistance is finite.

viii. A method has been devised for the accurate determination of the high-frequency inductance of closed conductors of extremely low inductance.

ix. The methods described in this report, with modifications or improvements, may be used for the direct-reading or null measurement of electrolytic conductivity, conductivity of molten metals, resistance, capacitance, or inductance.

VII SUGGESTIONS FOR FUTURE WORK

i. The methods described in this report may be adapted to the electrodeless measurement of the conductivity of molten metals, by modifying the design.

Because of the high temperatures at which such measurements would be made, magnetic materials must be eliminated and air-core toroids used. The toroid windings should be wound of some metal which does not oxidize readily, and the toroid casing should be made of a refractory material.

To maintain linearity in the measurement of such high conductivities as those of metals, some or all of the following changes should be made (see 9(5)):

a. Greatly reduce the cross-section area of the central hole

in the toroid assembly.

b. Greatly reduce the inductances of the driver and pickup toroids.

c. Reduce the frequency of operation.

A direct-reading, electrodeless, compact instrument for measuring the conductivity of molten metals should be of great use in metallurgical research and production, and the possibility of using this method for that purpose should be investigated. Perhaps the electrodeless method will ultimately be more useful in metallurgy than in the measurement of electrolytic conductivity.

ii. The direct-reading electrodeless conductivity-measuring method should be further investigated, aiming toward electrical and mechanical improvement of the toroid assembly, as well as improvement and simplification of the electronic circuits. Improvement of the toroid assembly might include better shielding of the toroids, improvement of their symmetry, increasing the spacing between them, and placing a magnetic shield, such as a permalloy ring, between them. The cause of the decrease in the ratio R_e/ρ at low conductivities (see Plate 26) should be investigated.

iii. A toroid assembly should be designed specifically for the Piccard-Frivold method. Use of high-permeability cores in this design should result in a considerable improvement in the form of greater equality between R_e' and R_e at balance, since a larger proportion of the flux of each toroid will be confined to its core, improving the symmetry.

The Piccard-Frivold method should be examined theoretically, to develop a complete and accurate equivalent circuit. An exhaustive experimental study should also be carried out, with the object of explaining and rectifying the unsatisfactory behavior observed in Plate 28.

iv. Other null methods should be investigated theoretically and experimentally, including that which was incorporated in the circuits developed for this research, but which was not used.

Another null method worthy of investigation, somewhat similar in basic principle to the Piccard-Frivold null method, involves the use of a bridging resistor connected from a voltage-divider across the driver toroid, to the ungrounded end of the pickup coil, which is untuned. The bridging resistance should be large compared with the reactance of the pickup coil, in order to get a 90^{o} phase shift. Polarity of the pickup coil should be such that the voltage applied to it by the bridging resistor is opposite in phase to that due to the circulating currents linking the toroid assembly. Balance may be obtained by adjusting either the bridging resistor or the voltage divider.

v. The effect of a conducting tank on the calibration of the electrodeless conductivity meter should be studied.

VIII ACKNOWLEDGEMENTS

The author wishes to express his gratitude to Dr. R. D. Bennett, Technical Director of the Naval Ordnance Laboratory, Washington, D.C., where this research was carried out, for finding time to supervise this research, in spite of his many duties.

Without Dr. Bennett's willingness to act as thesis supervisor, without the genereus arrangement whereby the Committee on the Graduate School of M.I.T. permitted this thesis to be done in absentia, and without the policy of the Naval Ordnance Laboratory of assisting its employes in every way, possible to obtain advanced degrees, this research would not have been undertaken.

APPENDIX A

1. Direct-reading Method with Tuned Pickup Toroid.

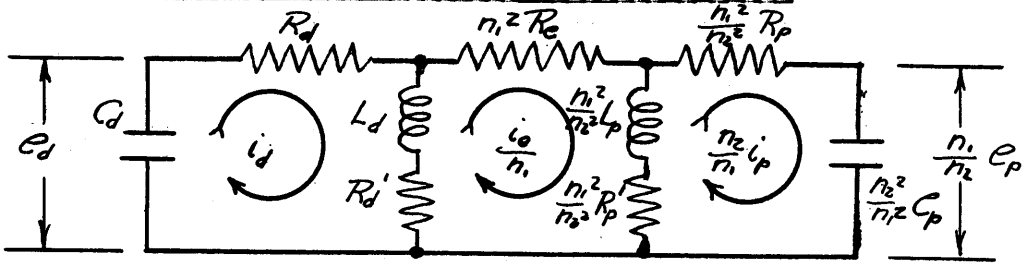

Fig. 1A

The equivalent circuit of the toroid assembly with tuned pickup (shown in Fig. 1A, which is the same as Plate 3(a)) is exact except for the omission of leakage inductance in series with $n_1^2 R_e$ and capacitance in parallel with $n_1^2 R_e$. These will be discussed later. This circuit was evolved by using the conventional equivalent T representation of a transformer. In Fig. 1A, if $Q_d \gg 1$ and $Q_p \gg 1$ (where $Q_d = \frac{\omega L_d}{R_d + R_d'}$ and $Q_p = \frac{\omega L_p}{R_p + R_p'}$), we can draw a simplified equivalent circuit as shown in Fig. 2A.

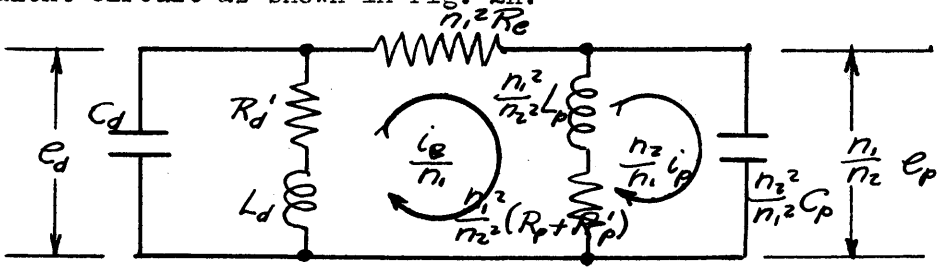

Fig. 2A

In Fig. 2A, if the pickup circuit is tuned to the frequency of e_d,

$$\frac{n_1}{n_2} e_p = \frac{i_e}{n_1} Z_p \frac{n_1^2}{n_2^2} \qquad (1A).$$

where $Z_p = Q_p \omega L_p$

Then $$e_p = \frac{n_2}{n_1}\left[\frac{e_d Z_p \frac{n_1^2}{n_2^2}}{n_1^2 R_e + Z_p \frac{n_1^2}{n_2^2}}\right] \tag{2A}$$

or $$e_p = \frac{n_2}{n_1}\left[\frac{e_d Q_p \omega L_p \frac{n_1^2}{n_2^2}}{n_1^2 R_e + Q_p \omega L_p \frac{n_1^2}{n_2^2}}\right] \tag{3A}.$$

Then $$\frac{e_p}{e_r} = \frac{n_2}{n_1}\left[\frac{1}{1 + \frac{R_e n_2^2}{Q_p \omega L_p}}\right] = \frac{n_2}{n_1}\left[\frac{1}{1 + \frac{R_e n_2^2}{Z_p}}\right] \tag{4A}.$$

When $R_e n_2^2 \rangle 100 Z_p$,

$$\frac{e_p}{e_r} \approx \frac{Z_p}{n_1 n_2 R_e} \tag{5A}$$

with an error of less than 1 percent. If $R_e n_2^2 = 0$,

$$\frac{e_p}{e_r} = \frac{n_2}{n_1} \tag{6A}$$

If the driver circuit is tuned to the same frequency as e_d, the input impedance is

$$Z_d' = Z_d \frac{\left[n_1^2 R_e + \frac{n_1^2}{n_2^2} Z_p\right]}{Z_d + n_1^2 R_e + \frac{n_1^2}{n_2^2} Z_p} \tag{7A}$$

where $Z_d = Q_d \omega L_d$.

Then

$$Z_d' = \frac{Q_d \omega L_d \left[n_1^2 R_e + \frac{n_1^2}{n_2^2} Q_d \omega L_d\right]}{Q_d \omega L_d + \frac{n_1^2}{n_2^2} Q_p \omega L_p + n_1^2 R_e} \tag{8A}.$$

$$\frac{Z_d'}{Z_d} = \frac{n_1^2 R_e + \frac{n_1^2}{n_2^2} Q_p \omega L_p}{Q_d \omega L_d + \frac{n_1^2}{n_2^2} Q_p \omega L_p + n_1^2 R_e} \tag{9A}.$$

(9A) shows how the input impedance is affected when the toroid assembly is immersed in a conducting medium. If $n_1^2 R_e \rangle\rangle Q_d \omega L_d + \frac{n_1^2}{n_2^2} Q_p \omega L_p$,

as is usually the case,

$$\frac{Z_d'}{Z_d} \approx 1 \tag{10A}$$

while if $n_1^2 R_e = 0$,

$$\frac{Z_d'}{Z_d} = \frac{\frac{n_1^2}{n_2^2} Q_p L_p}{Q_d L_d + \frac{n_1^2}{n_2^2} Q_p L_p} \tag{11A}$$

If the generator sypplying e_d has zero internal impedance (a condition that is strived for), the output impedance is given by

$$\frac{Z_p'}{Z_p} = \frac{n_2^2 R_e}{n_2^2 R_e + Q_p \omega L_p} \tag{12A}.$$

2. Direct-reading Method, Untuned Pickup Toroid.

In the case where the pickup circuit is untuned the equations will be determined in a more rigorous manner because the untuned arrangement is used in the direct-reading method and greater accuracy in the determination of e_p is required. The equivalent circuit for this case is shown in Fig. 3A.

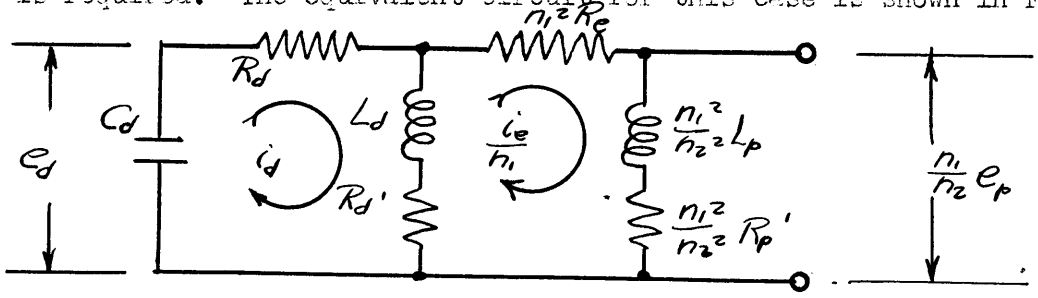

Fig. 3A

Writing the loop equations,

$$i_1 (R_d + R_d' + j\omega L_d) - i_e \left[\frac{R_d + j\omega L_d}{n_1} \right] + 0 = e_d \tag{13A}$$

$$i_1 (R_d' + j\omega L_d) - i_e \left[\frac{R_d'}{n_1} + n_1 R_e + \frac{n_1^2}{n_2^2} R_p' + j\omega \left(\frac{L_d}{n_1} + \frac{n_1}{n_2^2} L_p \right) \right] + 0 = 0 \tag{14A}$$

$$0 + i_e\left[\frac{n_1}{n_2^2}(R_p + j\omega L_p)\right] - e_p\left(\frac{n_1}{n_2}\right) = 0 \qquad (15A).$$

From these we get, by solving for e_p,

$$\frac{e_p}{e_r} = \frac{\left[R_d' + j\omega L_d\right]\left[\frac{n_1}{n_2^2}(R_p + j\omega L_p)\right]}{\left[R_d + R_d' + j\omega L_d\right]\left[\frac{R_d'}{n_1} + n_1 R_e + \frac{n_1}{n_2^2}R_p' + j\omega\left(\frac{L_d}{n_1} + \frac{n_1}{n_2^2}L_p\right)\right]\frac{n_1}{n_2} - \frac{n_1}{n_2}\left[\frac{(R_d' + j\omega L_d)^2}{n_1}\right]} \qquad (16A).$$

This may be rewritten as

$$\frac{e_p}{e_r} = \frac{\frac{n_2}{n_1}\left[R_d' + j\omega L_d\right]\left[R_p + j\omega L_p\right]}{R_d\left[R_d'\frac{n_2^2}{n_1^2} + n_2^2 R_e + R_p' + j\omega\left(L_d\frac{n_2^2}{n_1^2} + L_p\right)\right] + \left[n_2^2 R_e + R_p' + j\omega L_p\right]\left[R_d' + j\omega L_d\right]} \qquad (17A)$$

If $Q_p \gg 1$, $Q_d \gg 1$ and $n_2^2 R_e \gg \omega\left(L_d\frac{n_2^2}{n_1^2} + L_p\right)$

$$\frac{e_p}{e_r} \approx \frac{\frac{n_2}{n_1}(j\omega L_p)}{R_e n_2^2 + j\omega L_p} \qquad (18A)$$

Hence,

$$\left|\frac{e_p}{e_r}\right| = \frac{n_2}{n_1}\left[\frac{1}{\left(\frac{R_e n_2^2}{\omega L_p}\right)^2 + 1}\right]^{\frac{1}{2}} \qquad (19A).$$

If $\frac{R_e n_2^2}{\omega L_p} > 7.07$,

$$\left|\frac{e_p}{e_r}\right| \approx \frac{\omega L_p}{n_1 n_2 R_e} \qquad (20A)$$

with less than 1 percent error.

The input impedance variation is given by

$$\frac{Z_d'}{Z_d} = \frac{n_1^2 R_e + j\omega L_p\frac{n_1^2}{n_2^2}}{Q_d\omega L_d + n_1^2 R_e + j\omega L_p\frac{n_1^2}{n_2^2}} \qquad (21A).$$

If the generator has zero internal impedance, the output impedance is given by

$$\frac{Z_p'}{Z_p} = \frac{n_2^2 R_e}{n_2^2 R_e + j\omega L_p} \qquad (22A).$$

When the pickup circuit is untuned, there may be some distributed capacitance and circuit capacitance across it (due, for example, to capacitance to shield or cable capacitance). In addition, there may be a resistive load. These circuit elements will cause the pickup voltage to differ from the value given by (17A), (18A), (19A) or (20A). Using the circuit of Fig. 4A, we will evaluate the new voltage e_p' in terms of e_p.

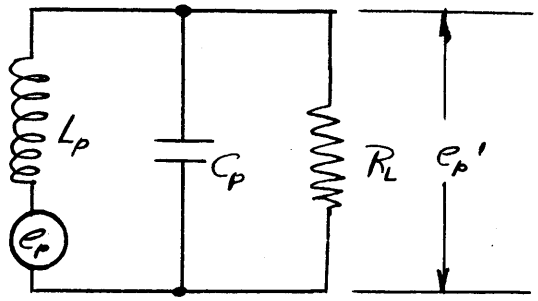

Fig. 4A.

In Fig. 4A, L_p is the low-frequency inductance of the pickup toroid, i.e. it is the inductance **at** a frequency lower than and remote from the frequency of resonance with the capacitance C_p which represents the total incidental capacitance. Since the correction now to be evaluated is a second-order effect, the resistance $R_p + R_p'$ of L_p is ignored since it has a third-order effect, provided $Q_p \gg 1$. Referring to Fig. 4A,

$$e_p' \doteq \frac{\left[\frac{R_L\left(\frac{-j}{\omega C_p}\right)}{R_L - \frac{j}{\omega C_p}}\right] e_p}{\frac{R_L\left(\frac{-j}{\omega C_p}\right)}{R_L - \frac{j}{\omega C_p}} + j\omega L_p} \qquad (23A)$$

$$\frac{e_p'}{e_p} = \frac{1}{1 + \frac{j\omega C_p}{\left[\frac{R_L\left(\frac{-j}{\omega C_p}\right)}{R_L - \frac{j}{\omega C_p}}\right]}} = \frac{1}{1 - \omega^2 L_p C_p + \frac{j\omega L_p}{R_L}} \qquad (24A)$$

C_p is actually not known directly; its effect is to increase the apparent pickup toroid inductance as measured in the presence of C_p at the operating frequency $f = \frac{\omega}{2\pi}$. In measuring the inductance at the operating frequency by a resonant method, a certain additional capacitance C_x is required to cause resonance. Then

$$\omega L_p [\omega C_p + \omega C_x] = 1 \qquad (25A),$$

or

$$\omega C_p = \frac{1}{\omega L_p} - \omega C_x \qquad (26A).$$

But $\omega C_x = \frac{1}{\omega L_p'}$, where L_p' is the apparent inductance at the operating frequency.

Hence $$\omega C_p = \frac{1}{\omega}\left[\frac{1}{L_p} - \frac{1}{L_p'}\right] = \frac{1}{\omega}\left[\frac{L_p' - L_p}{L_p L_p'}\right] \qquad (27A).$$

Therefore, $$\frac{e_p'}{e_p} = \frac{1}{\frac{L_p}{L_p'} + j\frac{\omega L_p}{R_L}} = \frac{1}{\omega L_p}\left[\frac{1}{\frac{1}{\omega L_p'} + \frac{1}{R_L}}\right] \qquad (28A)$$

Therefore, to get the true output voltage, (17A) and (18A) must be corrected by applying (28A). There only the absolute magnitude of the correction is required,

$$\left|\frac{e_p'}{e_p}\right| = \frac{R_L L_p'}{L_p}\left[\frac{1}{R_L^2 + (\omega L_p')^2}\right]^{\frac{1}{2}} \qquad (29A).$$

(29A) must be applied to (19A) and (20A). In the case of (20A) which will be most commonly used, the corrected voltage is then

$$\left|\frac{e_p'}{e_d}\right| = \frac{\omega L_p'}{n_1 n_2 R_e}\left[\frac{R_L^2}{(R_L)^2 + (\omega L_p')^2}\right]^{\frac{1}{2}} \qquad (30A).$$

3. Piccard-Frivold Null Method.

In the Piccard-Frivold null method, an additional loop in introduced into the equivalent circuit, representing the nulling loop. This loop is in opposite sense to the path in the conducting medium, with respect to one toroid; hence it is represented by an ideal transformer of -1 ratio in cascade with the balancing resistance R_e'. The equivalent circuit is shown in Fig. 5A. Note that the pickup circuit is tuned for added sensitivity.

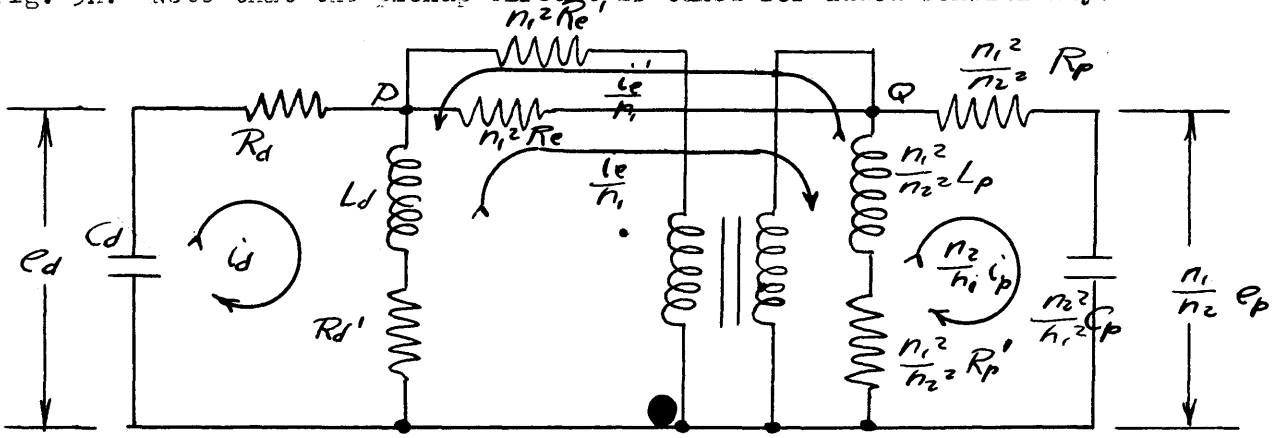

Fig. 5A

If a voltage e_d is applied, at balance the point Q is at zero potential. Then the balance condition is

$$R_e = R_e' \tag{31A}$$

and they may be considered to be in parallel as far as the driver toroid is concerned. The impedance of the input end at the resonant frequency of the driver circuit is then

$$\frac{Z_d'}{Z_d} = \frac{\frac{n_1^2 R_e}{2}}{\frac{n_1^2 R_e}{2} + Q_d \omega L_d} \tag{32A}$$

at balance.

By similar reasoning, the impedance looking into the pickup end is

$$\frac{Z_p'}{Z_p} = \frac{n_2^2 R_e / 2}{\frac{n_2^2 R_e}{2} + Q_p \omega L_p} \tag{33A}.$$

If $n_1^2 R_e \gg Q_p \omega L_p$, we find, using (5A), that the sensitivity at balance is given by

$$\frac{e_p}{e_d} - \frac{e_p + \Delta e_p}{e_d} = \frac{Q_p \omega L_p}{n_1 n_2} \left[\frac{1}{R_e} - \frac{1}{R_e + \Delta R_e} \right] \qquad (34A),$$

whence

$$\frac{\Delta e_p}{e_d} = - \frac{Q_p \omega L_p}{n_1 n_2 R_e} \frac{\Delta R_e}{R_e} \qquad (35A).$$

Then

$$\frac{\Delta e_p}{\frac{\Delta R_e}{R_e}} = - \frac{Q_p \omega L_p e_d}{n_1 n_2 R_e} \qquad (36A).$$

Thus, the sensitivity at balance to a given percentage change in R_e is inversely proportional to R_e.

4. Displacement Currents.

The resistance between the opposite faces of a centimeter cube is

$$R = \rho \text{ ohms} \qquad (37A)$$

where ρ is in ohm-cm. The capacitance between these same ends is

$$C = 8.842 \times 10^{-14} k \text{ farads} \qquad (38A)$$

where k is the dielectric constant. The impedance between the two faces of the cube is

$$Z = \frac{R(1 - j\omega RC)}{\omega^2 R^2 C^2 + 1} \qquad (39A)$$

or

$$Z = \frac{R \angle \tan^{-1} \omega RC}{(\omega^2 R^2 C^2 + 1)^{\frac{1}{2}}} \qquad (40A).$$

Substituting for R and C the values given by (37A) and (38A), we get

$$\frac{Z}{R} = \frac{\angle \tan^{-1} (8.842 \times 10^{-14} \omega \rho k)}{\left[(8.842 \times 10^{-14} \omega \rho k)^2 + 1 \right]^{\frac{1}{2}}} \qquad (41A)$$

or

$$\left| \frac{Z}{R} \right| = \frac{1}{\left[(8.842 \times 10^{-14} \omega \rho k)^2 + 1 \right]^{\frac{1}{2}}} \qquad (42A).$$

This is true of any medium in which the displacement current flow lines are everywhere parallel to the conduction current flow lines. If

$$8.842 \times 10^{-14} \omega \rho k \gg 10,$$

$$\frac{Z}{R} \approx \frac{\angle -90^\circ}{8.842 \times 10^{-14} \omega \rho k} \qquad (43A)$$

If the error in determining R is to be less than 1 percent,

$$8.842 \times 10^{-14} \omega \rho k < 0.02$$

In the Piccard-Frivold null method, the effect of displacement currents is to introduce a capacitive balance. The displacement currents introduce shunt capacitance across R_e and R_e'. If we call this capacitance C_e and C_e', the capacitive balance condition is $C_e = C_e'$.

5. Leakage Inductance.

As pointed out in the theory, leakage inductance is present only in the loop containing R_e. It is important only if of sufficient magnitude to alter the current flowing in this loop, and it is usually of much smaller magnitude.

In the direct-reading method with a tuned pickup toroid, the effect of the leakage inductance L_e is to modify (4A) to

$$\frac{e_p}{e_r} = \frac{n_2}{n_1}\left[\frac{1}{1 + \frac{n_2^2}{Z_t}(R_e + j\omega L_e)}\right] \qquad (44A),$$

and is less than 1 percent if $\omega L_e < 0.141 R_e$.

In the direct-reading method with untuned pickup toroid, the effect of leakage inductance is to modify (19A) to

$$\frac{e_p}{e_r} = \frac{n_2}{n_1}\left[\frac{1}{\left(\frac{R_e n_2^2}{\omega L_p}\right)^2 + \left(\frac{L_p + n^2 L_e}{L_p}\right)^2}\right]^{\frac{1}{2}} \qquad (45A).$$

$\frac{L_p + n_2^2 L_e}{L_p}$ is the ratio of the total inductance in the loop containing R_e, to the mutual inductance between that loop and the pickup toroid.

In the Piccard-Frivold null method, the leakage inductance imposes another balance condition, namely an inductive balance $L_e = L_e'$.

APPENDIX B

1. The Inductance Analogy.

If we have an inductor consisting of a single conductor, its inductance is given by

$$L = \frac{\phi}{I} \tag{1B}$$

where ϕ is the total magnetic flux set up by the current I. The magnetomotive force due to the current I around a path enclosing it is

$$MMF = \oint \vec{H} \cdot d\vec{l} = 4\pi I \tag{2B}$$

where $\vec{H}$ is the field due to the current I and $d\vec{l}$ is an element of the path.

Hence,

$$L = \frac{4\pi\phi}{MMF} \tag{3B}.$$

The ratio of MMF in a magnetic circuit, to the total magnetic flux, is called the magnetic reluctance, $\mathcal{R}$.

Hence

$$L = \frac{4\pi}{\mathcal{R}} \tag{4B}.$$

The reluctance of a cylindrical element in a medium of magnetic permeability μ is given by

$$\mathcal{R} = \frac{1}{\mu}\frac{dl}{A} \tag{5B}$$

where dl is the length of the element and A is its cross-sectional area. The resistance of the same element is

$$R_e = \rho\frac{dl}{A} \tag{6B}$$

where ρ is the resistivity of the medium. Eliminating $\frac{dl}{A}$ between (5B) and (6B), we get

$$\mathcal{R} = \frac{R_e}{\mu\rho} \tag{7B}.$$

Hence, if any three of the quantities in (7B) are known, the fourth may be determined. This relationship applies, furthermore, to any volume in which the boundary conditions for the magnetic field are the same as those for the electric field. It still further applies to two identical volumes such that if the boundary conditions for the magnetic field in one

are identical with those for the electric field in the other; a knowledge of μ and $\mathcal{R}$ in the former determines the relationship between ρ and $\mathcal{R}$ in the latter, or vice versa.

Since the inductance of the conductor linking a magnetic path is related to the reluctance of the path by (4B), the resistance of the path may be determined if the boundary conditions on the electric field correspond to those on the magnetic field. The relationship between resistance and inductance may be determined by eliminating $\mathcal{R}$ between (4B) and (7B), giving

$$R_e = \frac{4\pi\mu\rho}{L} \qquad (8B).$$

In particular, if the medium for which L is determined has a permeability of 1,

$$R_e = \frac{4\pi\rho}{L} \qquad (9B).$$

The validity of (8B) will be checked dimensionally. Writing the dimensional equation of (8B), we get

$$[\mu t^{-1}] = \frac{[\mu][\mu t^2 t^{-1}]}{\mu t}$$

$$[\mu t^{-1}] = [\mu t^{-1}]$$

(8B) is in emu. Converting to practical units, we get

$$R_e = \frac{4\pi\mu\rho}{10^9 L} \qquad (10B)$$

where R is in ohms, ρ is in ohm-cm, and L is in henrys. (9B) becomes

$$R_e = \frac{4\pi\rho}{10^9 L} \qquad (11B).$$

In terms of the conductivity $\sigma = \frac{1}{\rho}$,

$$R_e = \frac{4\pi}{10^9 \sigma L} \qquad (12B)$$

In practice, to determine the value of R_e for the conducting path linking the toroid casing, it is necessary to measure the inductance of a conductor of the same dimensions as the casing. We are interested in that

inductance which obtains when the current flow in the conductor is about the axis of the casing. Since we are dealing with a conducting path in which no current penetrates the casing, it is necessary to measure the high-frequency, or external, inductance of the conductor. If this inductance and the permeability of the medium in which it is measured are known, the ratio of R_c/ρ may be obtained from (12B).

2. Evaluation of Capacitance Errors in Measuring the Inductance of the Inductance Analogue.

In measuring the inductance of the toroidal conductor of the same dimensions as the toroid casing to determine the ratio R_c/ρ by the method of the inductance analogy, the conductor was cut along a plane passing through the toroid axis, and a thin sheet of polystyrene was placed between the two halves. Thus a loop was formed consisting of two equal inductances in series with two approximately equal capacitances, C_A and C_B (we say approximately equal because of the varying thickness of the dielectric material and the varying air gap between the material and the conductor). The resonant frequency of this circuit was measured by a resonance method. The capacitance between the two halves was measured at low frequency, giving the value C_P of C_A and C_B in parallel, from which the value C_S of C_A and C_B in series was determined. The inductance L could then be calculated from a knowledge of the resonant frequency and C_S.

If $C_A = C_B = C$, $C_P = 2C$ (13B),

while $C_S = C/2$ (14B).

Thus, $C_S = C_P/4$ (15B).

If $C_A \neq C_B$, $C_P = C_A + C_B$ (16B)

and $C_S = \dfrac{C_A C_B}{C_A + C_B}$ (17B)

or $$C_S = \frac{C_A C_B}{C_P} \qquad (18B).$$

Thus we see that when $C_A \neq C_B$, C_S cannot be determined from knowledge of C_P alone, since it depends also on the values of C_A and C_B. Since C_A and C_B cannot be measured separately, it must be assumed that they are equal, and it is necessary to determine the error arising from this assumption.

The assumed value of each condenser must be

$$C' = \frac{C_P}{2} = \frac{C_A + C_B}{2} \qquad (19B).$$

The assumed series capacitance is then

$$C_S' = \frac{C'}{2} = \frac{C_P}{4} = \frac{C_A + C_B}{4} \qquad (20B).$$

This is the capacitance calculated from the measured value of C_P; we wish to compare it with the true capacitance

$$C_S = \frac{C_A C_B}{C_A + C_B} \qquad (17B)$$

Let $C_A = C$ and $C_B = nC$. Then

$$C_S' = \frac{C}{4}(1+n) \qquad (21B)$$

and $$C_S = \frac{Cn}{(1+n)} \qquad (22B)$$

The percent error arising from the use of C_S' rather than C_S is

$$100\left(\frac{C_S' - C_S}{C_S}\right) \qquad (23B)$$

or $$Error = 100\left[\frac{\frac{C}{4}(1+n) - \frac{Cn}{(1+n)}}{\frac{Cn}{(1+n)}}\right] \qquad (24B).$$

$$Error = 100\left[\frac{(1+n)^2 - 4n}{n}\right] = \frac{100\,(n-1)^2}{n} \qquad (25B)$$

In the following table, the error is given as a function of n.

n	Percent Error
1.00	0
1.01	0.01
1.02	0.04
1.05	0.24
1.10	0.91
1.20	3.33
1.50	16.66

Thus we see that the error in assuming $C_A = C_B$ is less than one percent provided $\left(\frac{C_B - C_A}{C_A}\right) < 0.1$.

APPENDIX C

1. Toroid Design.

If we have a toroid of rectangular cross-section, with outer diameter d_2, inner diameter d_1, and axial height h, it can be easily shown that the inductance of a uniform winding on this toroid is [29]

$$L = 11.70 \times 10^{-9} \mu n^2 h \log_{10} \frac{d_2}{d_1} \text{ henry} \qquad (1C)$$

where μ is the permeability of the core, n is the number of turns on the winding, and dimensions are in inches.

It can also be shown that the d-c resistance of the winding is approximately

$$R_{DC} = \rho \frac{n^2 [2h + d_2 - d_1 + 4t]}{\frac{\pi^2}{8}(d_1 - \frac{t}{2})t} \qquad (2C)$$

where ρ is the resistivity of the wire used and t is the mean thickness of the winding. (2C) is derived from $R = \rho \frac{l}{A}$, where l is the total length of wire and A is the cross-sectional area of the wire. In (2C), $2h + d_2 - d_1 + 4t$ is the mean turn length, l_T and $n l_T = l$. $\pi(d_1 - \frac{t}{2})t$ in (2C) is the cross-sectional area of the winding. $\frac{\pi^2}{8}\frac{(d_1 - \frac{t}{2})t}{n}$ in (2C) is the cross-sectional area of the wire, and is obtained from $\pi(d_1 - \frac{t}{2})t$ by dividing by n, multiplying by $\frac{\pi}{4}$ to account for the space lost by using round wire, and multiplying by an additional space factor of 1/2 to include correction for the area taken up by the Formex insulation and for the area wasted in not having a layer winding.

The a-c resistance of a winding on an iron-core toroid of inductance L, due to core losses, is given by [30]

$$R_{AC} = \mu \{ L f a B_m + L f (c + ef) \} \qquad (3C),$$

where f is the frequency in cycles per second, $\mathcal{B}_m$ is the peak flux density in the core in gauss, and a, c, and e are empirically determined constants depending on the core material.

$\mathcal{B}_m$ is given by

$$\mathcal{B}_m = \frac{I n \mu (0.0353)}{d_1 + d_2} \qquad (4C),$$

where I is the rms current in the core in amperes, $\mathcal{B}_m$ is in gauss, and d_1 and d_2 are in inches. This is the mean value of $\mathcal{B}_m$ and is the value at a radius equal to $\frac{d_1+d_2}{4}$

Then $$R_{AC} = \left\{ \frac{2\pi f L I a n \mu (0.0353)}{2\pi (d_1+d_2)} + Lf(c+ef) \right\} \qquad (5C).$$

Since $$2\pi f L I = e \qquad (6C),$$

the voltage developed across the coil,

$$R_{AC} = \mu \left\{ \frac{e a n \mu (0.0353)}{2\pi (d_1+d_2)} + Lf(c+ef) \right\} \qquad (7C).$$

The total resistance R_T of the coil is

$$R_T = R_{AC} + R_{OC} \qquad (8C),$$

hence $$R_T = \mu \left\{ e_f n A \mu + Lf(c+ef) \right\} + n^2 P \qquad (9C),$$

where $$A = \frac{a(0.0353)}{2\pi (d_1+d_2)} \qquad (10C)$$

and $$P = \frac{8\rho}{\pi^2} \left[\frac{2h + d_2 - d_1 + 4t}{(d_1 - \frac{t}{2})t} \right] \qquad (11C).$$

Now $$R = \frac{4\pi f^2 L^2}{R_T} \qquad (12C),$$

where R is the parallel resonant resistance of a tuned circuit consisting of the winding and a lossless condenser at frequency f.

Eliminating R_T between (9C) and (12C), we get

$$\frac{4\pi f^2 L^2}{R} = \mu \left\{ e n A_\mu + L f (c + e f) \right\} + n^2 P \qquad (13C)$$

If we write

$$K^2 = \frac{1}{11.70 \times 10^{-9} \mu h \log_{10} \frac{d_2}{d_1}} \qquad (14C),$$

(1C) becomes $$L = \frac{n^2}{K^2} \qquad (15C).$$

Substituting this for L in (12C),

$$n^3 = \frac{R K^4}{4\pi^2 f^2} \left\{ e A_\mu^2 + n \left[\frac{\mu f (c + e f)}{K^2} + P \right] \right\} \qquad (16C).$$

Suppose we wish to design a toroid to have a given parallel resonant resistance R at a frequency f. We start with a specific core, selected from other considerations, which determines K, μ, c, e and A. A knowledge of the dimensions of the winding space (also chosen from other considerations) and of the resistivity of the wire determines P. e is chosen at some desired value, for example from a consideration of allowable power dissipation in the winding. R and f are given. Then (16C) is a cubic equation in n, all the coefficients being known. To solve for n, plot the right-hand and left-hand members on the same sheet of coordinate paper. The intersection of the two curves determines the only physically significant value of n.

The data on the TE no. 475866 cores, which are used in the toroid assembly, is as follows:

μ = 125
d_2 = 3.060 inches
d_1 = 1.938 inches
h = 0.500 inches
K = 2.62×10^3
a = 1.6×10^{-6}
c = 30×10^{-6}
e = 19×10^{-9}

In addition, the following design parameters were chosen:

Winding thickness t = 0.1 inch

Voltage across coil, e = 30 volts rms

f = 10,000 cps

Parallel resonant impedance, R = 10^6 ohms

Substituting all this data in (13C) and associated equations, and solving for n as outlined, we get: n = 737 turns.

This is the value calculated for the driver toroid: for the pickup toroid, e = 0 and the calculated value of n is: n = 722 turns.

The available winding area is given by

$$W.A. = \pi\left(d_1 - \frac{t}{2}\right)t \qquad (17C)$$

With the above dimensions, W.A. = 0.298 sq. ins., requiring about 2470 turns per sq. in. No. 25 B and S ga. heavy Formex insulated wire, which gives a winding of 2520 turns per sq. in., is used.

APPENDIX D

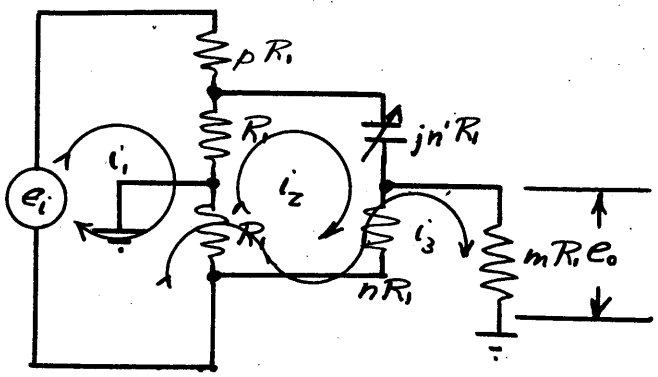

Fig. 1D

In the bridge-type R-C phase shifter in Fig. 1D, in which the bridge is supplied from a generator of internal emf e_i and source impedance pR_1, and develops a voltage e_o across the load mR_1, we wish to find the conditions under which $\left|\frac{e_o}{e_i}\right|$ is independent of the phase shift, as well as the value of $\left|\frac{e_o}{e_i}\right|$ and the expression for the phase shift, when these conditions are fulfilled. Writing the loop equations,

$$i_1 R_1 - i_2 R_1(1+n) + i_3 R_1(1+m+n) = 0 \tag{1D}$$

$$i_1(2R_1) + i_2 R_1[jn' - (2+n)] + i_3 R_1(1+n) = 0 \tag{2D}$$

$$i_1 R_1(2+p) - i_2(2R_1) + i_3 R_1 = e_i \tag{3D}.$$

Then

$$i_3 = \frac{R_1^2 \begin{vmatrix} 1 & -(1+n) & 0 \\ 2 & [jn'-(2+n)] & 0 \\ (2+p) & -2 & e_i \end{vmatrix}}{R_1^3 \begin{vmatrix} 1 & -(1+n) & (1+m+n) \\ 2 & [jn'-(2+n)] & (1+n) \\ (2+p) & -2 & 1 \end{vmatrix}} \tag{4D},$$

where m, n, n' and p are all real.

Expanding the determinants,

$$i_3 = \frac{e_i}{R_1} \frac{(jn'+n)}{\{jn'-(2+n) - (1+n)^2(2+p) - 4(1+m+n) - [jn'-(2+n)](2+p)(1+m+n) + 4(1+n)\}} \tag{5D}.$$

T his expression simplifies to

$$i_3 = \frac{e_i}{R_1} \frac{(n+jn')}{(n-jn')[(2+p)(1+m+n)-1]+p[1+2m-n^2]-2n^2} \qquad (6D).$$

If we set $p[1+2m-n^2] = 2n^2$,

$$p = \frac{2n^2}{1+2m-n^2} \qquad (7D)$$

and (6D) reduces to

$$i_3 = \frac{e_i}{R_1} \frac{(n+jn')}{(n-jn')[(2+p)(1+m+n)-1]} \qquad (8D)$$

or

$$i_3 = \frac{e_i}{R_1} \frac{\angle \tan^{-1}\frac{n'}{n}}{[(2+p)(1+m+n)-1]} \qquad (9D).$$

Then

$$e_o = i_3 m R_1 = \frac{e_i m \angle \tan^{-1}\frac{n'}{n}}{[(2+p)(1+m+n)-1]} \qquad (10D).$$

Hence, if (7D) is fulfilled, the ratio $\left|\frac{e_o}{e_i}\right|$ is independent of n' and the phase shift depends only on the ratio n/n'. It is unfortunate that the results apply only to variation in n', the impedance level of the capacitive arm, rather than to n, the impedance level of the resistive arm.

If m, n, n' and p are all multiplied by the same factor q, (10D) is altered to

$$e_o = \frac{e_i m \angle \tan^{-1}\frac{n'}{n}}{q[(2+p)(1+m+n)-1]} \qquad (11D).$$

In particular, if q=j, i. e. if all the resistive arms are made

capacitive and the capacitive branch is made resistive,

$$e_o = \frac{-j e_i m \angle \tan^{-1}\frac{n'}{n}}{[(2+p)(1+m+n)-1]} \qquad (12D),$$

where n' is now the impedance level of the resistive branch. The ratio $\left|\frac{e_o}{e_i}\right|$ is now independent of the impedance level of the resistive branch.

Using (7D), p may be eliminated from (10D), giving

$$e_o = \frac{e_i m(1+2m-n^2) \angle 2\tan^{-1}\frac{n'}{n}}{4m[1+m+n]+(1+n)^2} \qquad (13D).$$

Referring to (7D), let us decrease p to zero, at the same time increasing $1+2m-n^2$ to mainintain $2n^2$ constant. When $1+2m-n^2$ becomes very large, $2m \approx 1+2m-n^2$, and (7D) becomes

$$p \approx \frac{n^2}{m} \qquad (14D).$$

In the limit, when p becomes zero, m must simultaneously become infinite if n is to maintained constant. Then (10D) reduces to

$$e_o = \frac{e_i}{2} \angle \tan^{-1}\frac{n'}{n} \qquad (15D).$$

This is the special and commonly used case where the source has zero internal resistance and the load resistance is infinite. In this case, $\left|\frac{e_o}{e_i}\right|$ is independent of both n and n'.

Another special case occurs when p is increased indefinitely in (7D) and $1+2m-n^2$ is decreased to maintain $2n^2$ constant. In the limit, when $p \to \infty$,

$$n = (1+2m)^{\frac{1}{2}} \qquad (16D).$$

With this condition, (10D) reduces to

$$e_o = \frac{e_i\, m \quad \angle \tan^{-1}\frac{n'}{n}}{\rho(1+m+n)} \qquad (17D).$$

This is the case where the bridge is fed from a constant-current source, such as a pentode vacuum tube.

A third special case occurs when n= 1 and m=1. Then (7D) reduces to

$$p=1 \qquad (18D)$$

and (10D) reduces to

$$e_o = \frac{e_i \angle \tan^{-1}\frac{n'}{n}}{8} \qquad (19D).$$

Note that in general, if p is to be positive,

$$1+2m > n^2 \qquad (20D).$$

The smallest value of n for which m may be made infinitely small without requiring a negative value of p is n=1. For large values of n, the minimum value of m for p to be positive is

$$m \approx \frac{n^2}{2} \qquad (21D)$$

BIBLIOGRAPHY

Reference No.	Publication
1.	Acree, S. F.; Bennett, E.; Gray, G. H. and Goldberg, H.; J. Phys. Chem., vol. 42, pp. 871-896, Oct. 1938.
2.	Banerji, B. B.; "Electrode Capacity and Resistance of Electrolytes", Faraday Soc. Transactions, vol. 22, pp. 111-132, disc. 132-133, May 1936.
3.	Burton, E. E. and Pitt, A.; Phil. Mag. Supp. S. 7, Vd. 5, pp. 939-943, May 1928
4.	Dike, P. H.; "Bridge for Measurement of the Conductance of Electrolytes", Rev. Sci. Inst., vol. 2, pp. 379-395, July 1931.
5.	Ender, F.; "Electrolytic Conductivity Measurement", Zeits f. Elektrochem., vol. 43, pp. 217-233, April 1937.
6.	Falkenhagen, Hans; Book: "Electrolytes", Clarendon Press, Oxford, 1934, p. 82.
7.	Ibid., p. 90.
8.	Grube, G. and Speidel, H.; "Electrodeless Measurement of the Resistance of Metals and Alloys", Zeits. f. Elektrochem., vol. 46, pp. 233-242, March 1940.
9.	Hall, R. E. and Adams, L. H.; "Application of Thermionic Amplifier to Conductivity Measurements", Am. Chem. Soc., J., vol. 41, pp. 1515-1525, Oct. 1919.
10.	Haworth, H. F.; "Measurement of Electrolytic Resistance by Alternating Current", Faraday Soc., Trans., vol. 16, pp. 365-386, disc. 386-391, Feb. 1921; Electrician, vol. 85, pp. 443-445, Oct. 15, 1920 abstract.
11.	Jones, G. and Bollinger, G. M.; "Conductance of Electrolytes, Part II. Improvements in the Oscillator and Detector", Am. Chem. Soc., J., vol. 51, pp. 2407-2416, Aug. 1929.

Reference No. Publication

Jones, G. and Bollinger, G. M.;
"Conductance of Electrolytes, Part III. Design of Cells", ibid., vol. 53, pp. 411-451, Feb. 1931.

"Conductance of Electrolytes, Part IV. Validity of Ohm's Law for Electrolytes", ibid., vol. 53, pp. 1207-1212, April 1931.

"Conductance of Electrolytes, Part VII. Polarization", ibid., vol. 57, pp. 280-284, Feb. 1935.

Jones, G. and Bradshaw, B. C.;
"Conductance of Electrolytes, Part V. Redetermination of the Conductance of Standard Potassium Chloride Solutions in Absolute Units", ibid., vol. 55, pp. 1780-1800, May 1933.

Jones, G. and Christian, S. M.;
"Conductance of Electrolytes, Part VI. A.C. Galvanic Polarization", ibid., vol. 57, pp. 272-280, Feb. 1935.

Jones, G. and Josephs, R. C.;
"Conductivity of Electrolytes, Part I", ibid., vol. 50, pp. 1049-1092, April 1928.

12. Kohlraush;
Weid. Ann. vol. 60, p. 315, 1897; vol. 58, p. 514, 1896; vol. 56, p. 177, 1895; vol. 49, p. 225, 1893; vol. 26, p. 168, 1885; vol. 6, p. 9, 1879.

Kohlraush and Diesselhorst;
Weid. Ann. vol. 64, p. 417, 1896.

Kohlraush and Holborn;
Book: "Das Leitvermogen der Electrolyte", Teubner, Leipzig, 1916.

Kohlraush and Nippolt;
Pogg. Ann., vol. 138, pp. 280, 370, 1869.

13. Luder, W. F.;
"Precision Conductivity Bridge Assembly", Am. Chem. Soc., J., vol. 62, pp. 89-95, Jan. 1940.

14. Kraus, C. A. and Parker, H. C.;
"Calibration of Cells for Conductivity Measurements", Am. Chem. Soc., J., vol. 44, pp. 2422-2428, Nov. 1922

"Conductivity of Aqueous Solutions", ibid., vol. 44, pp. 2422-2428, Nov. 1922.

Reference No. Publication

15. Leeds and Northrup Company;
Catalog EN-94, Philadelphia, 1944.

16. Moore, B.;
"Improved Conductivity Cell", Journ. Sci. Instruments, vol. 9, pp. 389-390, Dec. 1932.

17. Parker, H. C.;
"Calibration of Cells for Conductance Measurements, Part II", Am. Chem. Soc., J.; vol. 45, pp. 1366-1379, June 1923.

Parker, H. C. and Parker, Elizabeth W.;
"Calibration of Cells for Conductance Measurements, Part III", ibid., vol. 46, pp. 312-335, Feb. 1924.

18. Piccard, A. and Frivold;
"Demonstration of Induction Currents Produced in Electrolytes without Electrodes", Archives des Sciences Physiques et Naturelles, Ser. 5, vol. 2, pp. 264-265, May-June 1920.

19. Powers, W. F. and Dull, M. F.;
"Measurement at Radio Frequencies of the Conductivity of Liquids without Immersed Electrodes", Journal Optical Society of America and Review of Scientific Instruments, vol. 17, pp. 323-325, Oct. 1928.

20. Riekhoff, H.;
Diss. Kiel, 1929; Ann. d. phys., vol. 5, p. 577, 1929.

Riekhoff, H. and Zahn,
Z. Phys., vol. 53, p. 619, 1929.

21. Schmid-Burgk, W.; Piwowarsky, E. and Nipper, H.;
"Electrical Conductivity of Fluid Cast Iron", Zeits. f. Metallkunde., vol. 28, pp. 224-227, Aug. 1936.

22. Shedlovsky, T.;
"Screened Bridge for Measurement of Electrolytic Conductivity. Part I, Theory of Capacity Errors. Part II, Description of Bridge", Am. Chem. Soc., J., vol. 52, pp. 1793-1805, May 1930.

"Conductivity Cell for Eliminating Electrode Effects in Conductivity Measurements", ibid., vol. 52, pp. 1806-1811, May 1930.

Reference No.	Publication
23.	Smith, F. A.; "Source of Error in Conductivity Measurements", Am. Chem. Soc., J., vol. 49, pp. 2167-2171, Sept. 1927.
24.	Taylor and Acree; "Studies in Measurement of the Electrical Conductivity of Solutions at Different Frequencies, VI", Am. Chem. Soc., J., vol. 38, p. 2403, 1916.
25.	Termen, F. E.; Book: "Radio Engineers' Handbook", McGraw-Hill Book Co., New York, 1943.
26.	Washburn, E. W.; "The Measurement of Electrolytic Conductivity. I. The Theory of the Design of Conductivity Cells", Am. Chem. Soc., J., vol. 38, p. 2431, 1916.
	Washburn, E. W. and Bell; "Apparatus for Measuring Conductivity of Electrolytes", ibid., vol. 35, p. 177, 1913.
	Washburn, E. W. and Parker, K.; "The Measurement of Electrolytic Conductivity. II. The Telephone Receiver as an Indicating Instrument", ibid., vol. 39, p. 235, 1917.
27.	Zahn, H.; Z. Phys. vol. 51, p. 350, 1928.
28.	National Bureau of Standards; Circular C74, "Radio Instruments and Measurements", equation (147), p. 250.
29.	Terman, F. E.; "Radio Engineers' Handbook", McGraw-Hill, 1943.
30.	Legg, V. E. and Given, F. J.; "Compressed Powdered Molybdenum Permalloy", BTS Monograph B-1243.

PLATE I

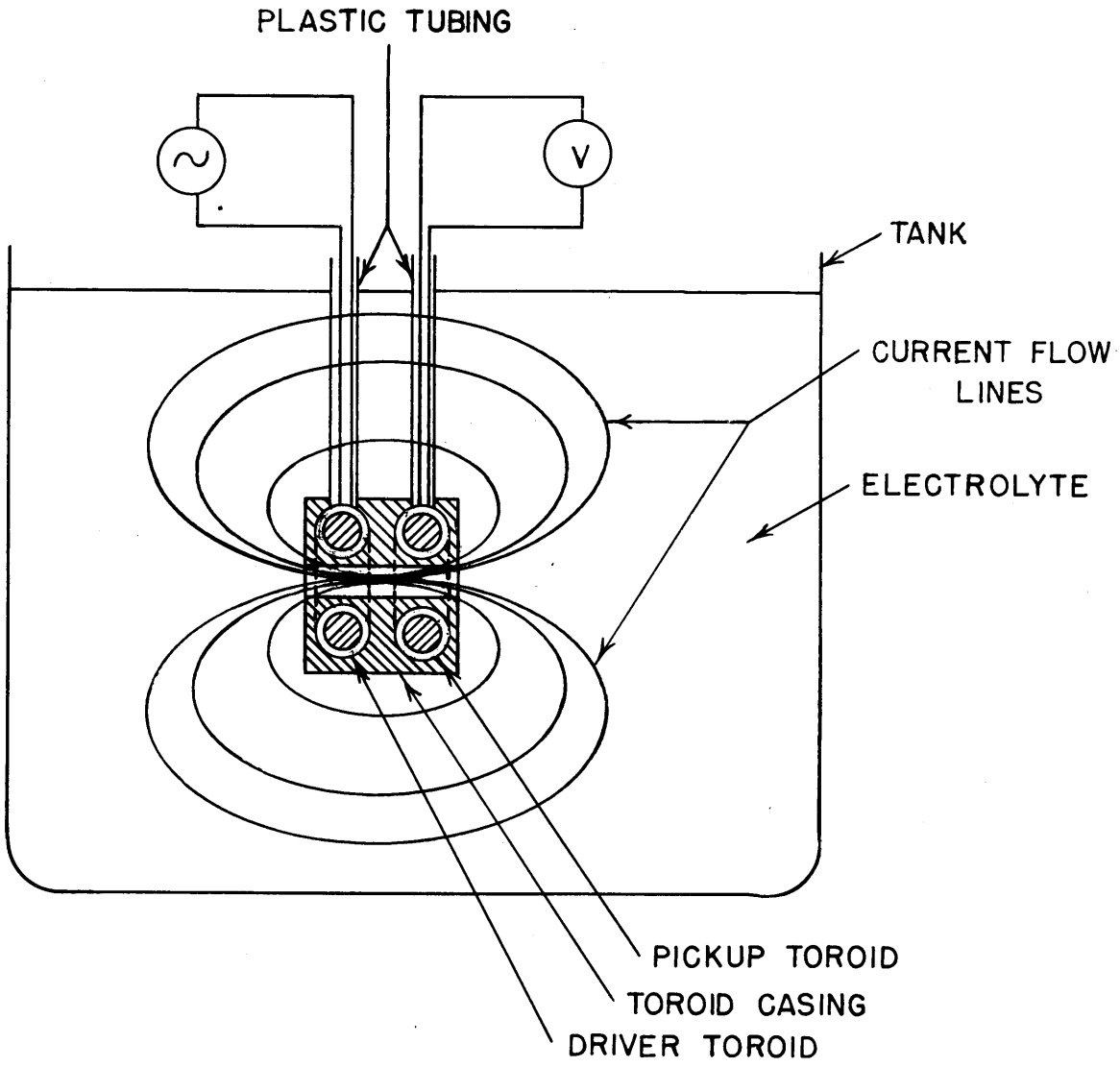
PLASTIC TUBING
V
TANK
CURRENT FLOW LINES
ELECTROLYTE
PICKUP TOROID
TOROID CASING
DRIVER TOROID

PLATE 2

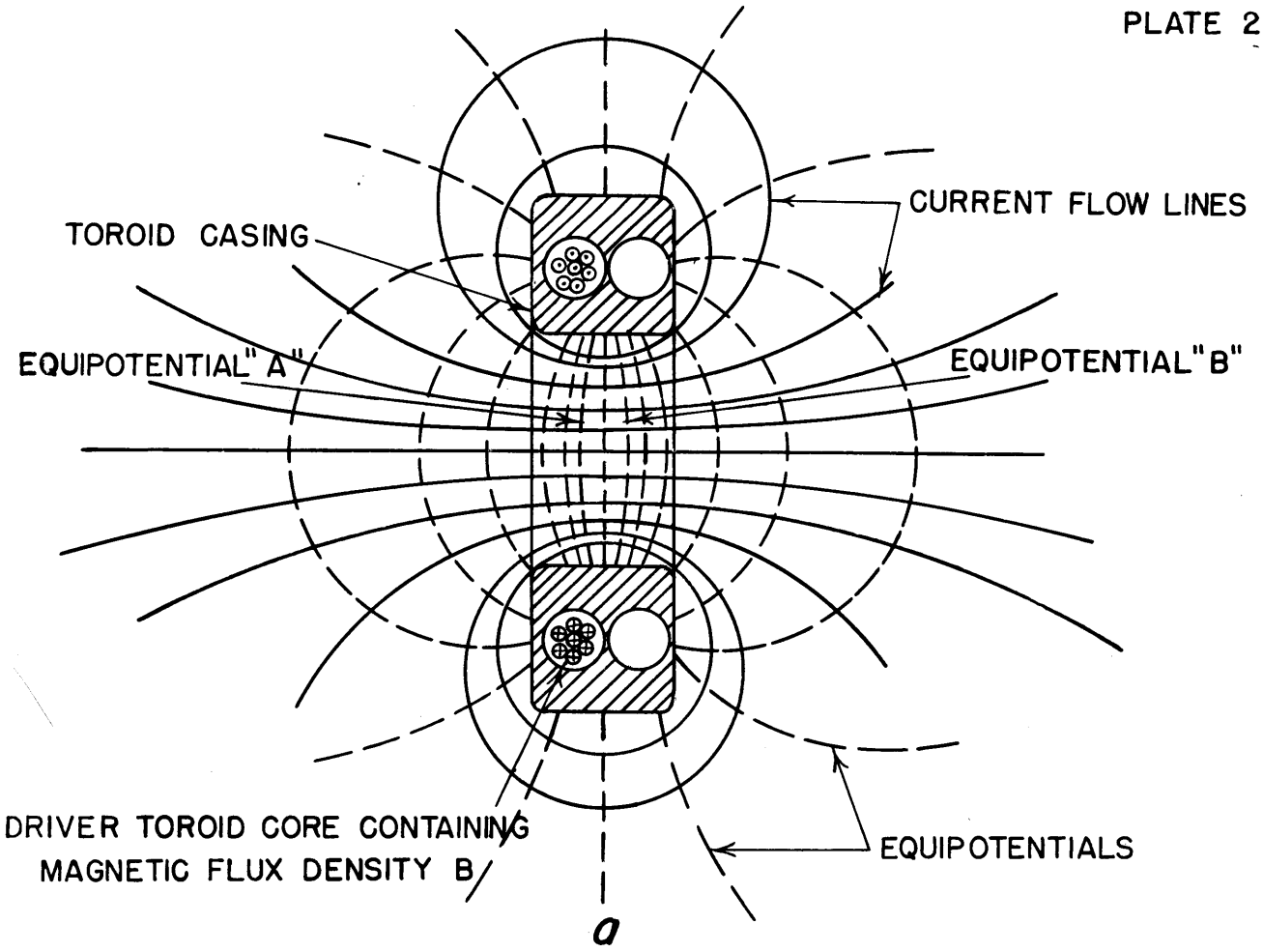
TOROID CASING
CURRENT FLOW LINES
EQUIPOTENTIAL "A"
EQUIPOTENTIAL "B"
DRIVER TOROID CORE CONTAINING
MAGNETIC FLUX DENSITY B
EQUIPOTENTIALS
a

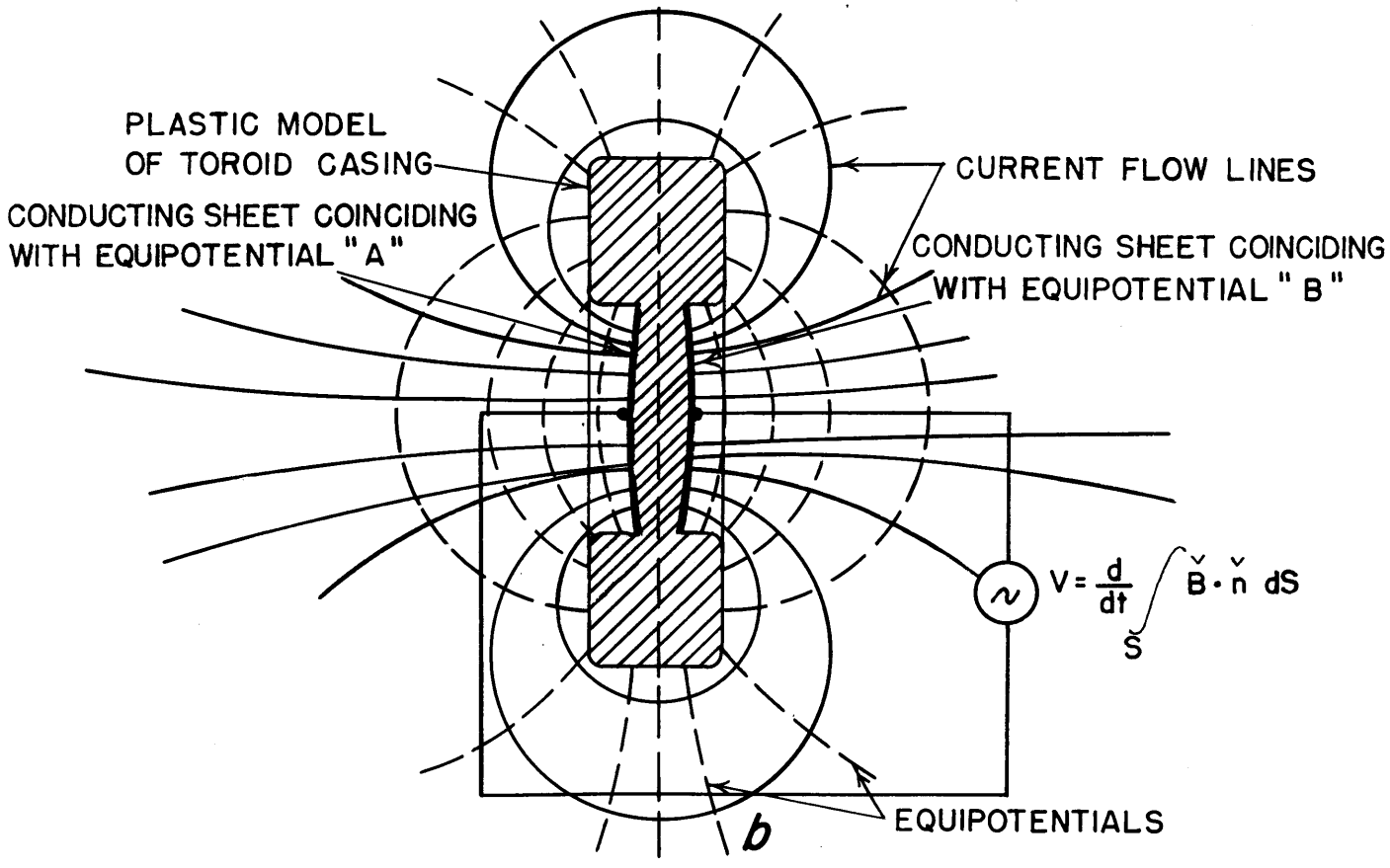
PLASTIC MODEL
OF TOROID CASING
CONDUCTING SHEET COINCIDING
WITH EQUIPOTENTIAL "A"
CURRENT FLOW LINES
CONDUCTING SHEET COINCIDING
WITH EQUIPOTENTIAL "B"
V = d/dt ∫S B · n dS
EQUIPOTENTIALS
b

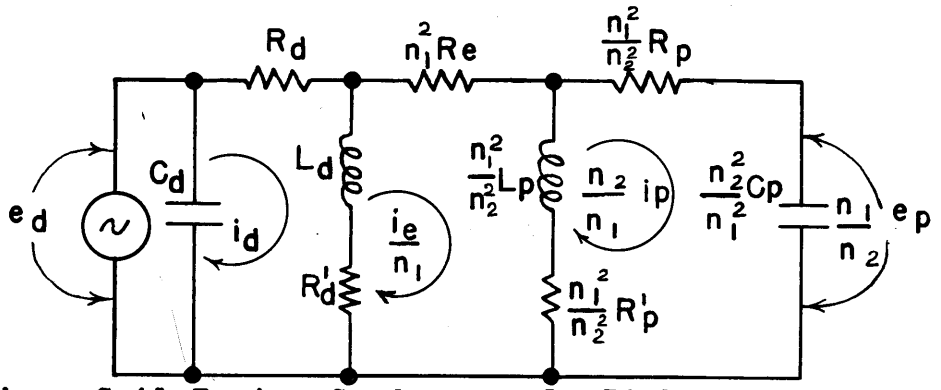

C_d Driver Coil Tuning Condenser	L_p Pickup Coil inductance
C_p Pickup Coil Tuning Condenser	n_1 Number turns on Driver Coil
e_d Driver voltage	n_2 Number turns on Pickup Coil
e_p Pickup voltage	R_d Driver Coil copper loss
i_e Current in electrolyte	R'_d Driver Coil core loss
i_d Current in Driver Coil	R_e Resistance of electrolyte
i_p Current in Pickup Coil	R_p Pickup Coil copper loss
L_d Driver Coil inductance	R'_p Pickup Coil core loss

(a)

EQUIVALENT CIRCUIT-DIRECT READING CONDUCTIVITY METER

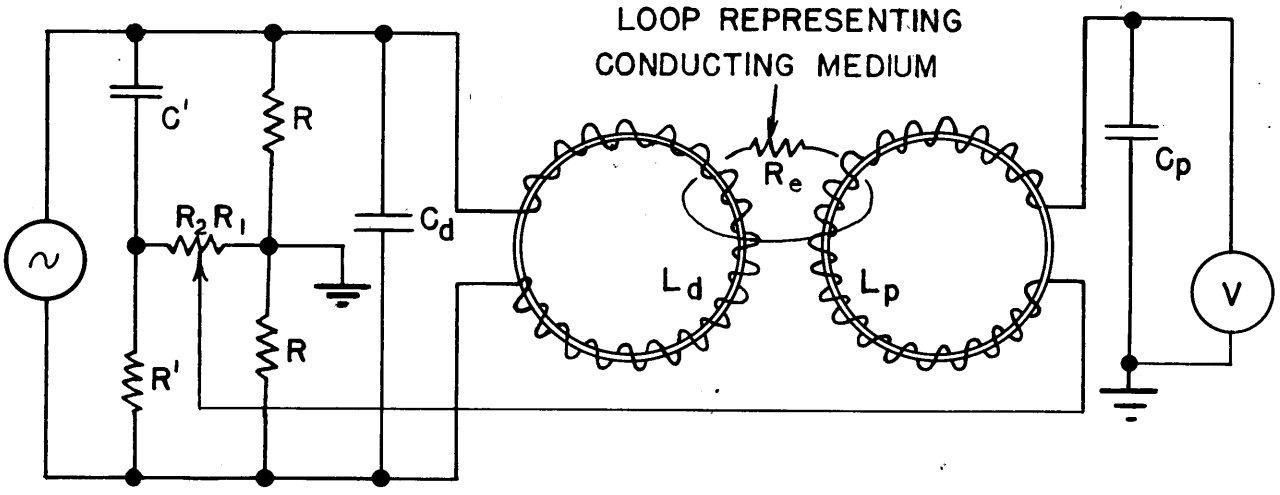

(b)

CIRCUIT OF NULL-TYPE CONDUCTIVITY METER

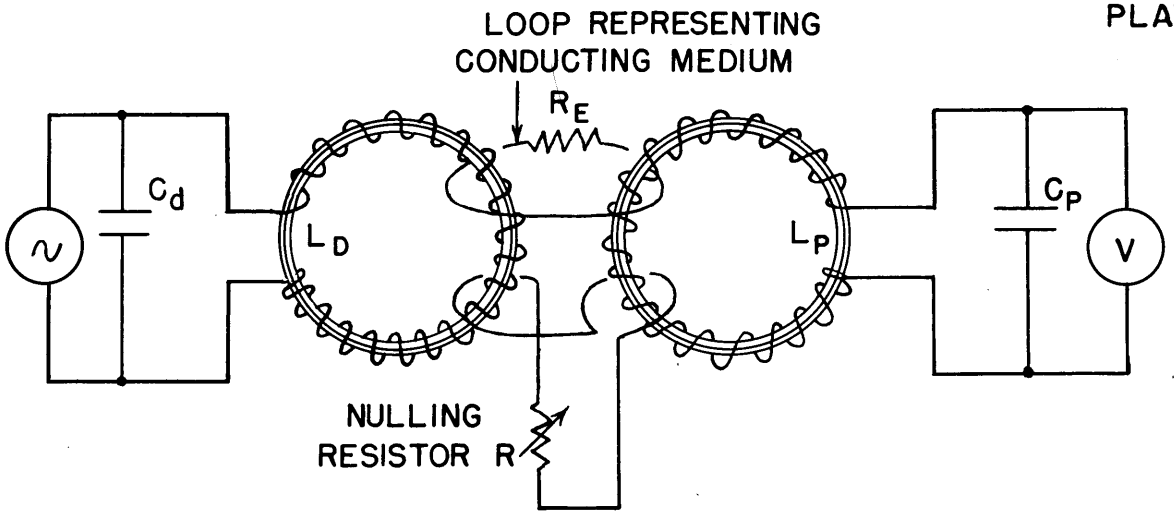

(a) PICCARD-FRIVOLD NULL-TYPE CONDUCTIVITY METER

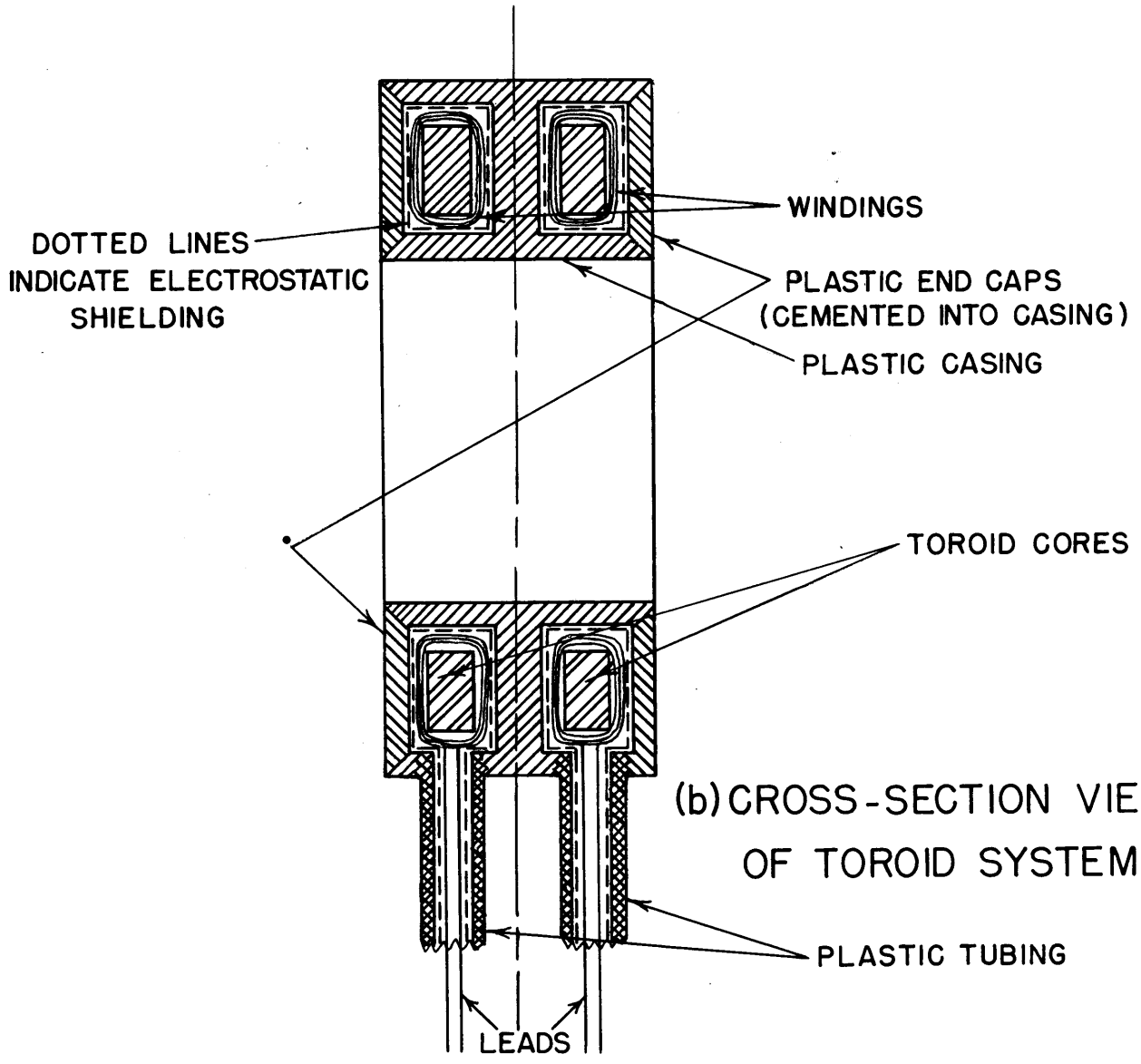

(b) CROSS-SECTION VIEW OF TOROID SYSTEM

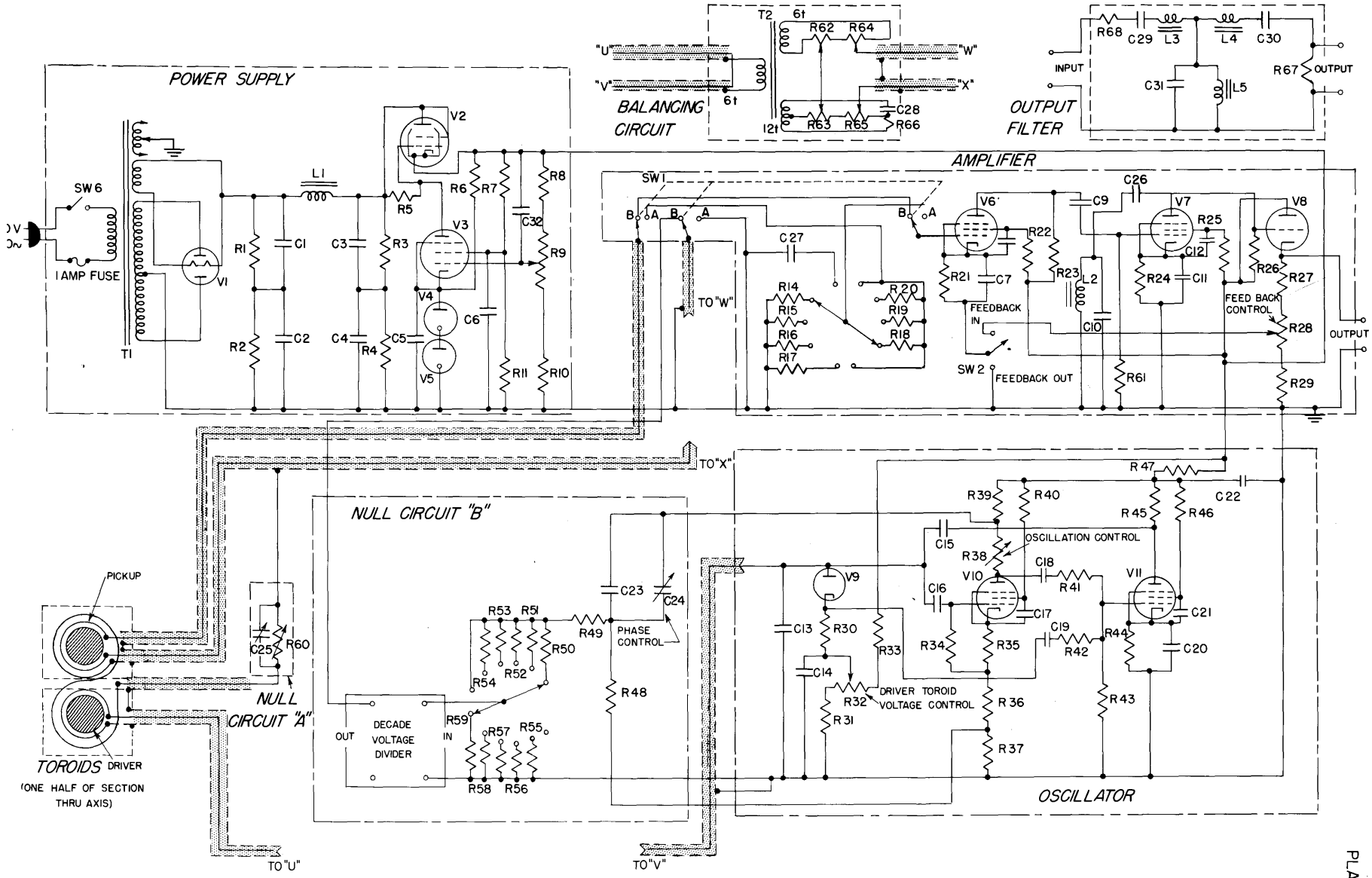

ELECTRODELESS CONDUCTIVITY METER

PLATE 5

PLATE 6

PLA

RESISTORS

	OHMS	TYPE
R_1	500,000	METALLIZED
R_2	500,000	"
R_3	500,000	"
R_4	500,000	"
R_5	500,000	"
R_6	80,000 ±1%	PRECISION
R_7	50,000	METALLIZED
R_8	180,000 ±1%	PRECISION
R_9	10,000	WIRE-WOUND POT.
R_{10}	100,000	PRECISION
R_{11}	250,000	METALLIZED
R_{14}	25 ±1%	PRECISION
R_{15}	250 ±1%	"
R_{16}	2,500 ±1%	"
R_{17}	25,000 ±1%	"
R_{18}	25,000 ±1%	"
R_{19}	24,800 ±1%	"
R_{20}	22,500 ±1%	"
R_{21}	1,500	METALLIZED
R_{22}	2,200,000	"
R_{23}	500,000	"
R_{24}	1,500	"
R_{25}	2,200,000	"
R_{26}	500,000	"
R_{27}	10,000 ±1%	PRECISION
R_{28}	2	WIRE-WOUND POT.
R_{29}	2 ±1%	PRECISION
R_{30}	50,000	METALLIZED
R_{31}	20,000 ±1%	PRECISION
R_{32}	10,000	WIRE-WOUND POT
R_{33}	150,000 ±1%	PRECISION
R_{34}	1,000,000	METALLIZED
R_{35}	100	"
R_{36}	20,000	"
R_{37}	160 ±1%	PRECISION

	OHMS
R_{38}	2,000
R_{39}	160 ±1%
R_{40}	120,000
R_{41}	50,000
R_{42}	50,000
R_{43}	1,000,000
R_{44}	1,500
R_{45}	500,000
R_{46}	2,200,000
R_{47}	1,000
R_{48}	2,270 ±1%
R_{49}	6.000 ±1%
R_{50}	10,000 ±1%
R_{51}	10,000 ±1%
R_{52}	9,990 ±1%
R_{53}	9,900 ±1%
R_{54}	9,000 ±1%
R_{55}	1,100 ±1%
R_{56}	101 ±1%
R_{57}	10.01 ±1%
R_{58}	1 ±1%
R_{59}	0.1 ±1%
R_{60}	DECADE R
R_{61}	1,000,000
R_{62}	2
R_{63}	2
R_{64}	100
R_{65}	100
R_{66}	8
R_{67}	1000 ±1%
R_{68}	1000 ±1%

ONE WATT RES.
ARE USED THRO

PLATE6 - LIST OF COMPONENTS

CAPACITORS

	MF.	VOLTAGE	TYPE
C_1	40	450	ELECTROL
C_2	40	450	"
C_3	40	450	"
C_4	40	450	"
C_5	4	150	PAPER
C_6	40	450	ELECTR
C_7	0.5		PAPER
C_8	0.005	450	"
C_9	0.002	450	"
C_{10}	0.00456		MICA
C_{11}	0.5		PAPER
C_{12}	0.005	450	"
C_{13}	0.00294		MICA
C_{14}	0.1	450	PAPER
C_{15}	0.002	450	"
C_{16}	0.001	450	"
C_{17}	0.5	450	"
C_{18}	0.04	450	"
C_{19}	0.04	450	"
C_{20}	25	25	"
C_{21}	0.05	450	"
C_{22}	8	450	"
C_{23}	0.0065		MICA
C_{24}	0.001		MICA TR
C_{25}	VARIABLE AIR		CONDENS
C_{26}	1	450	
C_{27}	0.00283		MICA
C_{28}	2		
C_{29}	0.00561 ± 1%		MICA
C_{30}	0.00561 ± 1%		MICA
C_{31}	0.045 ± 1%		MICA
C_{32}	1	450	PAPER

	OHMS	TYPE
R_{38}	2,000	WIRE-WOUND POT.
R_{39}	160 ± 1%	PRECISION
R_{40}	120,000	METALLIZED
R_{41}	50,000	"
R_{42}	50,000	"
R_{43}	1,000,000	"
R_{44}	1,500	"
R_{45}	500,000	"
R_{46}	2,200,000	"
R_{47}	1,000	"
R_{48}	2,270 ± 1%	PRECISION
R_{49}	6.000 ± 1%	"
R_{50}	10,000 ± 1%	"
R51	10,000 ± 1%	"
R52	9,990 ± 1%	"
R53	9,900 ± 1%	"
R54	9,000 ± 1%	"
R55	1,100 ± 1%	"
R56	101 ± 1%	"
R57	10.01 ± 1%	"
R58	1 ± 1%	"
R59	0.1 ± 1%	"
R60	DECADE RESISTANCE BOX	
R61	1,000,000	METALLIZED
R62	2	WIRE-WOUND POT.
R63	2	"
R64	100	"
R65	100	"
R66	8	METALLIZED
R67	1000 ± 1%	PRECISION
R68	1000 ± 1%	"

NE WATT RESISTORS
RE USED THROUGHOUT

TUBES

V_1	5W4
V_2	6V6
V_3	6SJ7
V_4	991
V_5	991
V_6	6SJ7
V_7	6SJ7
V_8	6J5
V_9	9005
V_{10}	6AC7
V_{11}	6SJ7

INDUCTORS

	HY.	
L_1	20	
L_2	0.055	Q=100
L_3	0.045 ±1%	Q=100
L_4	0.045 ±1%	Q=100
L_5	0.00561 ±1%	Q=100

TRANSFORMERS

T_1 POWER TRANSF.
700 V. C.T. HIGH VOLTAGE
5 V. 2 AMP.
6.3V. 2.5 AMP.

T_2 SPECIAL TRANSFORMER
WITH TURNS AS SHOWN

DRIVER AND PICKUP TOROIDS
DESCRIBED IN TEXT

L_2, L_3, L_4, L_5 AND T_2 WOUND WITH
NO. 24 B AND S GA. WIRE ON W.E. NO.
476930 MOLYBDENUM-PERMALLOY DUST CORES

TYPE
ELECTROLYTIC
"
"
"
PAPER
ELECTROLYTIC
PAPER
"
"
MICA
PAPER
"
MICA
PAPER
"
"
"
"
"
"
"
MICA
MICA TRIMMER
CONDENSER
MICA
MICA
MICA
MICA
PAPER

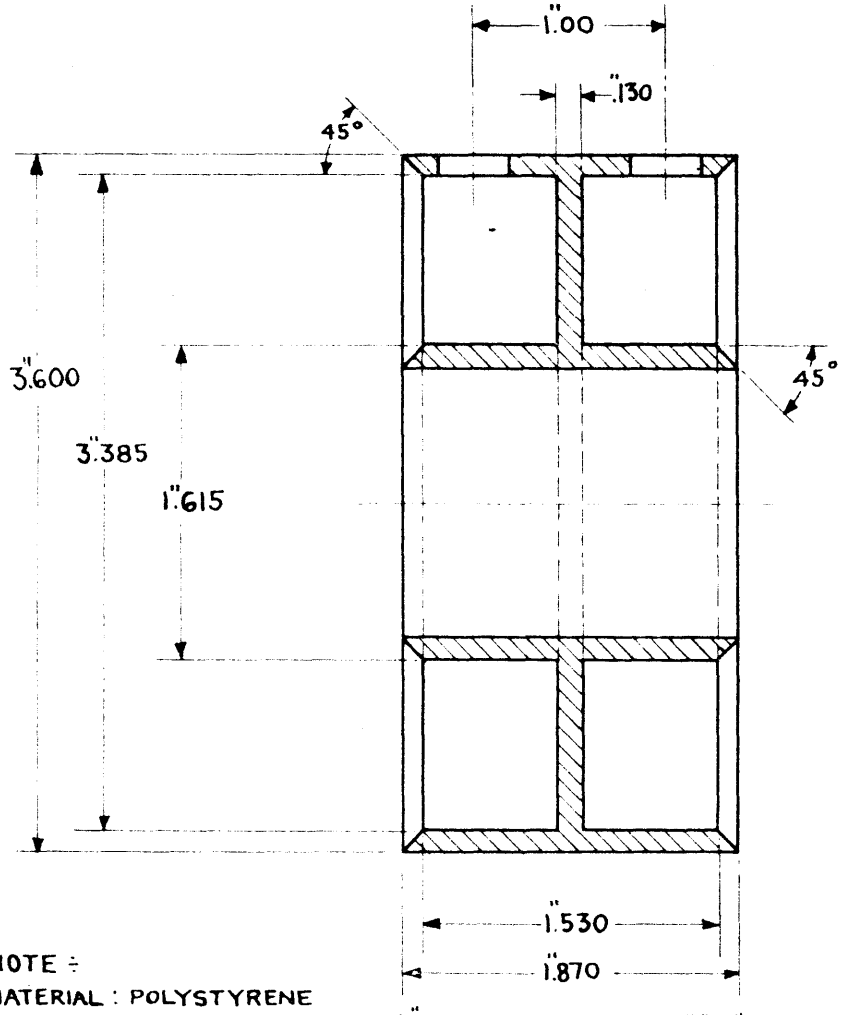

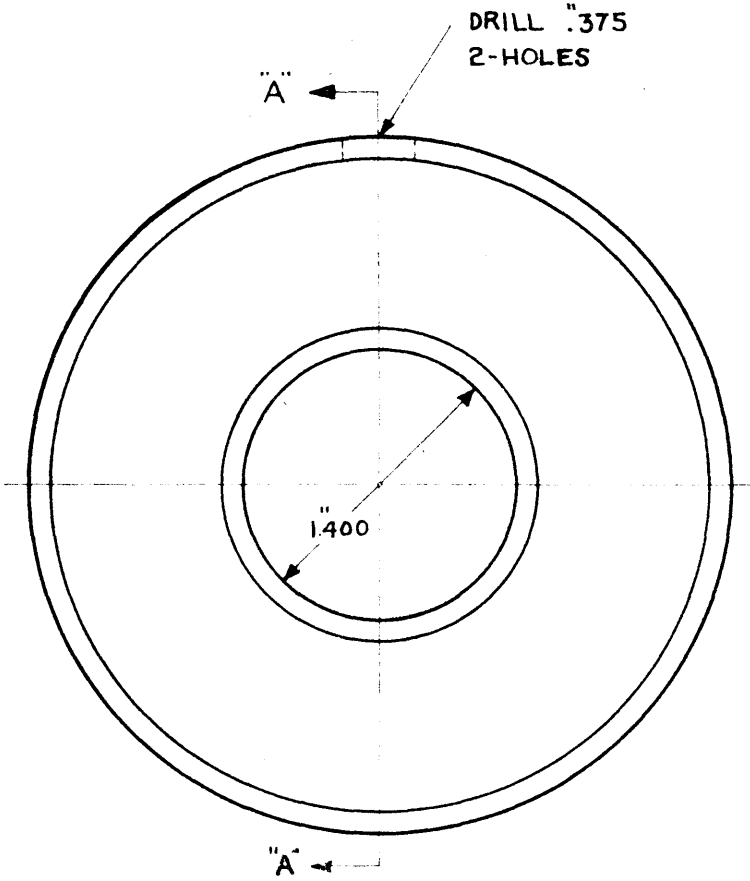

NOTE :
MATERIAL : POLYSTYRENE
TOLERANCES ON DIMENSIONS = ±.005

SECTION "A"-"A"

TOROID CASING

SCALE = FULL SIZE

PLATE 7

PLATE 7

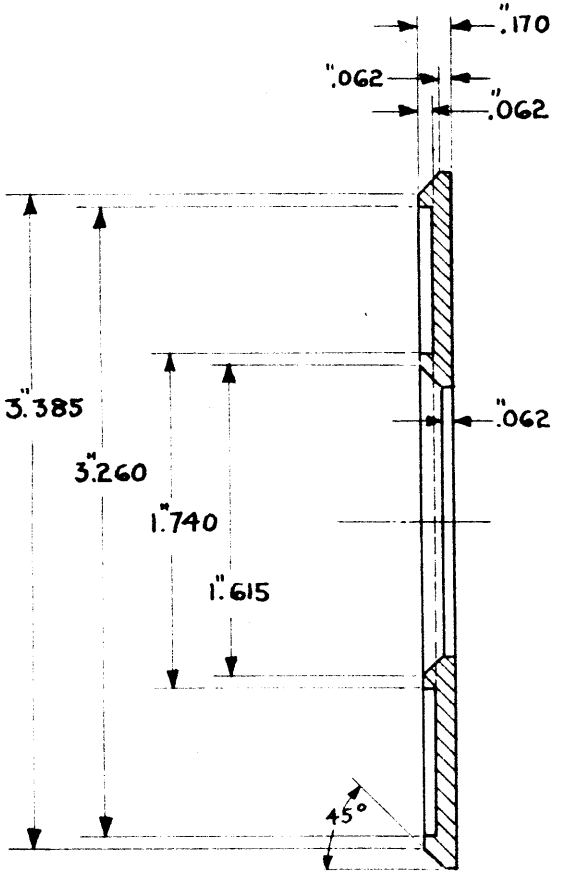

SECTION "A"-"A"

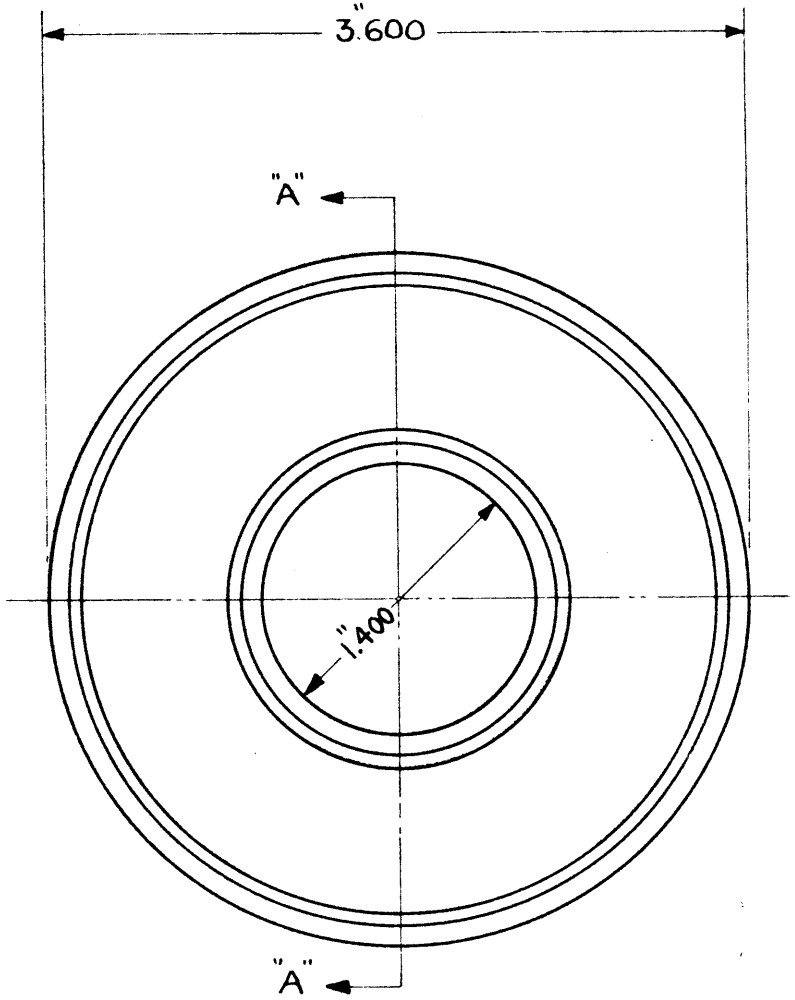

NOTE :-
MATERIAL : POLYSTYRENE
TOLERANCES ON DIMENSIONS = ±.005

END CAP
FOR TOROID CASING

SCALE = FULL SIZE

PLATE 8

PLATE 8

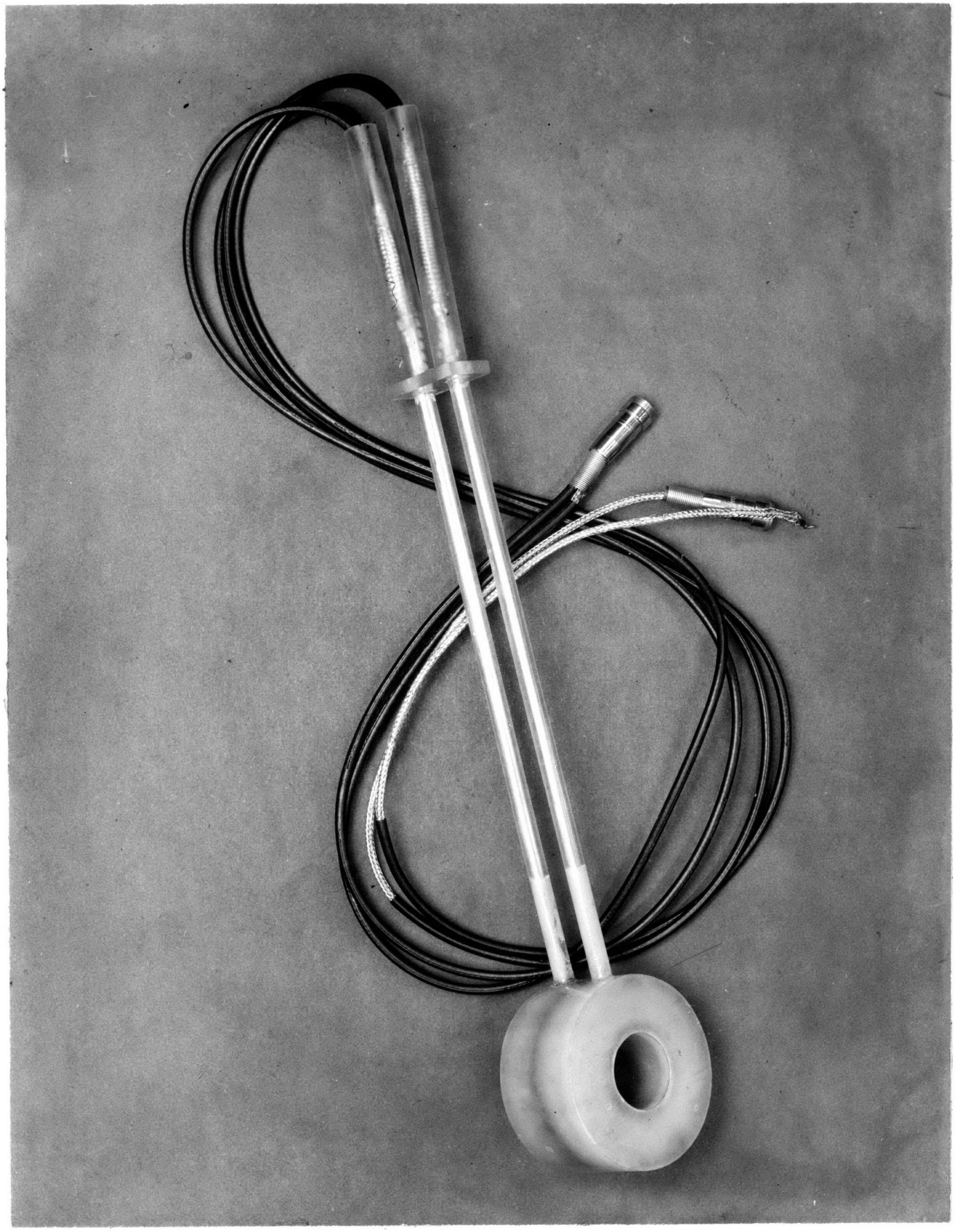

PLATE 10

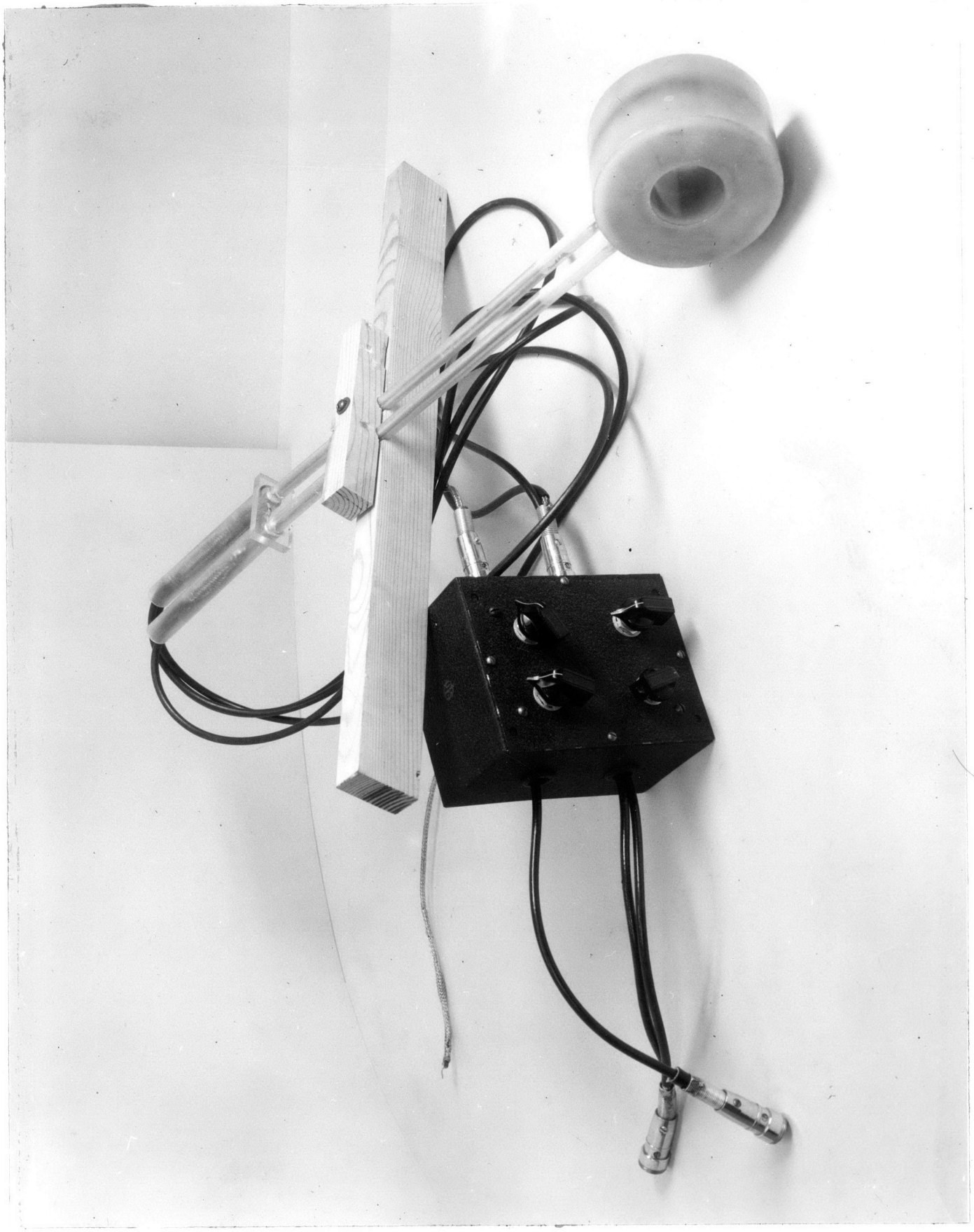

PLATE II

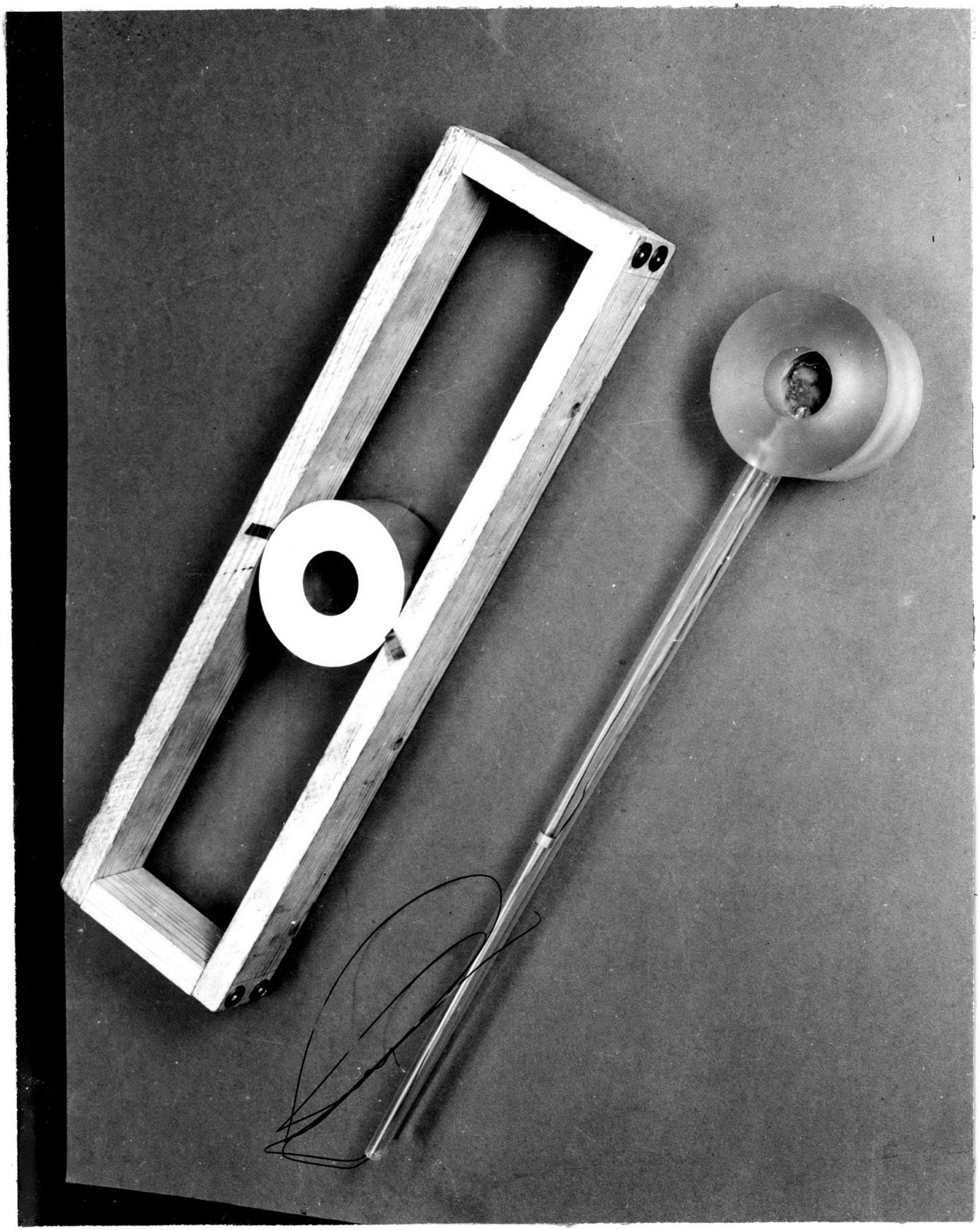

PLATE 12

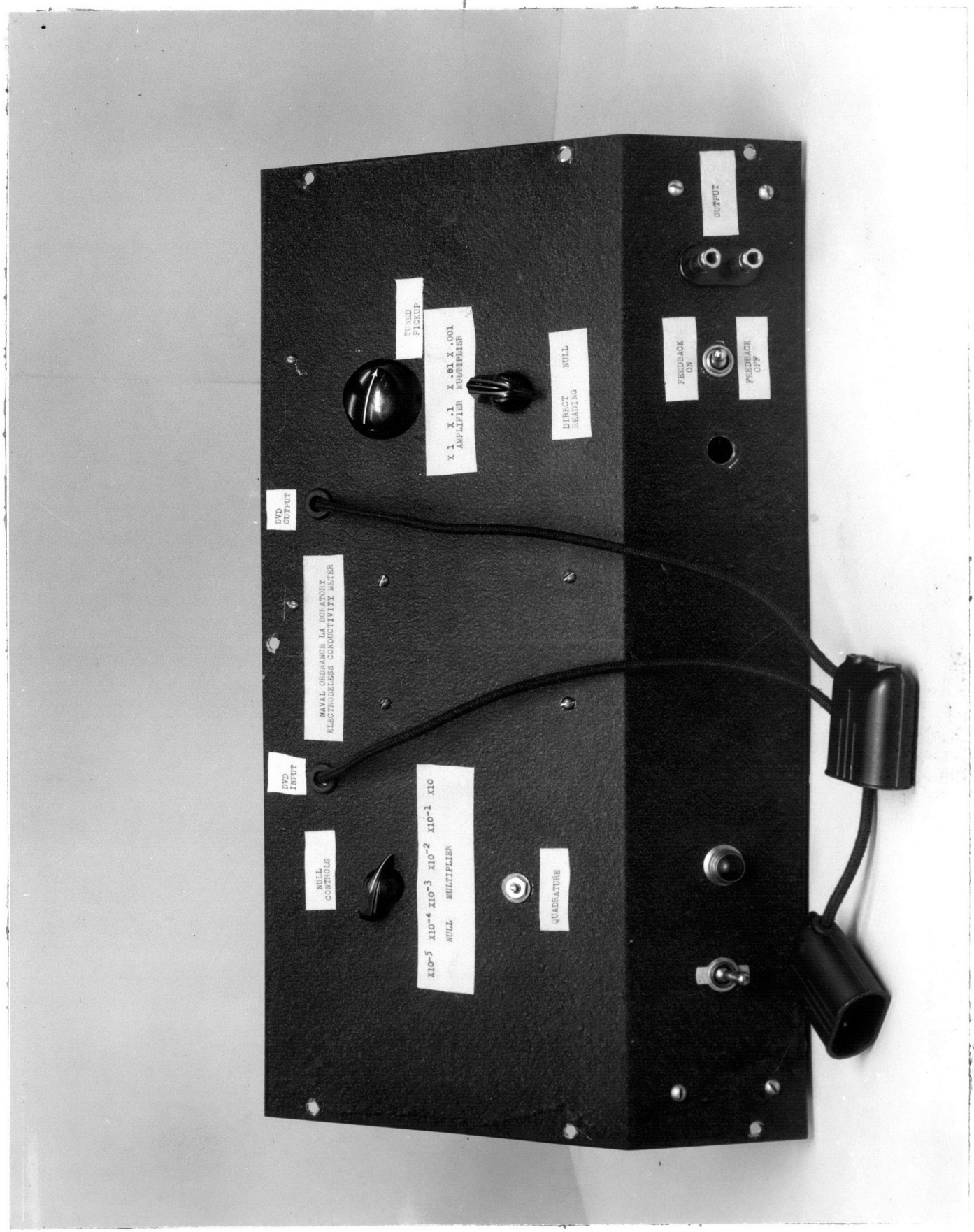
NAVAL ORDNANCE LA BORATORY
ELECTRODELESS CONDUCTIVITY METER
DVD OUTPUT
DVD INPUT
NULL CONTROLS
X10-5 X10-4 X10-3 X10-2 X10-1 X10
NULL MULTIPLIER
QUADRATURE
X 1 X.1 X.01 X.001
AMPLIFIER MAGNIFIER
TUNED PICKUP
DIRECT NULL READING
FEEDBACK ON
FEEDBACK OFF
OUTPUT

PLATE 13

PLATE 13

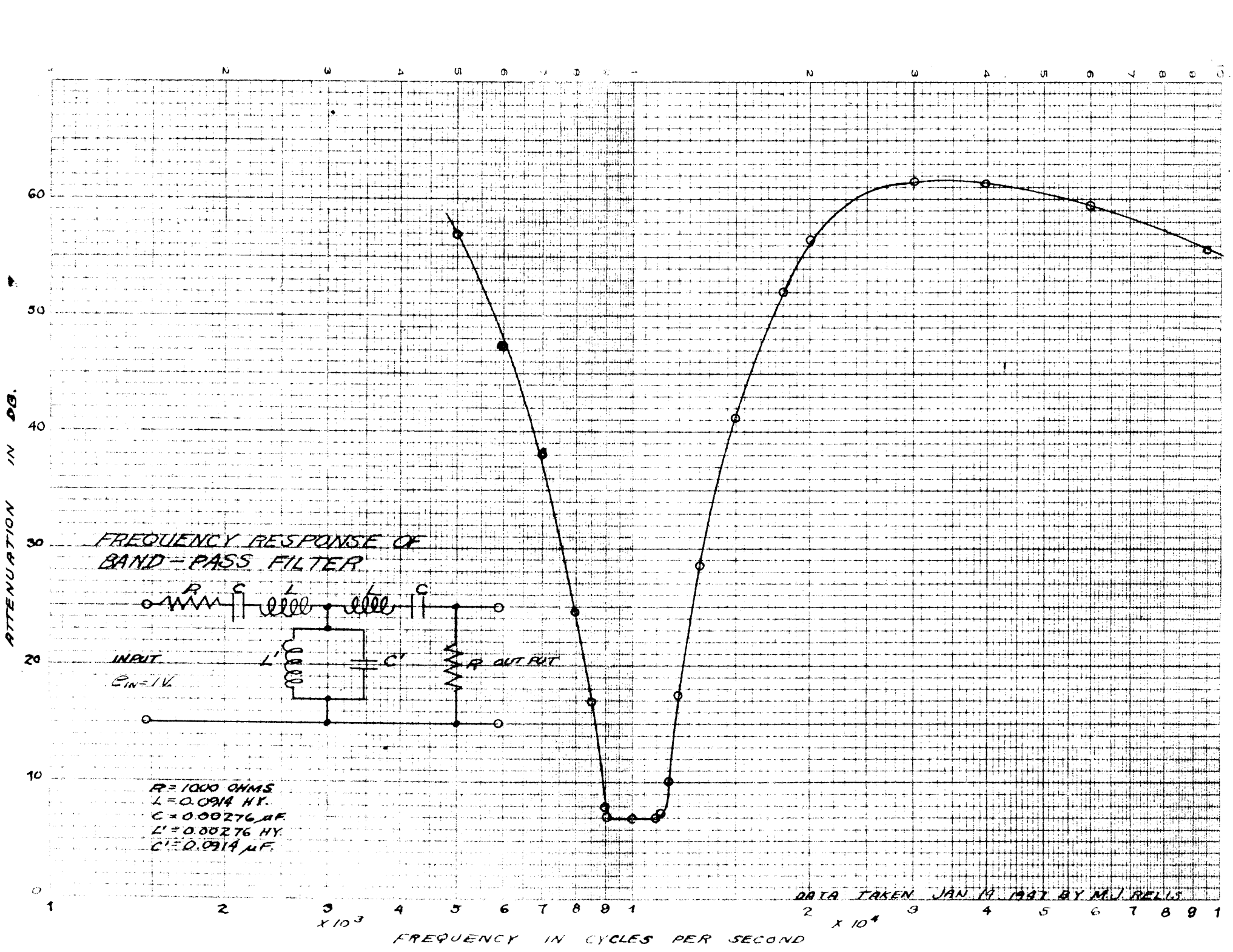
FREQUENCY RESPONSE OF
BAND-PASS FILTER
R
C
L
L
C
INPUT
e_{IN}=1V.
L'
C'
R
OUTPUT
R = 1000 OHMS
L = 0.0914 HY.
C = 0.00276 μF.
L' = 0.00276 HY.
C' = 0.0914 μF.
DATA TAKEN JAN 14 1941 BY M.J. RELLS
ATTENUATION IN DB.
0
10
20
30
40
50
60
1
2
3
4
5
6
7
8
9
1
2
3
4
5
6
7
8
9
1
X 10³
X 10⁴
FREQUENCY IN CYCLES PER SECOND

PLATE 14

FREQUENCY RESPONSE OF AMPLIFIER IN CASCADE WITH FILTER, WITH AND WITHOUT FEEDBACK

E_B = 300 V. C_K = 6.8 Ω

WITHOUT FEEDBACK, C_{OUT} = 10 MK

WITH FEEDBACK, C_{OUT} = 6.5 MK

GAIN IN DECIBELS

DATA TAKEN APR. 30, 1928, BY M. J. KELLY

PLATE 15

PLATE 16

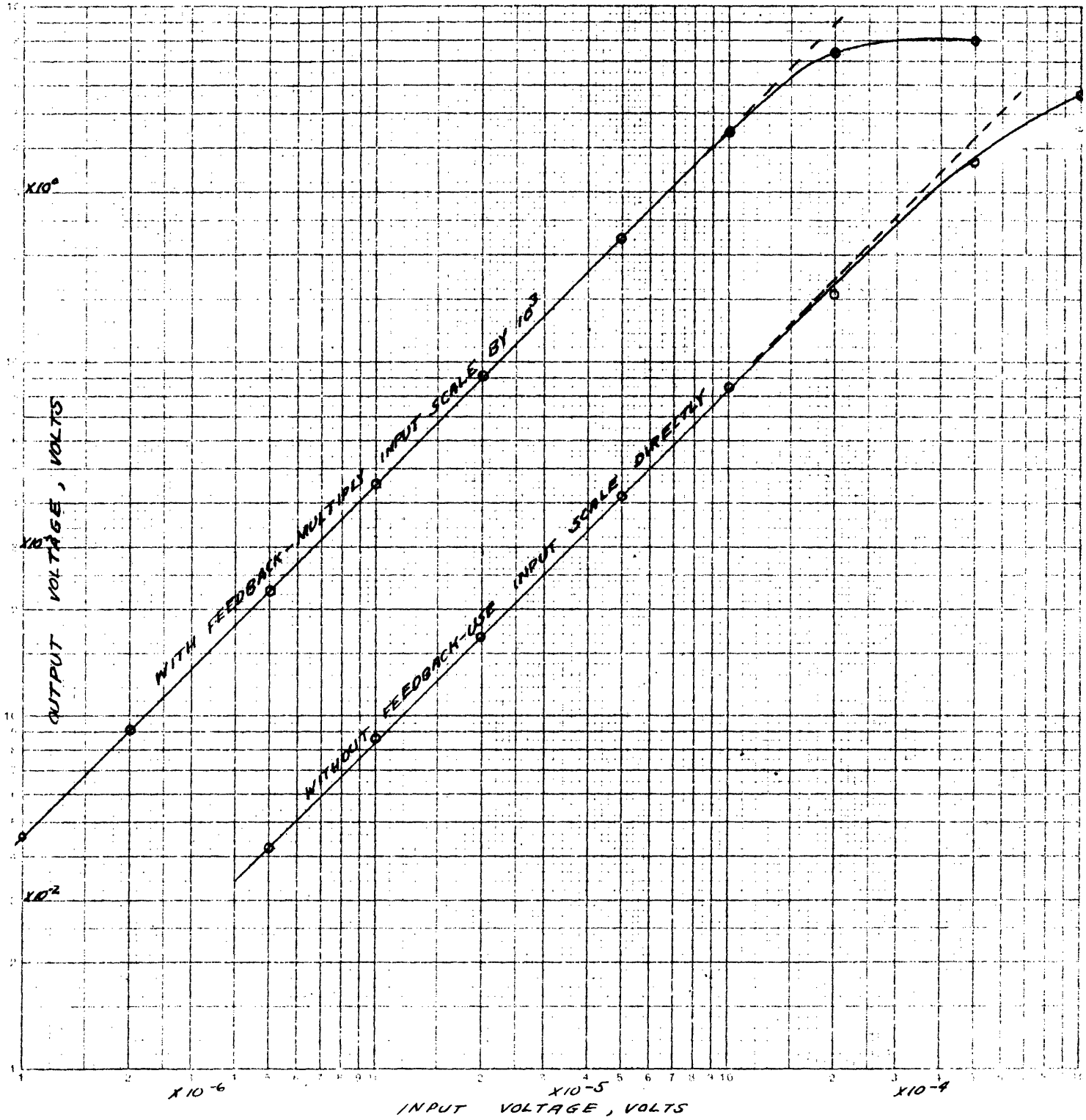

GAIN CHARACTERISTIC OF AMPLIFIER AT 10000 CPS

E_B = 300 V. E_f = 6.3 V.

DATA TAKEN APRIL 30, 1947 BY M. RELI.

(NO PLATE 17) PLATE 18

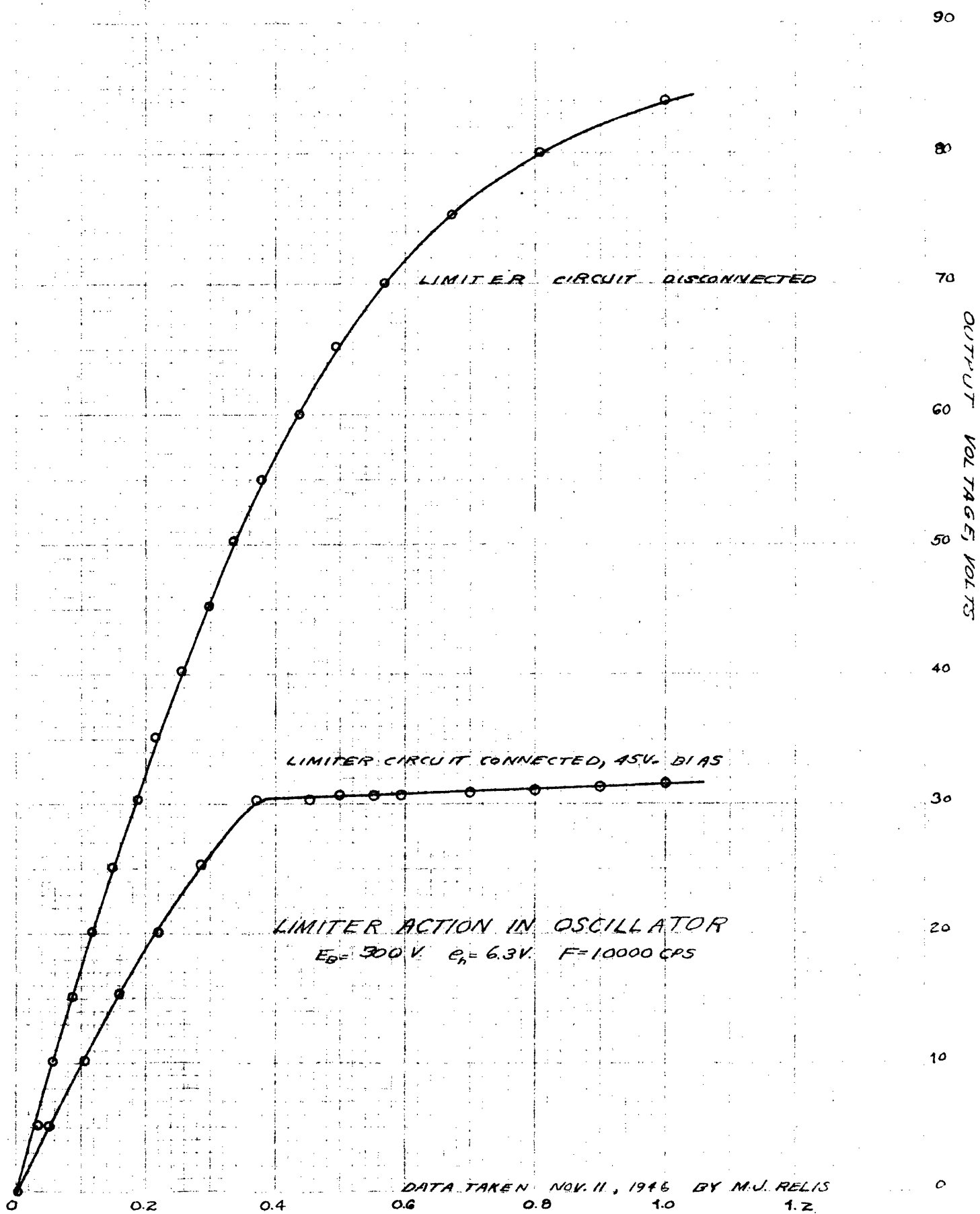

DETERMINATION OF R_{∞} OF [redacted] MODEL FROM RESISTANCE OF MODEL VS. RESISTIVITY OF ELECTROLYTE

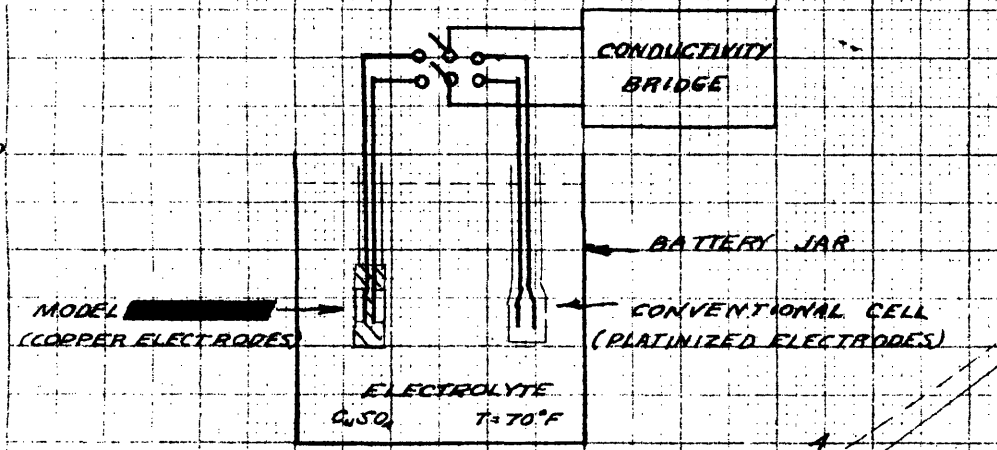

1 - FRESHLY BRIGHTENED MODEL ELECTRODES

NUMBERS INDICATE ORDER IN WHICH MEASUREMENTS WERE MADE

6 - FRESHLY BRIGHTENED MODEL ELECTRODES

R_{∞} = SLOPE OF SOLID LINE = 0.758

DATA TAKEN MARCH 19, 1947 BY M.J. RELLIS

RESISTANCE OF MODEL IN OHMS

0 100 200

RESISTIVITY OF ELECTROLYTE IN OHM-CM

0 100 200 300 400

PLATE 19

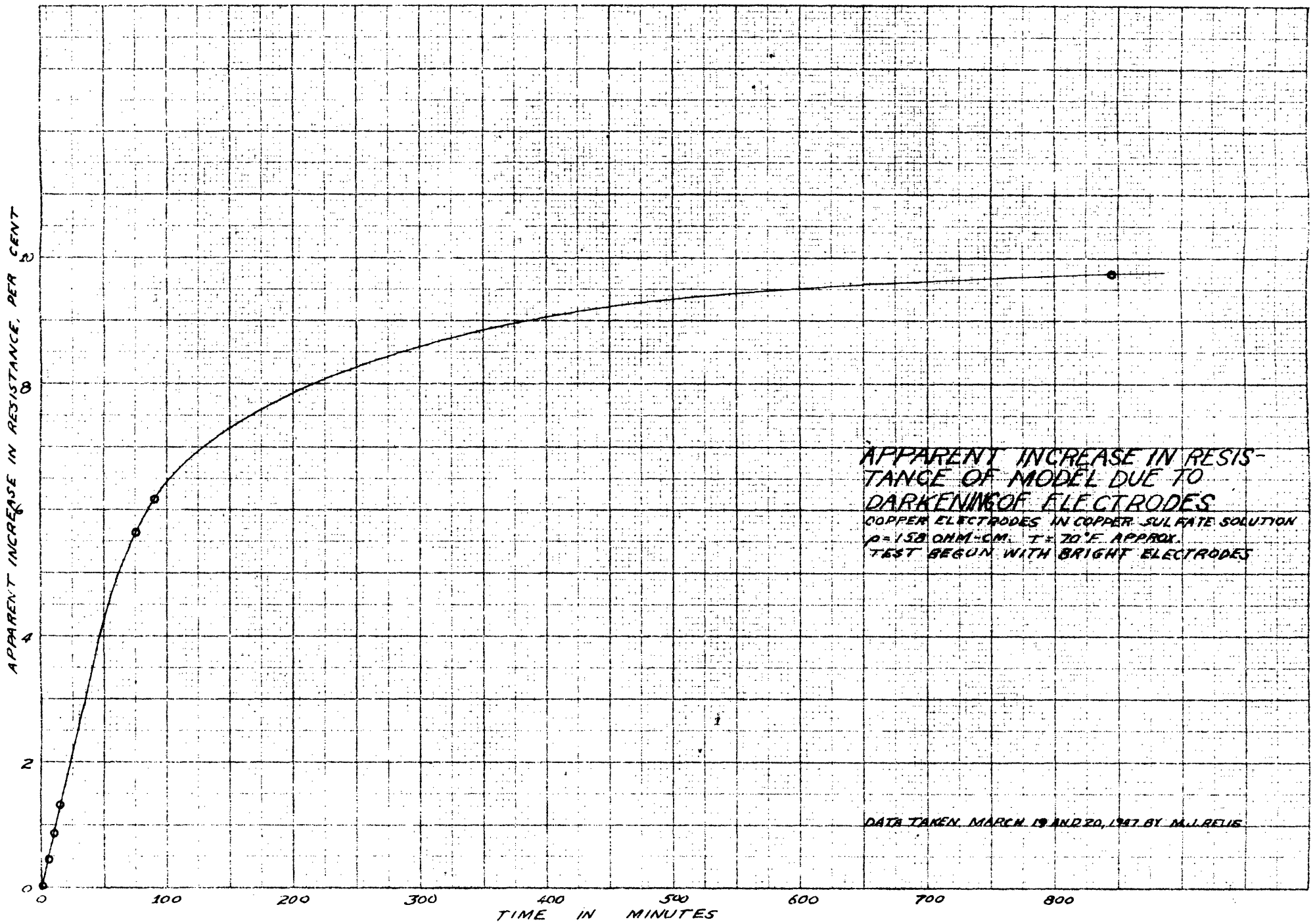
APPARENT INCREASE IN RESISTANCE, PER CENT
0
2
4
6
8
10
0
100
200
300
400
500
600
700
800
TIME IN MINUTES
APPARENT INCREASE IN RESISTANCE OF MODEL DUE TO DARKENING OF ELECTRODES
COPPER ELECTRODES IN COPPER SULFATE SOLUTION
ρ = 158 OHM-CM. T = 70°F APPROX.
TEST BEGUN WITH BRIGHT ELECTRODES
DATA TAKEN MARCH 19 AND 20, 1947 BY M.J. REILLY

PLATE 20

EFFECT OF PROXIMITY TO NON-CONDUCTING WALLS OF BATTERY JAR ON RESISTANCE OF MODEL OF TOROID ASSEMBLY

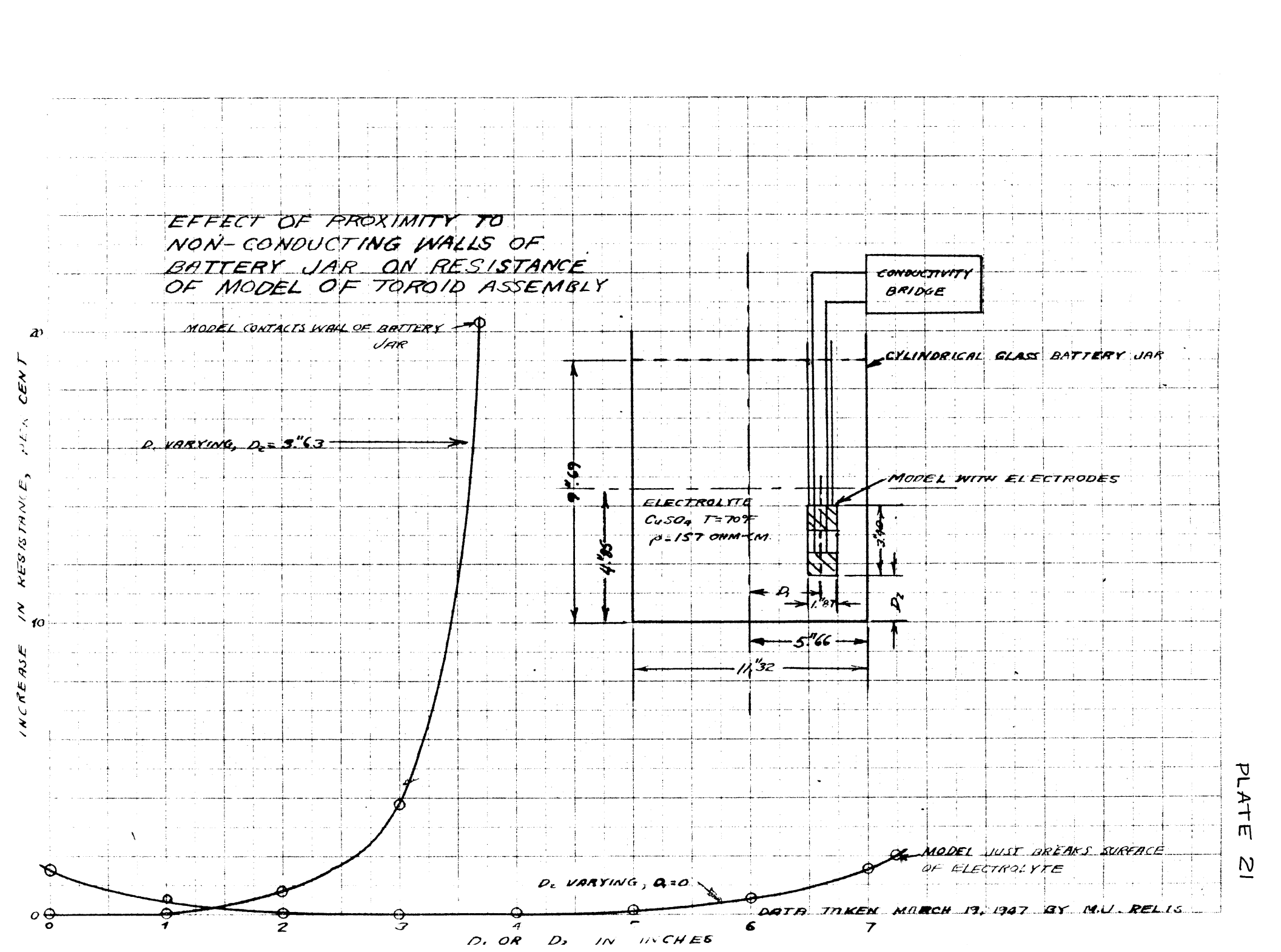

PLATE 21

DATA TAKEN NOV. 9, 1946 BY M. J. RELIS

CAPACITANCE IN HUNDREDS OF MICROMICROFARADS

0.2 0.3 0.4 0.5 0.6 0.7 0.8 0.9 1 2 3 4 5 6 7 8 9 10

FREQUENCY IN HUNDREDS OF MEGACYCLES PER SECOND

10 9 8 7 6 5 4 3 2 1

DETERMINATION OF INDUCTANCE FROM RESONANT FREQUENCY OF INDUCTANCE ANALOGUE VS. SERIES CAPACITANCE

F_1, C_1

F_2, C_2

$$L = \frac{1}{4\pi F_1 F_2 (C_1 C_2)^{\frac{1}{2}}}$$

$F_1 = 382$ MC/S $\quad F_2 = 100$ MC/S

$C_1 = 10$ μμF. $\quad C_2 = 150$ μμF.

$L = 0.0171$ μH.

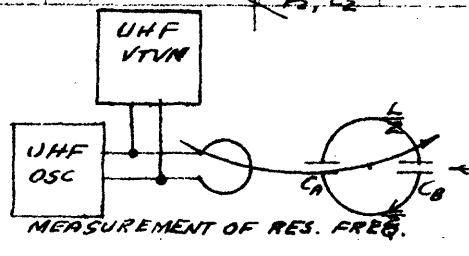

MEASUREMENT OF RES. FREQ.

← INDUCTANCE ANALOGUE →

MEASUREMENT OF PARALLEL CAP. $C_A + C_B$

SERIES CAP. TAKEN AS $\frac{C_A + C_B}{4}$

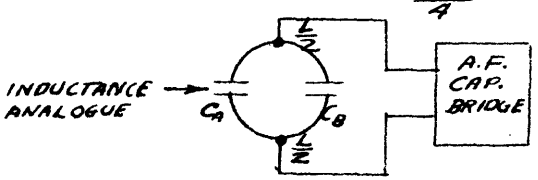

PLATE 22

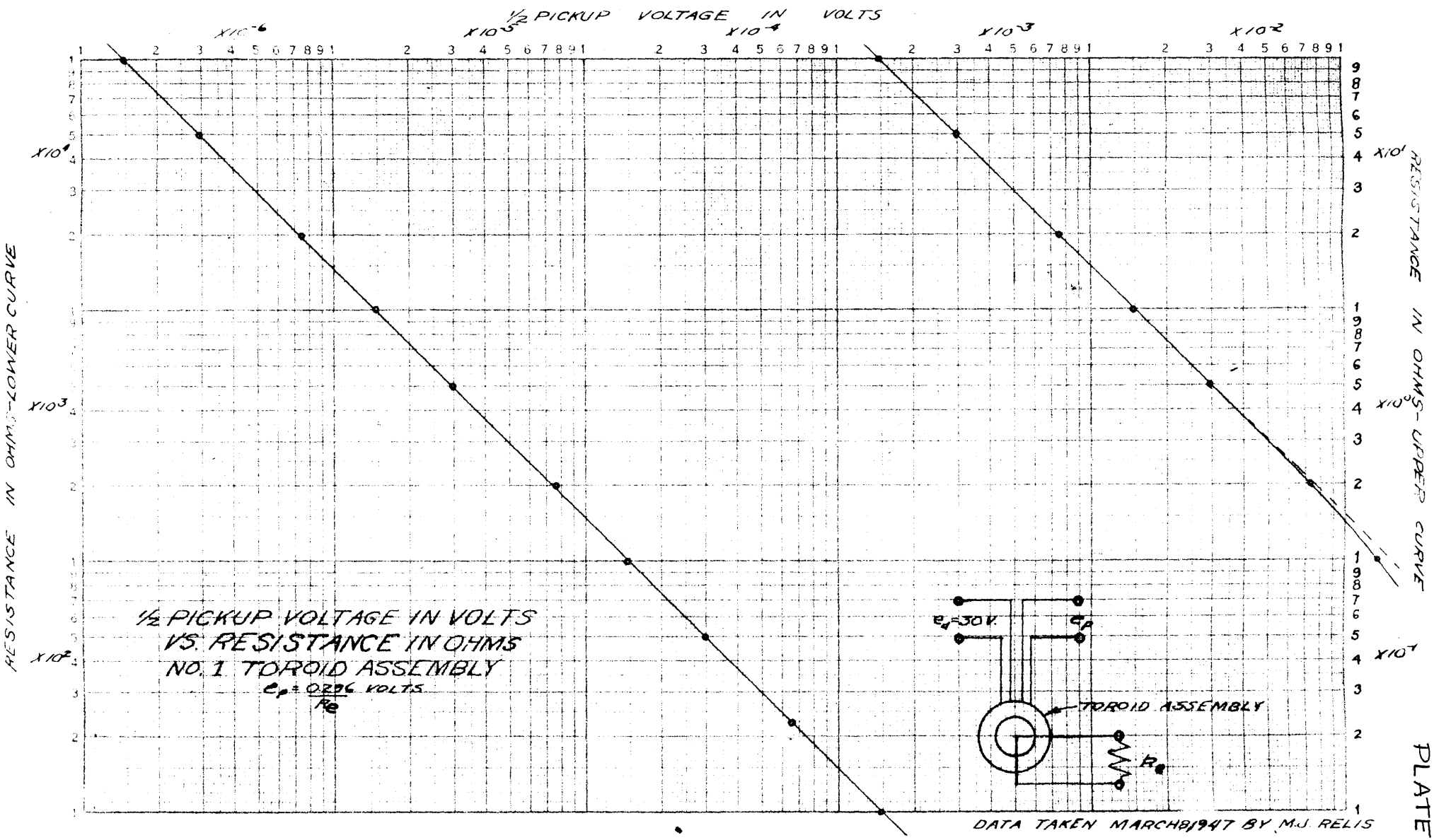
½ PICKUP VOLTAGE IN VOLTS
X10⁻⁶
X10⁻⁵
X10⁻⁴
X10⁻³
X10⁻²
X10⁴
X10³
X10²
X10¹
X10⁰
X10⁻¹
RESISTANCE IN OHMS-LOWER CURVE
RESISTANCE IN OHMS-UPPER CURVE
½ PICKUP VOLTAGE IN VOLTS
VS. RESISTANCE IN OHMS
NO. 1 TOROID ASSEMBLY
$e_p = \frac{0.006}{R_e}$ VOLTS
e_p=30 V.
e_p
TOROID ASSEMBLY
R_e
DATA TAKEN MARCH 8 1947 BY M.J. RELIS

PLATE 23

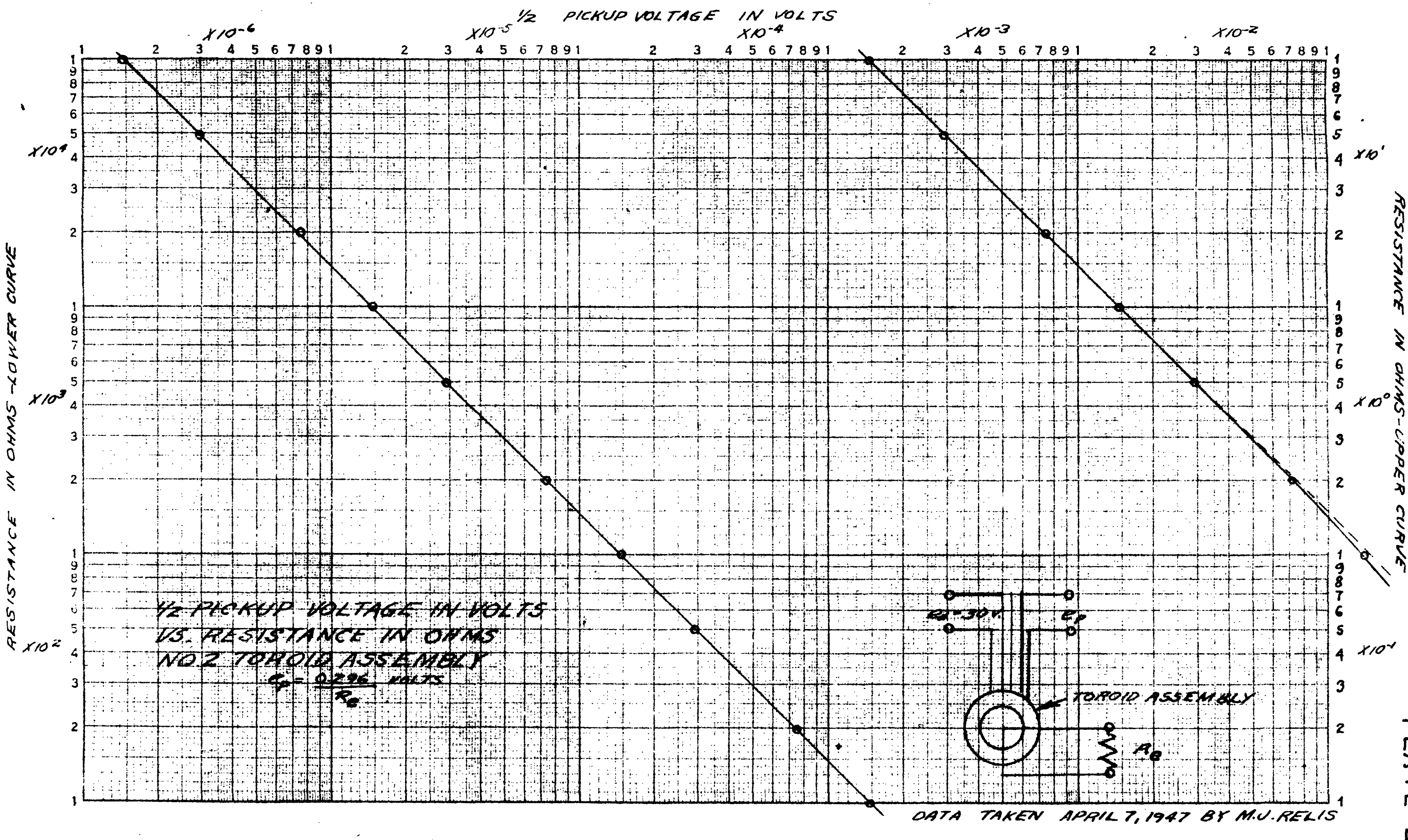
1/2 PICKUP VOLTAGE IN VOLTS
X10-6
X10-5
X10-4
X10-3
X10-2
RESISTANCE IN OHMS - LOWER CURVE
RESISTANCE IN OHMS - UPPER CURVE
X10⁴
X10³
X10²
X10¹
X10⁰
X10⁻¹
1/2 PICKUP VOLTAGE IN VOLTS
VS. RESISTANCE IN OHMS
NO.2 TOROID ASSEMBLY
$e_p = \frac{0.296}{R_e}$ VOLTS
Eg=30V.
Ep
TOROID ASSEMBLY
Re
DATA TAKEN APRIL 7, 1947 BY M.J. RELIS

PLATE 24

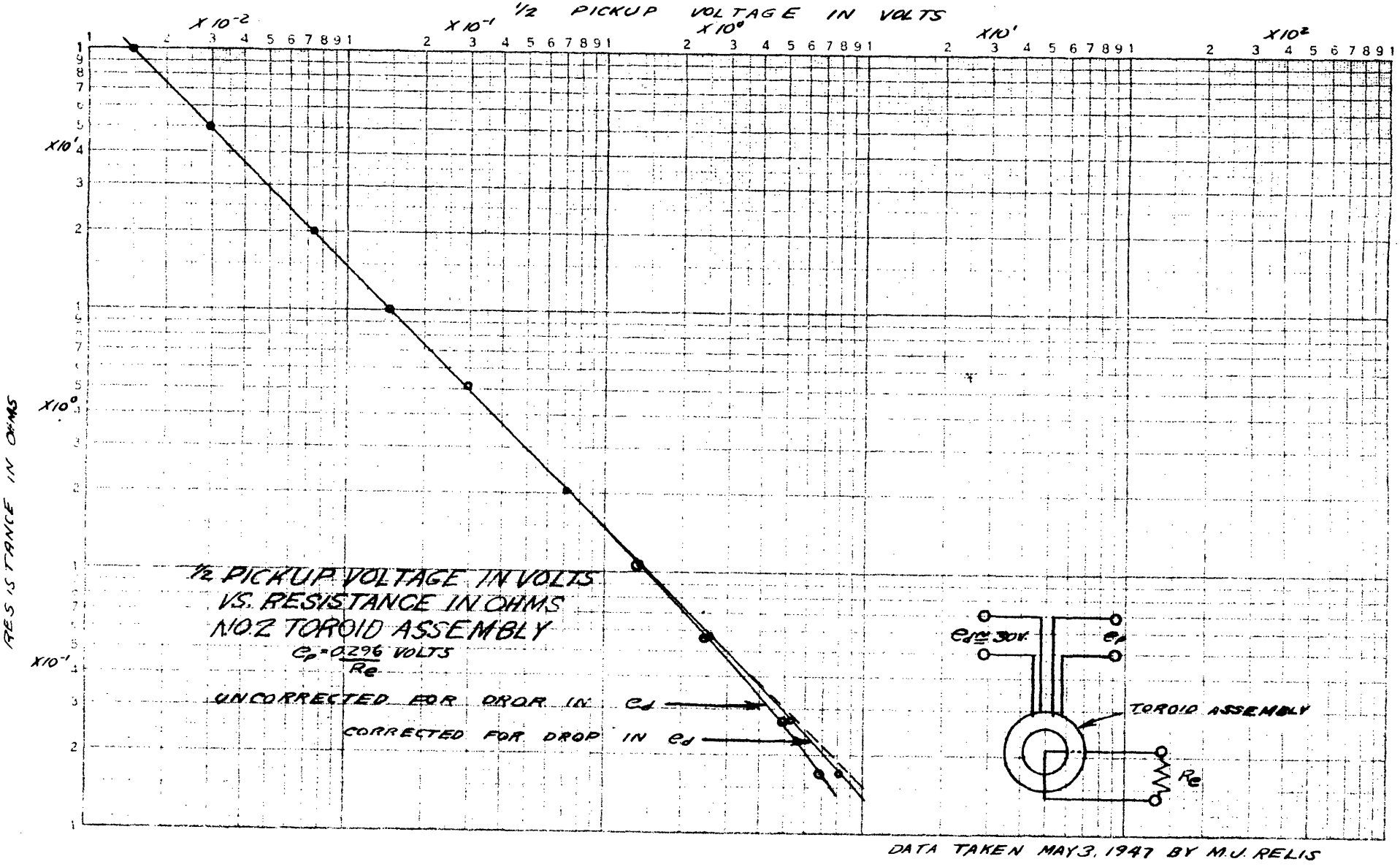
½ PICKUP VOLTAGE IN VOLTS
X 10⁻²
X 10⁻¹
X 10⁰
X 10¹
X 10²
RESISTANCE IN OHMS
X 10⁴
X 10³
X 10²
X 10¹
½ PICKUP VOLTAGE IN VOLTS
VS. RESISTANCE IN OHMS
NO.2 TOROID ASSEMBLY
$e_p = \frac{.0296}{Re}$ VOLTS
UNCORRECTED FOR DROP IN e_d
CORRECTED FOR DROP IN e_d
$e_d \cong 30V.$
e_d
TOROID ASSEMBLY
Re
DATA TAKEN MAY 3, 1947 BY M.J. RELIS

PLATE 25

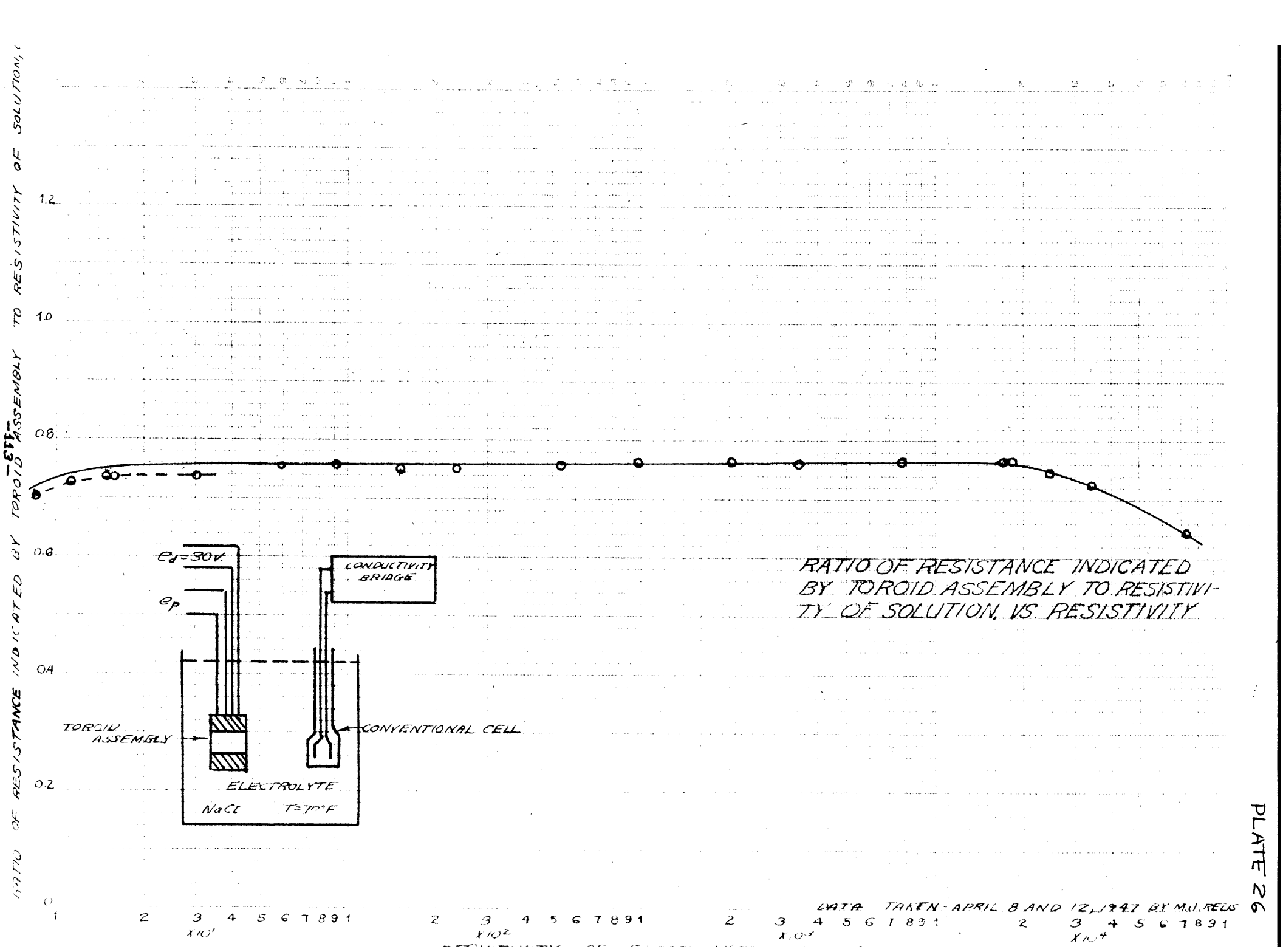
RATIO OF RESISTANCE INDICATED BY TOROID ASSEMBLY TO RESISTIVITY OF SOLUTION, VS. RESISTIVITY
-113-
1.2
1.0
0.8
0.6
0.4
0.2
0
1
2
3
4
5
6
7
8
9
1
X10¹
X10²
X10³
X10⁴
e_d=30v
e_p
CONDUCTIVITY BRIDGE
TOROID ASSEMBLY
CONVENTIONAL CELL
ELECTROLYTE
NaCl
T=70°F
DATA TAKEN-APRIL 8 AND 12, 1947 BY M.J. REUS
PLATE 26

RATIO OF RESISTANCE INDICATED BY TOROID ASSEMBLY TO RESISTIVITY OF SOLUTION, VS. RESISTIVITY, SHOWING EFFECT OF DISPLACEMENT CURRENTS

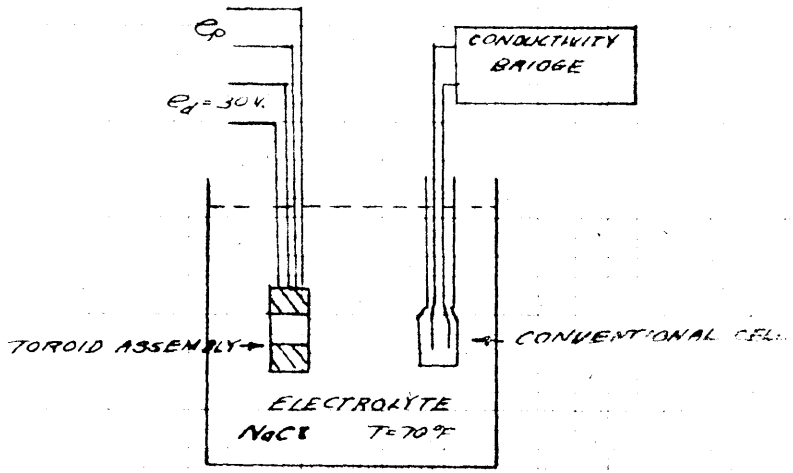

RATIO OF RESISTANCE INDICATED BY TOROID ASSEMBLY TO RESISTIVITY OF ELECTROLYTE

1.2
1.0
0.8
0.6
0.4
0.2
0

← EXPERIMENTAL CURVE; USE RESISTIVITY SCALE DIRECTLY

THEORETICAL CURVE; MULTIPLY RESISTIVITY SCALE BY 10^2 →

1 2 3 4 5 6 7 8 9 1 2 3 4 5 6 7 8 9 1 2 3 4 5 6 7 8 9 1

$\times 10^3$ $\times 10^4$ $\times 10^5$

DATA TAKEN APRIL 12, 1947, BY M.J. RELIS

PLATE 27

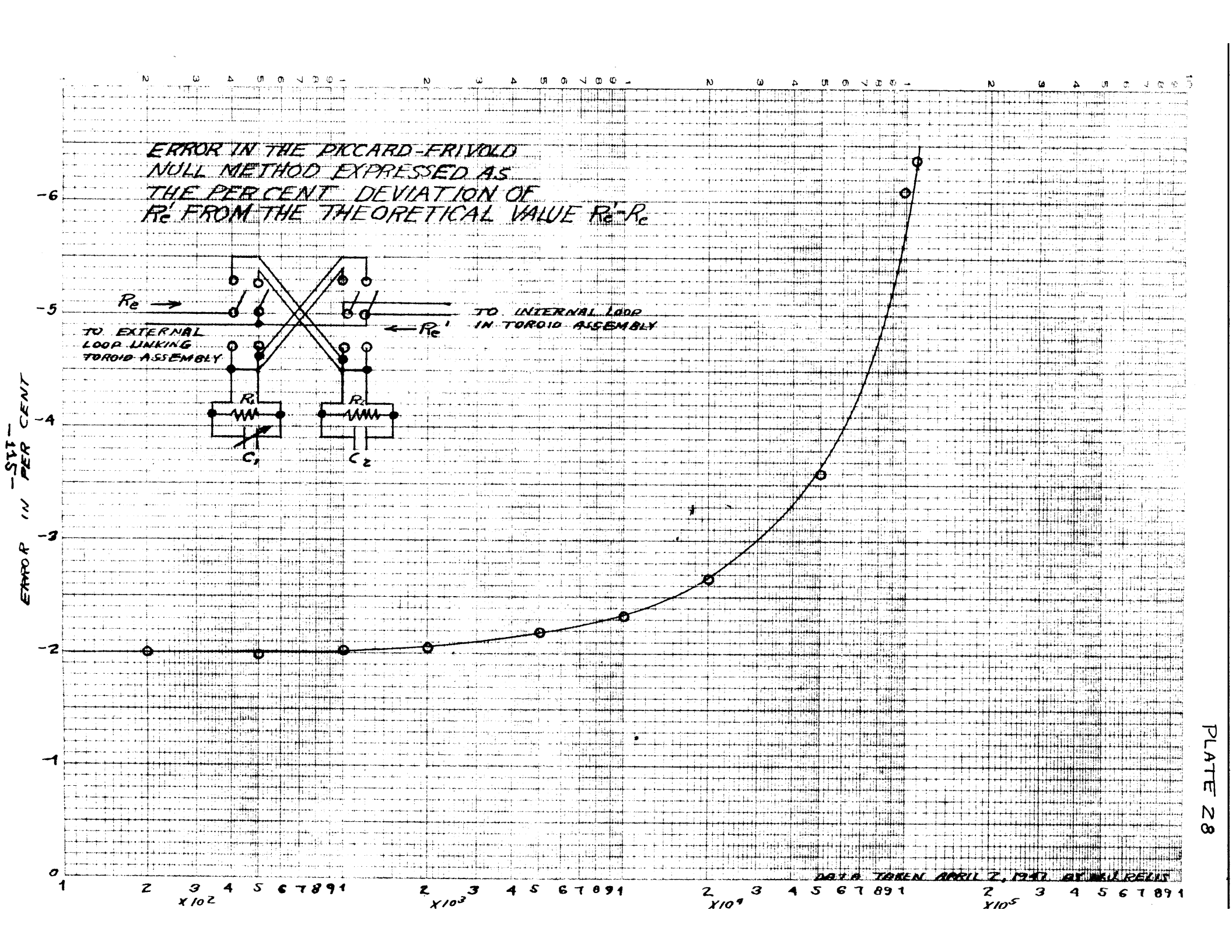
ERROR IN THE PICCARD-FRIVOLD NULL METHOD EXPRESSED AS THE PER CENT DEVIATION OF R_e' FROM THE THEORETICAL VALUE $R_e'-R_e$
R_e
TO EXTERNAL LOOP LINKING TOROID ASSEMBLY
R_e'
TO INTERNAL LOOP IN TOROID ASSEMBLY
R_1
R_2
C_1
C_2
ERROR IN PER CENT
-15-
0
-1
-2
-3
-4
-5
-6
1
2 3 4 5 6 7 8 9 1
X10²
X10³
X10⁴
X10⁵
DATA TAKEN APRIL 2, 1931 AT MT. WILSON

PLATE 28